Title
Perturbative Structure in Entanglement, Gauge Theory, and Holography

Author
Sivaramakrishnan, Allic Vijai

Publication Date
2017

Peer reviewed|Thesis/dissertation

UNIVERSITY OF CALIFORNIA

Los Angeles

Perturbative Structure in Entanglement, Gauge Theory, and Holography

A dissertation submitted in partial satisfaction

of the requirements for the degree

Doctor of Philosophy in Physics

by

Allic Vijai Sivaramakrishnan

2017

ABSTRACT OF THE DISSERTATION

Perturbative Structure in Entanglement, Gauge Theory, and Holography

by

Allic Vijai Sivaramakrishnan
Doctor of Philosophy in Physics
University of California, Los Angeles, 2017
Professor Per J. Kraus, Chair

We explore aspects of perturbative quantum field theory towards the goal of illuminating features of quantum gravity. In Chapter 1, we begin with the color-kinematic duality, a surprising relationship between gauge theoretic and kinematic properties of scattering amplitudes that, via the double-copy property, leads to a deep connection between gauge theory and gravity. We investigate the relationship between the color-kinematic duality and amplitude relations in ABJM theory and find that the duality is satisfied eight points without associated amplitude relations present in all other known instances of the duality.

In Chapter 2, we derive a basic consistency check for AdS_3/CFT_2, a tractable example of the well-known AdS/CFT duality. We show that, under certain mild assumptions on the light spectrum of the CFT, CFT correlators of light operators match those computed in AdS perturbatively in $1/N$: in a black hole background for high temperatures, and in thermal AdS for low temperatures.

Next we turn to entanglement entropy, an information-theoretic quantity that in the CFT may encode dual AdS geometry. Time-dependent entanglement entropy has been studied for generic excited states. However, localized unitary operators in particular are in correspondence with Hamiltonian perturbations, and are basic building blocks of local excitations. In Chapter 3, we detail these operators' locality properties as well as the differences between

excited states created by Hermitian operators and those created with localized unitary operators.

In Chapter 4, we initiate the perturbative exploration of entanglement entropy with a time-dependent Hamiltonian, computing past first order in perturbation theory. We find a universal structure of entanglement propagation: interactions entangle unentangled excitations according to entanglement diagrams that track the flow of entanglement. We provide diagrammatic tools to simplify computations of loop entanglement diagrams.

The dissertation of Allic Vijai Sivaramakrishnan is approved.

Michael Gutperle

Terence Chi-Shen Tao

Per J. Kraus, Committee Chair

University of California, Los Angeles

2017

To my mother, for refusing to be anything less than herself.

Contents

List of Figures

Acknowledgements

It is a pleasure to thank Per Kraus, my advisor, for his mentorship and collaboration. Learning from Per has been a privilege, and his unique approach to physics has sharpened my own abilities immensely. I also would like to thank Zvi Bern for his mentorship during my early work on scattering amplitudes. I would like to thank Michael Gutperle and Eric D'Hoker: along with Per Kraus and Zvi Bern, their encouragement, education, and many years of enjoyable and insightful interaction about physics or otherwise never failed to enrich my hours at UCLA. I would also like to thank Terence Tao for timely, effective advice.

I would like to thank my fellow graduate students in the group with whom I have spent much time, both in and out of physics, especially Scott Davies, Joshua Samani, Sean Litsey, JJ Stankowicz, Yi Li, Andrea Trivella, Mert Besken, Ashwin Hegde, and Michael Enciso. In addition, I would especially like to thank Julio Martinez for taking over Socal Grad Strings, as well as the time overlapped in the office late at night and on weekends. I thank River Snively for his intuition, skepticism, suspension of disbelief, and conversation both in our collaborations and otherwise. I would like to thank Eliot Hijano for years of stimulating, stimulated conversation: over, under, and somewhere in between. Outside of particle physics, I would like to thank Jeffrey Rosen, Daniel Montana, Marvin Thielk, Michael Liu, Yuliy Tsank, William Scott, Hernan Rosas, Tom Neiser, and Nathan Serafin for the unapologetic losses of productivity their acquaintance has incurred. I thank Chris Kampmeyer and Stanislav Culaclii for a musical interlude, and Josephine Barajas for a timely reminder.

Without these people, both this thesis and I would be less full. I also wish to thank quantum field theory in its many forms for providing lifetimes of deeply satisfying adventure. Finally, I thank my parents for everything.

Contribution of authors

Chapters 1, 3, and 4 are based on [1–3]. Chapter 2 is based on [4] in collaboration with Per Kraus and River Snively.

Vita

2011	B.A. (Physics), University of California, Berkeley
2011 – 2017	Teaching Assistant, Department of Physics and Astronomy, UCLA

Publications

"Color-Kinematic Duality in ABJM Theory Without Amplitude Relations,"
Sivaramakrishnan,A., Int.J.Mod.Phys. A32 (2017) no.02n03, 1750002
DOI: 10.1142/S0217751X17500026, arXiv:1402.1821 [hep-th]

"Localized Excitations from Localized Unitary Operators,"
Sivaramakrishnan,A., Annals Phys. 381 (2017) 41-67
DOI: 10.1016/j.aop.2017.03.012, arXiv:1604.00965 [hep-th]

"Black holes from CFT: Universality of correlators at large c,"
Kraus, P., Sivaramakrishnan,A., Snively, R., JHEP 1708 (2017) 084
JHEP 1708 (2017) 084 arXiv:1706.00771 [hep-th]

"Entanglement Entropy with a Time-dependent Hamiltonian,"
Sivaramakrishnan, A., arXiv:1709.09776 [hep-th]

Chapter 1

Color-Kinematic Duality in ABJM Theory Without Amplitude Relations

We explicitly show that the Bern-Carrasco-Johansson color-kinematic duality holds at tree level through at least eight points in Aharony-Bergman-Jafferis-Maldacena theory with gauge group SU(N) x SU(N). At six points we give the explicit form of numerators in terms of amplitudes, displaying the generalized gauge freedom that leads to amplitude relations. However, at eight points no amplitude relations follow from the duality, so the diagram numerators are fixed unique functions of partial amplitudes. We provide the explicit amplitude-numerator decomposition and the numerator relations for eight-point amplitudes.

1.1 Introduction

Studies of scattering amplitudes have uncovered important insights into gauge and gravity theories. In particular, Bern, Carrasco, and Johansson (BCJ) found a surprising duality between the color factors and kinematic numerator factors that comprise diagrams in Yang-Mills theory [5]. The color-kinematic duality implies nontrivial amplitude relations. These amplitude relations have been studied in both field theory and string theory [6–8]. The color-kinematic duality appears to extend to loop level, as confirmed in a variety of examples with

varying levels of supersymmetry [9–13]. While there has been some progress in understanding the origin of the duality from a Lagrangian vantage point [14–16], further work is needed.

The color-kinematic duality reveals new structures in gravity through a surprisingly simple gauge-gravity correspondence. Kinematic numerators satisfying the color-kinematic duality provide the link: by replacing color factors with numerators that satisfy the duality, gauge-theory amplitudes are converted into gravity amplitudes [5, 9], revealing a double-copy structure of gravity. A connection between gravity and Yang-Mills theory has long been known at tree level from the Kawai-Lewellen-Tye relations [17], but the double-copy property of gravity reveals a more extensive correspondence, one that appears to extend to loop level. This property has advanced the study of supergravity's properties, especially in uncovering unexpected ultraviolet cancellations at high loop orders [18–21]. More generally, the double-copy relation allows us to directly study the effects of any newly uncovered properties of gauge-theory amplitudes on corresponding gravity amplitudes.

In Yang-Mills theory, BCJ amplitude relations come from a residual generalized gauge freedom present in kinematic numerators even after imposing that the duality between color and kinematics is manifest [5,8,22–24]. There have also been string-theory studies to investigate the residual gauge invariance in the duality between color and kinematics in Yang-Mills theory [6, 7]. While there has been progress in understanding the underlying structure behind the duality and the residual gauge invariance [15, 25], further clarification is needed. To gain additional insight, it is important to study a wide variety of cases where the duality holds.

In particular, the color-kinematic duality has been found in three-dimensional Chern-Simons-matter theories: the $\mathcal{N} = 8$ Bagger-Lambert-Gustavsson (BLG) theory and the $\mathcal{N} = 6$ Aharony-Bergman-Jafferis-Maldacena (ABJM) theory [26, 27]. BLG theory turns out to be a special case of ABJM theory. These cases are quite interesting because a Lie three-algebra, not a Lie two-algebra, defines the gauge structure of these theories. These Chern-Simons-matter theories would appear to have rather different properties than gauge

theory. The color-kinematic duality is governed by gauge-group relations, so the presence of the duality in ABJM-type theories shows that the duality is more general than previously appreciated.

We address the color-kinematic duality in ABJM theory. The first nontrivial example of the duality in this theory was first given in ref. [26]: the six-point all-scalar amplitude. While this manuscript was in preparation, ref. [28] noted briefly that the duality holds up to ten points, but surprisingly found no BCJ amplitude relations at eight points or higher. Details and explicit expressions for the eight-point computation were not provided.

In this note, we provide details and explicit expressions of the eight-point computation, and we independently confirm the surprising result that the color-kinematic duality holds at eight points without BCJ amplitude relations. Demonstrating that there are no BCJ amplitude relations is non-trivial, and has significant implications for the color-kinematic duality. In all previously known gauge-theory examples, enforcing the color-kinematic duality has produced BCJ amplitude relations, and the two are therefore often considered synonymous. Our result confirms that, on the contrary, the two can be independent properties of scattering amplitudes. The eight-point process is the simplest example in which the color-kinematic duality holds without the residual freedom that produces BCJ amplitude relations, warranting a detailed study. To this end, we provide the explicit numerator decomposition of the eight-point amplitudes as well as the BCJ numerator relations.

Another curious feature that may be connected is that at lower points, the double-copy property holds [26, 27], but starting at eight points it does not [28]: applying the double-copy procedure to the eight-point kinematic numerators does not produce the appropriate gravity numerators. The eight-point ABJM amplitude is the only known instance in which the color-kinematic duality holds but the double-copy property fails. Examining the eight-point amplitudes in some detail may therefore further illuminate the connection between the color-kinematic duality and the double-copy property.

In this note, we start by presenting relatively explicit forms of the six point numerators

in ABJM theory that satisfy the duality between color and kinematics. This has not been given previously and is the first nontrivial case where the duality holds. (At four points the duality is trivial and for odd points the amplitudes vanish.) We then confirm that the duality between color and kinematics holds at eight points for bosonic external states, but does not generate BCJ amplitude relations. In an ancillary online file [29], we present a set of independent eight-point amplitudes in terms of numerators, and the numerator relations implied by the color-kinematic duality.

This note is organized as follows. In Sec. 2, we review the necessary background. Sec. 2.1 describes the color-kinematic duality in Yang-Mills theory. Then, in Sec. 2.2 we explain the construction of partial amplitudes and how the color-kinematic duality leaves behind a residual freedom that gives rise to BCJ amplitude relations. Sec. 2.3 presents relevant properties of the three-algebra formulation of ABJM theory. Sec. 3 contains our results: demonstration of the color-kinematic duality through eight points. In Sec. 3.1, we show the trivial case: four points. We demonstrate the first non-trivial case – six points – and present numerator solutions in terms of amplitudes in Sec. 3.2. In Sec. 3.3 we detail the eight-point case. We explain how to construct the eight-point partial amplitudes from numerators, and confirm that the color-kinematic duality is satisfied but does not imply BCJ amplitude relations. In Sec. 4 we discuss the implications of the eight-point result and future directions.

1.2 Review

1.2.1 The color-kinematic duality in Yang-Mills theory

In Yang-Mills theory, tree amplitudes can in general be written as

$$\mathcal{A}(1,2,\ldots,n) = \sum_i \frac{c_i n_i}{\prod_{\alpha_i} s_{\alpha_i}}, \tag{1.2.1}$$

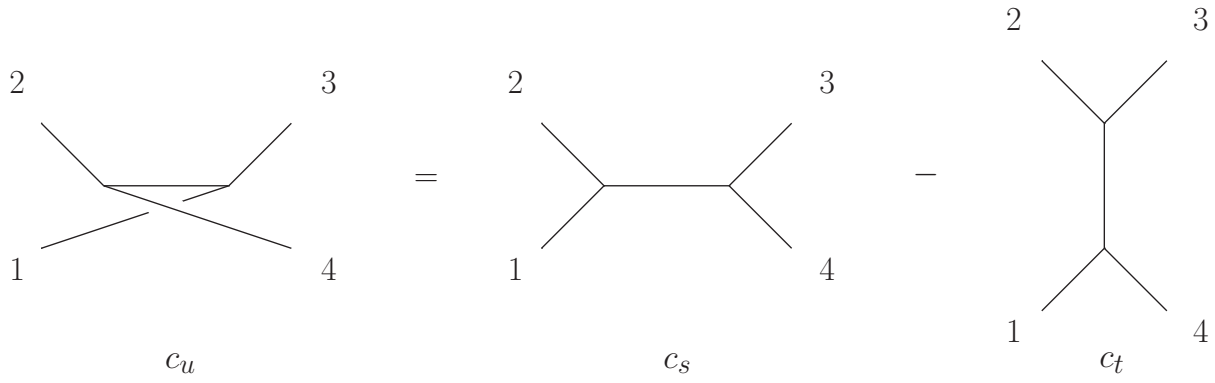

Figure 1.1: Diagrammatic representation of the Jacobi relation.

where the sum runs over diagrams with only cubic vertices. In general, any terms not of this form can be put into this form by multiplying and dividing by appropriate propagators. Here, c_i are products of structure constants and we suppress the coupling constant and helicity labels. The n_i are kinematic numerators: functions of momenta and polarization vectors. Each color factor c_i is in one-to-one correspondence with a diagram with a specific propagator structure. The s_{α_i} in the denominator are the Feynman propagators for the i-th diagram, where s_{α_i} are the kinematic invariants of the scattering process.

The c_i are not an independent set and are related by Jacobi identities, as shown in fig. 1.1. BCJ proposed the color-kinematics duality, wherein the numerators n_i obey the same relations and symmetries under relabelling [5]. For instance,

$$c_1 = c_2 + c_3 \Rightarrow n_1 = n_2 + n_3. \tag{1.2.2}$$

$$c_1 \to -c_1 \Rightarrow n_1 \to -n_1. \tag{1.2.3}$$

BCJ also noted that replacing c_i with n_i that satisfy the duality in (1.2.1) gives the scattering amplitude $\mathcal{M}(1, 2, \ldots, n)$ in gravity. This connection between gravity and gauge theory is known as the double-copy property of gravity. At tree level, these properties have been proven in various ways [8, 14, 30]. The color-kinematic duality is a basic property of gauge and gravity theories that deserves further study, especially to understand the underlying

symmetry.

1.2.2 Amplitude relations from the color-kinematic duality in Yang-Mills theory

The simplicity of the color-kinematic duality and double-copy property suggests a novel principle in gauge theories and gravity. Here, we review how amplitude relations follow from the color-kinematic duality in Yang-Mills theory. We also note that such amplitude relations arise from string theory [7, 25]. The color-kinematic duality has also been directly studied in string theory [6].

In Yang-Mills theory, we can write the color-decomposition in (1.2.1) in terms of color-ordered amplitudes and traces over gauge-group generators. At tree level, this trace decomposition is [31]

$$\mathcal{A}(1,2,\ldots,n) = \sum_{\sigma \in S_n/Z_n} \mathrm{Tr}(T^{\sigma_1} T^{\sigma_2} \ldots T^{\sigma_n}) A(\sigma_1, \sigma_2, \ldots \sigma_n), \tag{1.2.4}$$

where S_n/Z_n is all leg orderings unrelated by cyclic permutation. The color-ordered amplitudes are in terms of numerators divided by propagators, as in (1.2.1). These amplitudes obey symmetry properties. They are invariant under cyclic permutations of indices. They have symmetry under reversal: $A(1,2,\ldots,n) = (-1)^n A(n,\ldots,2,1)$. These amplitudes obey the photon-decoupling identity:

$$\sum_{\sigma \in cyclic} A(1, \sigma(2,3,\ldots,n)) = 0, \tag{1.2.5}$$

and more generally the Kleiss-Kuijf (KK) relations [32].

$$A(1, \{\alpha\}, n, \{\beta\}) = (-1)^{n_\beta} \sum_{\{\sigma\}_i \in OP(\{\alpha\}, \{\beta^T\})} A(1, \{\sigma\}_i, n). \tag{1.2.6}$$

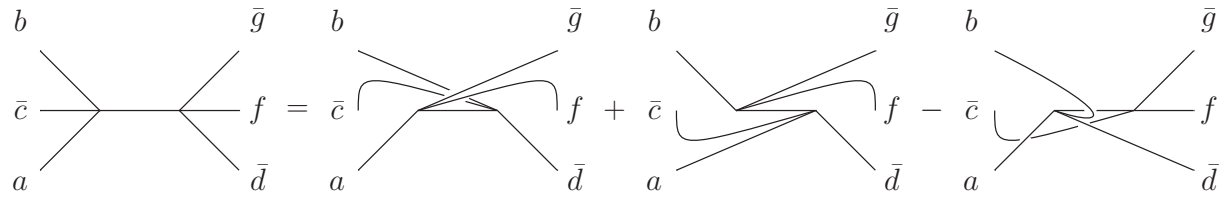

Figure 1.2: Diagrammatic representation of the generalized Jacobi relation.

Here, $OP(\{\alpha\}, \{\beta^T\})$ is the set of permutations which preserve the order of each set. The set $\{\beta^T\}$ is $\{\beta\}$ but with reversed ordering. Using these identities, we can choose a set of $(n-2)!$ color-ordered amplitudes as a KK-independent basis.

In eq. (1.2.1) the tree amplitudes are written in terms of numerators. The duality between color and kinematics immediately implies that we can write the amplitude in terms of the same number of numerators as independent color factors. In principle, the $(n-2)!$ amplitudes and $(n-2)!$ numerators in this basis could uniquely specify each other. However, it turns out that the numerators are not unique – they can be shifted by kinematic functions in such a way that the basis amplitudes remain unchanged. See refs. [5, 6, 14] for details. This freedom is a residual generalized gauge freedom, or "residual freedom". In other words, the $(n-2)!$ equations for the basis amplitudes in terms of basis numerators are non-invertible. Only $(n-3)!$ of the $(n-2)!$ numerators are independent, resulting in $(n-2)! - (n-3)!$ amplitude relations, known as BCJ amplitude relations.

1.2.3 The three-algebra formulation of ABJM theory

We will consider ABJM theory, a theory of M2 branes [33]. This theory admits a natural Lie three-algebra formulation analogous to the Lie two-algebra defining the gauge symmetry of Yang-Mills theory. ABJM theory is a Chern-Simons-matter gauge theory with gauge-group $SU(N) \times SU(N)$. Matter fields are bi-fundamental, and map between the two gauge groups: they are written in terms of group elements $(T^a)^{b\bar{c}} : V_1 \to V_2$ where V_1 and V_2 are the vector spaces of group elements from the first and second $SU(N)$ groups. Indices are barred to

distinguish between the two vector spaces. The index a is an adjoint index, while indices $b, \bar{c}$ are fundamental and anti-fundamental. We do not use different notation for adjoint and (anti-)fundamental indices as we often show only the adjoint indices. The reader should keep in mind that multiplication of group elements involves contracting fundamental and anti-fundamental indices. The group elements T^a are related by a triple product:

$$[T^a, T^b; \bar{T}^{\bar{c}}] = f^{ab\bar{c}}{}_d T^d, \qquad [T^a, T^b; \bar{T}^{\bar{c}}] = T^a \bar{T}^{\bar{c}} T^b - T^b \bar{T}^{\bar{c}} T^a. \tag{1.2.7}$$

Indices are raised and lowered with the metric $\mathrm{Tr}(T^a \bar{T}^{\bar{b}}) = h^{a\bar{b}}$. The unbarred and barred indices are antisymmetric amongst each other separately, but not together: they are adjoint indices in two different gauge groups. For example, $f^{ab\bar{c}\bar{d}} = -f^{ba\bar{c}\bar{d}} = f^{ba\bar{d}\bar{c}}$. One can write $f^{ac\bar{b}\bar{d}}$ or $f^{a\bar{b}c\bar{d}}$ as they are the same. The structure constants obey a generalized four-term Jacobi relation illustrated in fig. 1.2:

$$f^{ab\bar{c}}{}_e f^{ef\bar{g}}{}_d = f^{af\bar{g}}{}_e f^{eb\bar{c}}{}_d + f^{bf\bar{g}}{}_e f^{ae\bar{c}}{}_d - f_{\bar{e}}{}^{f\bar{g}\bar{c}} f^{ab\bar{e}}{}_d. \tag{1.2.8}$$

ABJM amplitudes are only nonzero for even numbers of external particles due to the theory's bi-fundamental nature.

The color-ordering and numerator decomposition of ABJM amplitudes proceed along the same lines as in Yang-Mills theory. The ABJM numerator decomposition takes the same form (1.2.1), but the color factors are now products of the four-index structure constants and the sum runs over diagrams with only quartic vertices. Unlike in Yang-Mills theory, generic numerators in the three-algebra formulation of ABJM theory are non-local. The structure constant has four indices, but the matter is coupled to the gauge field by a cubic interaction. The propagators in the color-kinematic decomposition of ABJM amplitudes (1.2.1) specify a graph with four-point interactions, and so some of the propagators that specify three-point interactions must be absorbed into the numerator. The color factors in the numerator decomposition can be expanded into the trace over strings of generators,

schematically $\mathrm{Tr}(T^a \bar{T}^{\bar{b}} \ldots)$, by using the following identities:

$$f^{ab\bar{c}\bar{d}} = \mathrm{Tr}([T^a \bar{T}^{\bar{c}} T^b - T^b \bar{T}^{\bar{c}} T^a] \bar{T}^{\bar{d}}), \tag{1.2.9}$$

$$(T^a)^i{}_{\bar{j}} \, (\bar{T}^{\bar{b}})^{\bar{m}}{}_n \, h_{a\bar{b}} = \delta^{\bar{m}}_{\bar{j}} \, \delta^i_n. \tag{1.2.10}$$

The numerator decomposition can therefore be converted into a sum over color-ordered amplitudes, just as in Yang-Mills theory. Color-ordered $2m$-point amplitudes are defined by

$$\begin{aligned} \mathcal{A}(\bar{1}, 2, \bar{3}, \ldots, \overline{2m-1}, 2m) = \sum_{\sigma \in S'_{2m}/Z_{2m}} & \mathrm{Tr}(\bar{T}^{\bar{\sigma}_1} T^{\sigma_2} \bar{T}^{\bar{\sigma}_3} \ldots \bar{T}^{\bar{\sigma}_{2m-1}} T^{\sigma_{2m}}) \\ & \times A(\bar{\sigma}_1, \sigma_2, \bar{\sigma}_3, \ldots, \bar{\sigma}_{2m-1} \sigma_{2m}). \end{aligned} \tag{1.2.11}$$

The set S'_{2m}/Z_{2m} is all orderings that have alternating barred and unbarred legs and are unrelated by cyclic permutation. The color-ordered amplitudes can be written in terms of numerators. One color factor is the sum of different trace-strings with different signs, and these signs determine the relative signs of the numerators in the color-ordered amplitudes. For example, consider a color factor $c_i \equiv f^{13\bar{2}\bar{4}} = \mathrm{Tr}([T^1 \bar{T}^{\bar{2}} T^3 - T^3 \bar{T}^{\bar{2}} T^1] \bar{T}^{\bar{4}})$. The associated numerator n_i will enter $A(1\bar{2}3\bar{4})$ and $A(3\bar{2}1\bar{4})$, but with opposite signs. The color-ordered ABJM amplitudes have symmetries similar to those of Yang-Mills amplitudes upon inversion and cyclic permutation. For amplitudes with external bosonic states

$$A_{2m}(\bar{1}, 2, \bar{3}, \ldots, \overline{2m-1}, 2m) = A_{2m}(\bar{3}, 4, \ldots, \overline{2m-1}, 2m, \bar{1}, 2), \tag{1.2.12}$$

$$A_{2m}(\bar{1}, 2, \bar{3}, \ldots, \overline{2m-1}, 2m) = (-1)^{2m-1} A(\bar{1}, 2m, \overline{2m-1}, \ldots, \bar{3}, 2). \tag{1.2.13}$$

The amplitudes obey KK-type identities, though these identities are not entirely understood beyond six points [28]. Such identities are linear relations between amplitudes with integer coefficients, just as in Yang-Mills theory. In the following, we sometimes denote barred and unbarred indices by even and odd particle labels. We do not need to keep track of ordering

between the two types of indices. For a more detailed review of ABJM theory's three-algebra formulation, see refs. [28, 34].

1.3 The color-kinematic duality in ABJM theory

Evidence for the color-kinematic duality in ABJM theory was recently found in tree-level scattering amplitudes [26]. Testing the duality in ABJM theory proceeds just as in Yang-Mills theory: requiring the numerators satisfy the duality between kinematics and color generates BCJ amplitude identities, which can be verified by using the explicit amplitudes. Details of how to calculate the explicit amplitudes, as well as some lower-point examples, are described in ref. [35].

We describe the color-kinematic duality at four, six, and eight points. The color-kinematic duality is trivially satisfied at four points. At six and eight points, we consider amplitudes with bosonic external states. The six-point case is the first non-trivial instance of the duality [28]. Next, we explicitly demonstrate the duality for six points as a warmup to our work at eight points. Duality-satisfying six-point numerators in terms of amplitudes are provided, as these do not appear elsewhere in the literature. At eight points, we show how to construct the amplitudes in terms of numerators. Numerical analysis shows that the numerators satisfy the color-kinematic duality but do not have any residual freedom – they are uniquely specified by amplitudes. We give explicit expressions for the generalized Jacobi identities the numerators satisfy and the eight-point amplitudes in terms of numerators in the attached files online [29]. All our analysis is for three dimensional on-shell momenta, consistent with the space-time dimension of the theory. As ref. [27] found, implications of the color-kinematic duality change when these conditions are relaxed: when momenta are off-shell or taken in more than three dimensions, the freedom that produces the BCJ amplitude relation at six points is no longer present.

1.3.1 Four points

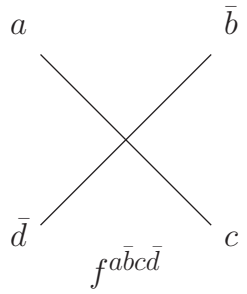

Figure 1.3: The four-point diagram with its associated color factor. This diagram is the elementary vertex of ABJM theory in the three-algebra formulation.

In the three-algebra formulation of ABJM theory, the vertex associated with $f^{a\bar{b}c\bar{d}}$ comes from a four-point diagram, illustrated in fig. 1.3, with a non-local numerator. At four points, there is only one independent color-ordered amplitude after accounting for amplitude symmetries. When assembling the indices on a structure constant, one must choose a convention: whether to begin with an unbarred or barred index, and whether to move clockwise or counter-clockwise. We chose to begin from an unbarred index and move clockwise in the diagram. We also use the convention that all momenta are incoming. With these conventions the four-point superamplitude is [35]

$$A(1,\bar{2},3,\bar{4}) = \frac{\delta^{(3)}(P)\delta^{(6)}(Q)}{\langle 14\rangle\langle 34\rangle} f^{a_1\bar{a}_2a_3\bar{a}_4}. \tag{1.3.1}$$

The delta functions conserve momentum $P^{\alpha\beta} = \sum_i p_i^{\alpha\beta}$ and supermomentum $Q^{\alpha I} = \sum_i q_i^{\alpha I}$. As we have $\mathcal{N} = 6$ real supercharges, these can be grouped into 3 complex Grassmann-valued spinors. We have $q_i^{\alpha I} = \lambda_i^\alpha \eta^I$ for the i-th particle. The label I is the index for the $SO(6)$ R-symmetry, and α labels the supercharge number, running from one to three [34, 35]. The amplitude is written using spinor-helicity formalism (see e.g. [31]).

1.3.2 Six points

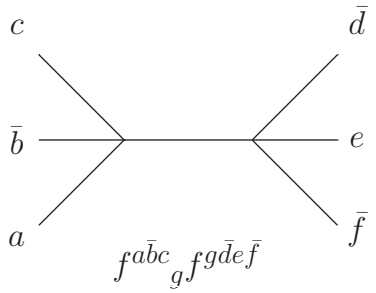

Figure 1.4: The six-point diagram with its associated color factor. This diagram does not have left-right reflection symmetry.

At six points, the color-kinematic duality holds [26, 27]. We present explicit formulas showing how it holds. The six-point color factors are products of two structure constants, and obey the generalized Jacobi identity (1.2.8). The full amplitude has nine independent channels:

$$\mathcal{A}(1,2,3,4,5,6) = \frac{c_1 n_1}{s_{123}} + \frac{c_2 n_2}{s_{156}} + \frac{c_3 n_3}{s_{126}} + \frac{c_4 n_4}{s_{134}} + \frac{c_5 n_5}{s_{125}} + \frac{c_6 n_6}{s_{124}} + \frac{c_7 n_7}{s_{136}} + \frac{c_8 n_8}{s_{145}} + \frac{c_9 n_9}{s_{146}}. \quad (1.3.2)$$

The kinematic invariants are $s_{ijk} = (p_i + p_j + p_k)^2$. The pole structure specifies the diagram, and so fixes the color factor up to an overall sign:

$$\begin{aligned} c_1 &= f^{123}{}_a f^{a456}, \qquad c_2 = f^{561}{}_a f^{a234}, \qquad c_3 = f^{345}{}_a f^{a612}, \\ c_4 &= f^{134}{}_a f^{a562}, \qquad c_5 = f^{521}{}_a f^{a436}, \qquad c_6 = f^{365}{}_a f^{a124}, \\ c_7 &= f^{163}{}_a f^{a254}, \qquad c_8 = f^{541}{}_a f^{a632}, \qquad c_9 = f^{325}{}_a f^{a416}. \end{aligned} \quad (1.3.3)$$

There are five amplitudes independent under the KK-type relations. We choose the following

amplitudes as our basis amplitudes:

$$A(1,2,3,4,5,6) = \frac{n_1}{s_{123}} + \frac{n_2}{s_{156}} + \frac{n_3}{s_{126}}, \qquad A(1,4,3,6,5,2) = \frac{n_4}{s_{134}} + \frac{n_5}{s_{125}} + \frac{n_6}{s_{124}},$$
$$A(1,6,3,2,5,4) = \frac{n_7}{s_{136}} + \frac{n_8}{s_{145}} + \frac{n_9}{s_{146}}, \qquad A(1,4,3,2,5,6) = -\frac{n_4}{s_{134}} - \frac{n_2}{s_{156}} - \frac{n_9}{s_{146}},$$

$$A(1,6,3,4,5,2) = -\frac{n_7}{s_{136}} - \frac{n_5}{s_{125}} - \frac{n_3}{s_{126}}. \tag{1.3.4}$$

The relative sign of each numerator is conveniently determined by switching to the trace expansion of its color factor. Next, we require that the numerators satisfy the duality between color and kinematics. Each numerator must obey the same identities as its sibling color factor:

$$n_5 = -n_2 + n_3 + n_4, \qquad n_6 = n_1 - n_2 + n_4,$$
$$n_8 = n_1 - n_3 + n_7, \qquad n_9 = n_2 - n_3 + n_7.$$

We can choose $\{n_1, n_2, n_3, n_4, n_7\}$ as a basis independent under the color-kinematic duality. There are now five independent numerators, the same number as the KK-independent amplitudes. Our set of KK-independent amplitudes are now

$$\begin{aligned}
A(1,2,3,4,5,6) \equiv A_1 &= \frac{n_1}{s_{123}} + \frac{n_2}{s_{156}} + \frac{n_3}{s_{126}} \\
A(1,4,3,6,5,2) \equiv A_2 &= \frac{n_4}{s_{134}} + \frac{-n_2 + n_3 + n_4}{s_{125}} + \frac{n_1 - n_2 + n_4}{s_{124}} \\
A(1,6,3,2,5,4) \equiv A_3 &= \frac{n_7}{s_{136}} + \frac{n_1 - n_3 + n_7}{s_{145}} + \frac{n_2 - n_3 + n_7}{s_{146}} \\
A(1,4,3,2,5,6) \equiv A_4 &= -\frac{n_4}{s_{134}} - \frac{n_2}{s_{156}} - \frac{n_2 - n_3 + n_7}{s_{146}} \\
A(1,6,3,4,5,2) \equiv A_5 &= -\frac{n_7}{s_{136}} - \frac{-n_2 + n_3 + n_4}{s_{125}} - \frac{n_3}{s_{126}}.
\end{aligned} \tag{1.3.5}$$

We can solve for the numerators one by one and find that one numerator drops out of our equations. To be concrete, we begin by solving for n_1: choosing one of the amplitude-

numerator equations above and solving for n_1 in terms of an amplitude and the remaining numerators, we substitute this expression for n_1 into the remaining amplitude equations. The equations now relate the five amplitudes to four numerators. We solve for n_2 and n_3 in the same way, leaving two equations that relate the five amplitudes to n_4 and n_7. When solving for n_4 in one equation and substituting the result into the remaining equation, we find that n_7 drops out. What remains is an equation relating the five amplitudes – this is the BCJ amplitude relation. One of the five numerators is arbitrary. In other words, the coefficient matrix of the numerators in the amplitude equations has rank four, while there are five numerators. This is similar to the situation in Yang-Mills theory [5].

We may therefore choose one numerator to have an arbitrary value. As the remaining numerators depend on this numerator, the remaining numerators depend on our choice. A convenient choice is to simply set n_7 to zero and solve for the remaining numerators in terms of amplitudes. Imposing three-dimensional momentum conservation produces a lengthy expression, so we display the solution using the original kinematic invariants:

$$\begin{aligned} n_1 &= s_{123}\left(A_1 + \frac{A}{s_{234}} + \frac{E}{D}\left(\frac{1}{s_{345}} - \frac{B}{C}\frac{1}{s_{234}}\right)\right), & n_2 &= -A + \frac{BE}{CD}, \\ n_4 &= s_{134}\left(-A_4 + \left(A - \frac{BE}{CD}\right)\left(\frac{1}{s_{234}} + \frac{1}{s_{235}}\right) - \frac{E}{D}\frac{1}{s_{235}}\right), & n_3 &= -\frac{E}{D}. \end{aligned} \tag{1.3.6}$$

The quantities A, B, C, D, E have been defined for convenience and are

$$
\begin{aligned}
A =& \frac{-\frac{A_3}{s_{123}} + \frac{A_1}{s_{236}}}{\frac{1}{s_{123}s_{235}} - \frac{1}{s_{234}s_{236}}} \\
B =& -\frac{\frac{1}{s_{235}} + \frac{1}{s_{236}}}{s_{123}} - \frac{1}{s_{236}s_{345}} \\
C =& \frac{1}{s_{123}s_{235}} - \frac{1}{s_{234}s_{236}} \\
D =& -B\left(-\frac{-\left(\frac{1}{s_{234}}+\frac{1}{s_{235}}\right)\left(-\frac{1}{s_{134}}-\frac{1}{s_{346}}-\frac{1}{s_{356}}\right)+\frac{\frac{1}{s_{346}}+\frac{1}{s_{356}}}{s_{134}}}{s_{123}} - \frac{1}{s_{134}s_{234}s_{356}}\right) \\
&+ C\left(-\frac{-\frac{1}{s_{134}s_{346}} + \frac{-\frac{1}{s_{134}}-\frac{1}{s_{346}}-\frac{1}{s_{356}}}{s_{235}}}{s_{123}} - \frac{1}{s_{134}s_{345}s_{356}}\right) \\
E =& C\left(-\frac{\frac{A_2}{s_{134}} - A_4\left(-\frac{1}{s_{134}}-\frac{1}{s_{346}}-\frac{1}{s_{356}}\right)}{s_{123}} + \frac{A_1}{s_{134}s_{356}}\right. \\
&\left. + A\left(\frac{-\left(\frac{1}{s_{234}}+\frac{1}{s_{235}}\right)\left(-\frac{1}{s_{134}}-\frac{1}{s_{346}}-\frac{1}{s_{356}}\right)+\frac{\frac{1}{s_{346}}+\frac{1}{s_{356}}}{s_{134}}}{s_{123}} + \frac{1}{s_{134}s_{234}s_{356}}\right)\right).
\end{aligned}
\tag{1.3.7}
$$

We now substitute the solutions for n_1, n_2, n_3, n_4 into the expression for A_5 in (1.3.5). Since n_7 drops out, it leaves behind a single nontrivial BCJ amplitude relation between the five partial amplitudes. We have confirmed that this relation holds numerically in the actual amplitudes by plugging in explicit values for the amplitudes, which were obtained in ref. [35]. The six-point case is discussed further in ref. [28], which gives the BCJ amplitude relation and checks it for the superamplitude. While in Yang-Mills theory the freedom to adjust numerators may be used to keep the color-kinematic numerators local, in the three-algebra formulation of ABJM theory numerators are inherently non-local. The freedom to adjust n_7 cannot be used to make the remaining numerators local functions.

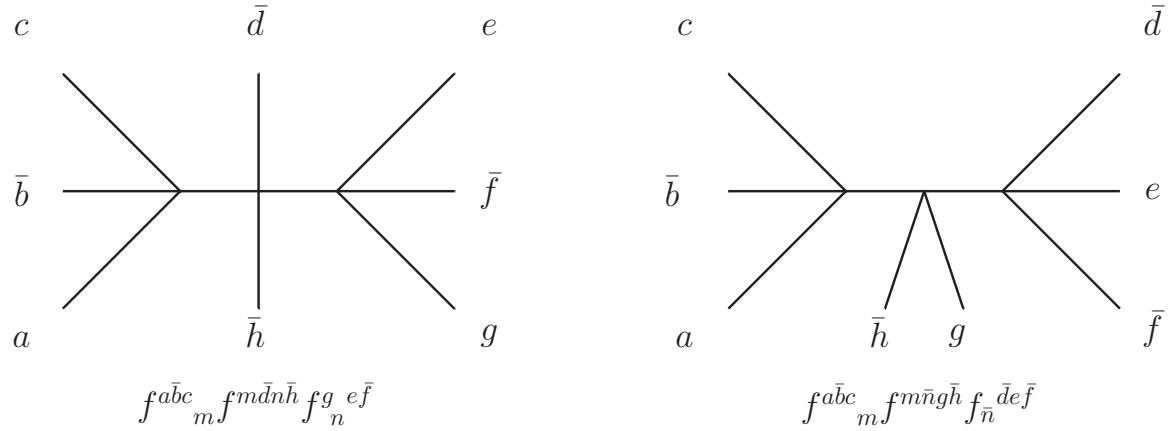

Figure 1.5: The two diagrams that contribute numerators to the ABJM color-stripped amplitude. The left diagram has a color factor of the form $f^{a\bar{b}c}{}_m f^{m\bar{d}n\bar{h}} f^{g}{}_{n}{}^{e\bar{f}}$. The external indices in the middle are both barred or, for a different leg ordering than shown above, both unbarred. The right diagram has a color factor of the form $f^{a\bar{b}c}{}_m f^{m\bar{n}g\bar{h}} f_{\bar{n}}{}^{\bar{d}e\bar{f}}$. One middle index is barred while the other is not.

1.3.3 Eight points

The eight-point case proceeds in the same fashion as the six-point case. The two distinct diagrams that contribute are shown in fig. 1.5. For clarity, we provide one color-stripped amplitude from which all others are obtained by relabelling. In this amplitude, we label each numerator by the color factor it is associated with, suppressing the summed indices on the structure constants. For example, we denote the numerator associated with the color factor $f^{1\bar{2}3}{}_a f^{a\bar{4}\bar{8}b} f^{57}{}_b{}^{\bar{6}}$ as $n_{123,48,576}$. In assigning the color-factors, we use the convention that the summed indices of the color factors are as close together as possible, and the right-most structure constant has an index which is higher than the left-most structure constant's indices. We suppress the bars and take odd and even labels to correspond to the barred and

unbarred indices separately. The color-stripped amplitude then is

$$\begin{aligned} A(1,2,3,4,5,6,7,8) = &- \frac{n_{132,48,576}}{s_{123}s_{567}} - \frac{n_{354,62,718}}{s_{345}s_{781}} + \frac{n_{324,51,768}}{s_{234}s_{678}} + \frac{n_{546,73,182}}{s_{456}s_{812}} \\ &- \frac{n_{132,78,546}}{s_{123}s_{456}} - \frac{n_{354,12,768}}{s_{345}s_{678}} - \frac{n_{576,34,182}}{s_{567}s_{812}} - \frac{n_{718,56,324}}{s_{781}s_{234}} \\ &+ \frac{n_{576,18,324}}{s_{567}s_{234}} + \frac{n_{718,32,546}}{s_{781}s_{456}} + \frac{n_{132,54,768}}{s_{123}s_{678}} + \frac{n_{354,76,182}}{s_{345}s_{812}}. \end{aligned} \tag{1.3.8}$$

All other color-stripped eight-point amplitudes can be obtained from this expression by relabelling. The signs of each numerator depends on the trace string's contribution to each color factor, similar to the Yang-Mills case [5]. The eight-point amplitude has 216 different color factors, and therefore 216 corresponding numerators. We have checked that our numerator representation of the color-stripped amplitudes obey the correct cyclic permutation properties and KK-type identities as listed in ref. [28]. We repeat these symmetries below, using the bar-unbar notation for clarity. The symmetries are

$$\text{Cyclic shift by } 2m\text{:} \quad A(1\bar{2}3\bar{4}5\bar{6}7\bar{8}) = A(7\bar{8}1\bar{2}3\bar{4}5\bar{6}), \tag{1.3.9}$$

$$\text{Reversal:} \quad A(1\bar{2}3\bar{4}5\bar{6}7\bar{8}) = -A(1\bar{8}7\bar{6}5\bar{4}3\bar{2}), \tag{1.3.10}$$

where m is an arbitrary integer. An example of an eight-point KK-type identity satisfied by our amplitudes is

$$\begin{aligned} &- A(12345876) - A(14325876) + A(16385274) + A(16385472) \\ &+ A(16783254) + A(12763854) + A(14763852) + A(16783452) \\ &+ A(16723854) + A(16743852) + A(16327854) + A(16347852) \\ &+ A(16387254) + A(16387452) + A(14367852) + A(12367854) = 0. \end{aligned} \tag{1.3.11}$$

There are 57 amplitudes independent under the KK-type identities. We call these the KK amplitudes. The basis was chosen by eliminating all linear dependence between amplitudes

written in terms of numerators. As in Yang-Mills theory, we know the resulting linear amplitude relations are not BCJ amplitude relations, because no generalized Jacobi relations have been used. Eliminating the linear dependence between amplitudes in this step corresponds to exhausting the KK-type amplitude relations. No closed form for the KK-type identities have been found, but the number of basis amplitudes agrees with the result in ref. [28]. We choose a set of KK amplitudes and present a sample below. The full set of equations is contained in an attached file online [29].

$$\begin{aligned}
A(12345876) =& -\frac{n_1}{s_{123}s_{876}} - \frac{n_2}{s_{123}s_{587}} - \frac{n_7}{s_{123}s_{458}} + \frac{n_{28}}{s_{587}s_{612}} - \frac{n_{30}}{s_{458}s_{612}} - \frac{n_{36}}{s_{345}s_{612}} \\
& - \frac{n_{136}}{s_{458}s_{761}} - \frac{n_{139}}{s_{345}s_{761}} + \frac{n_{144}}{s_{234}s_{761}} + \frac{n_{163}}{s_{234}s_{876}} + \frac{n_{164}}{s_{234}s_{587}} + \frac{n_{208}}{s_{345}s_{876}}, \\
A(12365478) =& \frac{n_5}{s_{123}s_{478}} - \frac{n_8}{s_{123}s_{547}} + \frac{n_9}{s_{123}s_{654}} + \frac{n_{48}}{s_{547}s_{812}} - \frac{n_{49}}{s_{654}s_{812}} - \frac{n_{51}}{s_{365}s_{812}} \\
& + \frac{n_{154}}{s_{654}s_{781}} - \frac{n_{155}}{s_{365}s_{781}} + \frac{n_{160}}{s_{236}s_{781}} - \frac{n_{171}}{s_{236}s_{478}} + \frac{n_{173}}{s_{236}s_{547}} - \frac{n_{212}}{s_{365}s_{478}}, \\
A(12365874) =& \frac{n_2}{s_{123}s_{587}} - \frac{n_3}{s_{123}s_{658}} - \frac{n_5}{s_{123}s_{874}} + \frac{n_{11}}{s_{412}s_{587}} - \frac{n_{12}}{s_{412}s_{658}} - \frac{n_{18}}{s_{365}s_{412}} \\
& - \frac{n_{100}}{s_{658}s_{741}} - \frac{n_{103}}{s_{365}s_{741}} + \frac{n_{107}}{s_{236}s_{741}} + \frac{n_{170}}{s_{236}s_{587}} + \frac{n_{171}}{s_{236}s_{874}} + \frac{n_{212}}{s_{365}s_{874}}.
\end{aligned}$$

The four-term generalized Jacobi relations the numerators must satisfy according to the color-kinematic duality are also listed in an attached file online. These relations are solved, and all numerators are specified by the 57 basis numerators. After imposing the Jacobi relations, the 57 amplitude equations are expressed in terms of the 57 basis numerators. Here, the number of KK amplitudes and numerators independent under the generalized Jacobi relations are the same, just as in Yang-Mills theory. However, the surprise here is that these equations turn out to be invertible. Solving the system analytically is difficult, but it is straightforward to check invertibility numerically by using explicit values for the three-dimensional momentum that obey momentum conservation. In other words, the numerators have no residual freedom: each numerator is uniquely specified as a function of gauge-invariant amplitudes. Without residual freedom, the eight-point amplitudes have no BCJ

amplitude relations. The lack of BCJ amplitude relations is a surprising result.

At eight points, the color-kinematic duality is automatically satisfied. Through the numerator decomposition the amplitudes obey the KK-type identities manifestly, and unlike in Yang-Mills theory, there are no BCJ amplitudes relations to check.

1.4 Discussion

We have examined bosonic amplitudes through eight points in ABJM theory and found that the duality between color and kinematics holds, but at eight points attendant BCJ amplitude relations are not present. The color-kinematic duality specifies the eight-point numerators as unique functions of gauge-invariant partial amplitudes. We also have given explicit expressions necessary for analysis of ABJM amplitudes that do not appear in the literature. At six points, we have solved for a basis of color-kinematic numerators in terms of amplitudes. At eight points, we presented a set of amplitudes independent under the Kleiss-Kuijf relations in terms of numerators, as well as the relations the numerators satisfy according to the color-kinematic duality. The full eight-point expressions can be found in an ancillary online file [29].

The eight-point amplitude-numerator decomposition we provided can be used to study possible relations between ABJM amplitudes, or equivalently between ABJM numerators [28]. A recent twistor string construction for ABJM theory may also provide insight [36]. BLG theory is a special case of ABJM theory, and possesses the color-kinematic duality, residual freedom, and the double-copy property [28]. The mapping between BLG and ABJM amplitudes is straightforward at four and six points, but is not fully understood at eight points [28] and needs further investigation. While in ABJM theory the double-copy procedure leads to supergravity amplitudes at lower points, at eight points the double-copy property fails [28]. One might suspect that there is a connection between the simultaneous disappearances of the double-copy property and residual freedom. Further study of the eight point ABJM amplitudes may provide insight into the double-copy property through

side-by-side comparison with BLG amplitudes.

Using the data we have provided, further analysis of the eight-point ABJM amplitudes may provide important clues about the color-kinematic duality, residual freedom, and the double-copy property. The presence of the color-kinematic duality in ABJM theory without associated BCJ amplitude relations emphasizes the basic role numerators play in the duality compared to the amplitude relations. The eight-point ABJM amplitudes are the lowest-point amplitudes that allow the color-kinematic duality without possessing residual freedom to rearrange the numerators or yielding gravity amplitudes via the double-copy property. These amplitudes therefore provide an interesting avenue for further understanding the role of these properties in the duality between color and kinematics.

Chapter 2

Black holes from CFT: Universality of correlators at large c

Two-dimensional conformal field theories at large central charge and with a sufficiently sparse spectrum of light states have been shown to exhibit universal thermodynamics [37]. This thermodynamics matches that of AdS_3 gravity, with a Hawking-Page transition between thermal AdS and the BTZ black hole. We extend these results to correlation functions of light operators. Upon making some additional assumptions, such as large c factorization of correlators, we establish that the thermal AdS and BTZ solutions emerge as the universal backgrounds for the computation of correlators. In particular, Witten diagrams computed on these backgrounds yield the CFT correlators, order by order in a large c expansion, with exponentially small corrections. In pure CFT terms, our result is that thermal correlators of light operators are determined entirely by light spectrum data. Our analysis is based on the constraints of modular invariance applied to the torus two-point function.

2.1 Introduction

In classical physics, black holes have a clear meaning as representing the inevitable endpoint of the gravitational collapse of suitably dense configurations of matter. In the quantum

world, by contrast, the precise status of black hole solutions is a far more subtle question that continues to provoke debate; see e.g. [38]. A basic question is whether standard black hole geometries, realized in the quantum theory as coherent states of the gravitational field, are in some sense close to the actual solutions resulting from the collapse of matter in a particular microstate, or instead, do the actual solutions look dramatically different, with the usual black hole only arising as an effective description after some sort of coarse graining? Some version of the latter scenario seems nearly inescapable if one demands that black hole evaporation be described by a unitary S-matrix governed by more-or-less ordinary laws of physics (no macroscopic violations of locality, etc.) [39, 40].

The AdS/CFT correspondence offers a framework to address such questions without resorting to ad hoc speculations. In this paper we consider observables that are under good theoretical control, namely boundary correlation functions of low dimension operators computed in the thermal ensemble. We pose the question: under what conditions are such correlation functions, at sufficiently high temperature, accurately computed by Witten diagrams in the standard black hole geometry?

We work in the context of the AdS_3/CFT_2 correspondence, which provides several technical advantages while retaining the essential physical elements present in higher dimensional examples. Our guiding philosophy is that we wish to deduce the emergence of black hole physics while only making well-motivated assumptions about the CFT in the low energy and low temperature regime. The key feature that allows us to proceed in this manner is modular invariance of the CFT partition function and correlators. A number of other works have used modular invariance to probe the AdS/CFT correspondence, for example [41–49]. Our basic result can be stated as follows. Under some mild assumptions corresponding to what one thinks of as a good holographic CFT at low energies, high temperature correlation functions computed at large central charge are indeed given, order by order in bulk perturbation theory, by Witten diagrams computed in the Euclidean BTZ geometry, with

deviations being exponentially small in the central charge.[1] To see a breakdown of the black hole geometry at the level of thermal correlators one therefore needs to either examine these exponentially small terms, or consider kinematical configurations, such as large Lorentzian time separations, that take one outside our assumptions.

Our work is the natural extension of the work of Hartman, Keller, and Stoica (HKS) [37]. HKS assumed a sufficiently sparse spectrum of states at energies below the black hole threshold, and then used modular invariance to deduce that at large c the thermal free energy matches that of thermal AdS and BTZ in the low and high temperature regimes respectively. We will assume the same sparseness conditions as HKS, and in addition make some assumptions about the strength of couplings in the low energy theory. These assumptions are described in more detail in the next section. We make reference to light (L), medium (M), and heavy (H) operators,[2] according to the value of their conformal dimension Δ.[3] Light operators obey $\Delta < \Delta_c$, where Δ_c is held fixed as $c \to \infty$. Medium operators lie in the range $\Delta_c < \Delta < c/12$, where the upper limit is the black hole threshold. Heavy operators obey $\Delta > c/12$, and create black hole microstates. Our approach is to compute a quantity defined with respect to a given Δ_c, perform an asymptotic expansion in $1/c$, and then send $\Delta_c \to \infty$. We make the usual holographic CFT assumption of large c factorization, which is the statement that correlators of light operators admit an asymptotic expansion in powers of $1/\sqrt{c}$, and that the spectrum of such operators organizes into single-trace and multi-trace operators (a nice, general discussion may be found in [50]). Our next assumption concerns the growth of light correlators computed in medium energy states; we assume that such correlators grow at most polynomially in the medium energy dimension, which, as we discuss, is the natural expectation. This assumption is necessary to ensure that correlators of light operators computed at low temperature receive negligible contributions from states of energy $\Delta \sim c$, which would represent a breakdown of low energy effective field theory.

[1] In this work we only consider one-point and two-point correlators, but we expect our results to extend to higher point correlators.

[2] Note that our usage of light, medium, and heavy differs from that of HKS.

[3] $\Delta = h + \overline{h}$ is the total scaling dimension.

Finally we make a technical assumption regarding the expansion of low temperature thermal correlators.

We then proceed to study the implications of modular invariance on one-point and two-point thermal correlators. The one-point function is not so easy to study in isolation, because when expanded as a sum over states the terms in the sum have no definite sign, making it hard to deduce bounds. So we instead focus first on the two-point function, which does admit an expansion in terms of positive quantities, and then later circle back to the one-point function using these results. As already stated, our main result is that in the high temperature regime, $T > 1/2\pi$, these correlators, to all orders in the $1/\sqrt{c}$ expansion, are computed from Witten diagrams in the Euclidean BTZ geometry. Thermal one-point functions have a typical size of $1/\sqrt{c}$. From the bulk point of view, this is the statement that scalar fields vanish in the classical limit, which we can think of as a version of a no-hair theorem derived from CFT considerations. Of course, such a result is not surprising given that HKS already established that the thermodynamics of the CFT is in universal agreement with the hairless BTZ solution. We should also emphasize that this version of the no-hair statement concerns solutions that dominate in the canonical ensemble; it allows for the existence of novel solutions that dominate at fixed energy rather than fixed temperature.

The rest of this paper is organized as follows. In section 2, we review the HKS argument that we extend to prove our main result. In section 3 we state and motivate the assumptions necessary for our argument. In section 4, we use the modular bootstrap to prove one of our main results: under our assumptions, thermal two-point functions of light operators are determined by the light sector of the theory to all orders in an asymptotic expansion in $1/\sqrt{c}$. In section 5, we show that our two-point function result implies that thermal one-point functions of light operators are also determined by the light sector in the same way. We conclude with a brief discussion of possible extensions of this work. Appendix A contains certain calculational details that we omitted in section 4.

2.2 Review of the HKS argument

In this section we review results from ref. [37] for the partition function of a 1+1-dimensional large-c CFT living on a circle. We first divide the spectrum into light (L) and heavy (H) states,

$$L = \{E \leq \epsilon\}\,, \qquad H = \{E > \epsilon\}\,. \tag{2.2.1}$$

However, we bring to the reader's attention that in all other parts of this paper we use a different definition of "light" (as in the introduction); in this section only we are adopting the terminology in HKS. Energy is related to scaling dimension as

$$E = \Delta - \frac{c}{12}. \tag{2.2.2}$$

The L, H contributions to the partition function are

$$Z_L = \sum_L e^{-\beta E}, \qquad Z_H = \sum_H e^{-\beta E}, \tag{2.2.3}$$

where β is the inverse temperature and the sum is over all states in the relevant range. HKS use modular invariance to show that at large c a theory with a sufficiently sparse light spectrum obeys $\log Z \approx \log Z_L \approx \beta c/12$ at temperature $\beta > 2\pi$. The precise meaning of $\approx$ will become apparent.

The L, H contributions to the modular-transformed partition function ($\beta \to \beta' = 4\pi^2/\beta$) are denoted

$$Z'_L = \sum_L e^{-\beta' E}, \qquad Z'_H = \sum_H e^{-\beta' E}. \tag{2.2.4}$$

Modular invariance implies

$$Z_L - Z'_L = Z'_H - Z_H. \tag{2.2.5}$$

What Z_L gains under modular transformation, Z_H loses.

Assume $\beta > 2\pi$. We want a bound on $Z_H = Z'_H - Z_L + Z'_L$ relative to Z_L. Because every

term in the partition function sum is positive, Z_H can be bounded in terms of Z'_H,

$$Z_H = \sum_H e^{(\beta'-\beta)E} e^{-\beta' E} \leq e^{(\beta'-\beta)\epsilon} Z'_H. \tag{2.2.6}$$

This implies a bound on $Z_H - Z'_H$,

$$Z_H - Z'_H \leq Z'_H (e^{(\beta'-\beta)\epsilon} - 1). \tag{2.2.7}$$

We can now use modular invariance (2.2.5) to exchange $Z_H - Z'_H$ for $Z'_L - Z_L$ to obtain a bound on Z'_H in terms of Z_L,

$$Z'_H \leq (1 - e^{(\beta'-\beta)\epsilon})^{-1} (Z_L - Z'_L) \leq (1 - e^{(\beta'-\beta)\epsilon})^{-1} Z_L. \tag{2.2.8}$$

According to (2.2.6) this bound translates into a bound on Z_H in terms of Z_L.

$$Z_H \leq \frac{e^{(\beta'-\beta)\epsilon}}{1 - e^{(\beta'-\beta)\epsilon}} Z_L. \tag{2.2.9}$$

It follows that

$$\ln Z_L \leq \ln Z = \ln(Z_L + Z_H) \leq \ln Z_L - \ln(1 - e^{(\beta'-\beta)\epsilon}). \tag{2.2.10}$$

Using modular invariance, one obtains a similar expression for $\beta < 2\pi$. So far, everything holds for an arbitrary compact, unitary, CFT.

We now consider a family of CFTs with a large c limit. Taking ϵ to be independent of c, we then have that at large c,

$$\log Z = \begin{cases} \log Z_L + \mathcal{O}(c^0), & \beta > 2\pi, \\ \log Z'_L + \mathcal{O}(c^0), & \beta < 2\pi \ . \end{cases} \tag{2.2.11}$$

Next, it's easy to see that $\log Z_L = \beta c/12 + \mathcal{O}(c^0)$ provided that the following sparseness condition is obeyed,

$$\rho(E) \lesssim e^{2\pi(E+\frac{c}{12})} = e^{2\pi\Delta} \qquad E \leq \epsilon, \tag{2.2.12}$$

where $\lesssim$ is defined in footnote 4. We will have more to say about this assumption in the next section. Under this assumption we then have

$$\log Z = \begin{cases} \beta c/12 + \mathcal{O}(c^0), & \beta > 2\pi, \\ \beta' c/12 + \mathcal{O}(c^0), & \beta < 2\pi \ . \end{cases} \tag{2.2.13}$$

This result for the partition function implies a Cardy density of states for $E > c/12$,

$$\rho(E) \approx e^{2\pi\sqrt{\frac{c}{3}E}}, \qquad E > c/12, \tag{2.2.14}$$

where the smooth function $\rho(E)$ is obtained by averaging the microscopic density of states over a small energy window.

$\rho(E)$ is non-universal for $0 < E < c/12$. However, the assumption (2.2.12) implies $\log \rho(E) \leq \pi c/6 + 2\pi E$ in this range, and at large c. These states never dominate in the canonical ensemble.

The main takeaway message is that the sparseness assumption together with modular invariance at large c implies a universal result for the leading behavior (in c) of the canonical partition function, and this result furthermore matches the partition function obtained from AdS_3 gravity in the classical limit.

2.3 Assumptions

In this section we lay out the precise assumptions that will be invoked in our correlation function analysis, and discuss the motivation for these assumptions, which come from expectations about which properties we expect of a CFT with a "good" holographic dual. In

stating our assumptions we are thinking in terms of a family or sequence of CFTs such that we can take $c \to \infty$ within this space of CFTs. Each member of the family is assumed to be a compact, unitary, CFT.

In the following, light, medium, and heavy operators are defined as having scaling dimensions:

$$L = \{0 \leq \Delta \leq \Delta_c\} \ , \quad M = \{\Delta_c < \Delta \leq \frac{c}{12} + \epsilon\} \ , \quad H = \{\Delta > \frac{c}{12} + \epsilon\} \ . \tag{2.3.1}$$

Here ϵ is held fixed as $c \to \infty$. The cutoff Δ_c is taken to infinity *after* performing the large-c expansion.

Assumption 1: Sparse spectrum

This condition is widely discussed in the AdS/CFT literature, e.g. [50, 51], and a specific version of it was noted in the last section. At the crudest level, we should demand that as $c \to \infty$ the number of local operators with dimension below any fixed value should remain finite. A diverging number of operators could invalidate the usual loop expansion in the bulk: a growing number of light fields running in loops could make loop diagrams compete with or dominate over tree diagrams. HKS assume a specific version of this statement, namely that the density of operators at dimension Δ should obey[4]

$$\rho(\Delta) \lesssim e^{2\pi\Delta} \ , \quad \Delta \leq \frac{c}{12} + \tilde{\epsilon} \ . \tag{2.3.2}$$

The quantity $\tilde{\epsilon}$ is eventually taken to zero; we distinguish it from the quantity ϵ introduced below, which remains finite at large c.

As reviewed in the previous section, HKS showed that their sparseness assumption on

[4]Following HKS, the inequality $e^x \lesssim e^y$ means that $\lim x/y \leq 1$. So, for example, the right hand side of the inequality in (2.3.2) could be multiplied by a polynomial in Δ.

the light spectrum implied that

$$\rho(\Delta) \lesssim e^{2\pi\Delta} \ , \quad \Delta \leq \frac{c}{6} \ , \tag{2.3.3}$$

as well as

$$\rho(\Delta) \approx e^{2\pi\sqrt{\frac{c}{3}(\Delta - \frac{c}{12})}} \ , \quad \Delta > \frac{c}{6} \ . \tag{2.3.4}$$

The density of states (2.3.4) coincides with Cardy's formula, but now in a different regime of validity, since the derivation of Cardy's formula is only valid for $\Delta \gg c$ at fixed c.

The results of HKS can also be stated in terms of the partition function as,

$$Z(\beta) \approx \begin{cases} e^{\frac{\beta c}{12}} \ , & \beta > 2\pi \\ e^{\frac{\pi^2 c}{3\beta}} \ , & \beta < 2\pi \ . \end{cases} \tag{2.3.5}$$

These partition functions coincide with those of thermal AdS or BTZ solutions in the bulk. We should note that the sparseness condition (2.3.2) is rather mild, allowing in particular for a stringy growth of states.

Assumption 2: Factorization of light correlators

We now make a standard assumption that corresponds to having a weakly coupled low energy field theory in the bulk. Let $\{O_i\}$ be a collection of operators whose dimensions are all bounded in the large c limit. We assume the asymptotic expansion[5]

$$\langle 0|O_1(x_1)\dots O_n(x_n)|0\rangle \sim \sum_{k=0}^{\infty} \frac{1}{c^{k/2}} G_n^{(k)}(x_i) \ , \quad c \to \infty \ . \tag{2.3.6}$$

We also assume that the light operator spectrum can be organized into single-trace and multi-trace operators. Namely, we have a collection of single-trace operators whose connected $k > 2$ point functions amongst each other vanish in the large c limit. Then we have multi-trace operators whose dimension in the large c limit equals the sum of dimensions of their single-

[5]We assume that operators are normalized such that their two-point functions have unit coefficient.

trace constituents, and whose correlators in the large c limit are obtained in terms of their constituents by Wick contractions.

The objects $G_n^{(k)}(x_i)$ computed for single-trace operators are what one computes in the bulk via Witten diagrams in AdS, order by order in the bulk loop expansion. Following [51], we expect that there is a one-to-one correspondence between such CFT correlators that obey crossing constraints and those obtained from theories in AdS. Note though that since the sparseness condition allows for the bulk theory to be stringy in nature, when we refer to "Witten diagrams" we are not demanding that the bulk theory necessarily be local with higher derivative interaction terms suppressed at the AdS scale, rather we also admit the case of bulk amplitudes computed from a worldsheet construction with string tension at the AdS scale. The question of whether a more restrictive sparseness condition, along with modular invariance, implies locality below the AdS scale is discussed in [52].

Assumption 3: Growth of light correlators in medium energy states

To state this assumption, we let $\{O_i\}$ denote a collection of light operators, with $\Delta_i < \Delta_c$, where the cutoff Δ_c is held fixed as $c \to \infty$, and we let O_A denote a medium operator, obeying $\Delta_c < \Delta_A < \frac{c}{12} + \epsilon$. Our assumption is that for all sufficiently large Δ_c and c, there exists some number K and positive number p (which are allowed to depend on n and on the positions x_i) such that

$$|\langle A|O_1(x_1)\dots O_n(x_n)|A\rangle| < K(\Delta_A)^p \ . \tag{2.3.7}$$

Essentially, we are allowing light correlators in medium states to grow with c as long as they do so in a sub-exponential manner.

The bulk intuition behind this assumption is the following. We expect there to exist bulk solutions with scalar fields taking macroscopic values, but which are not so heavy as to create black holes. Finite gravitational back reaction allows for fields taking values $\phi \sim \sqrt{c}$, so that the matter stress tensor behaves as $T_{\mu\nu} \sim c \sim G_N^{-1}$. If now we compute the n-point function of the CFT operator O_ϕ dual to the bulk field ϕ, we will obtain a result that behaves as $c^{n/2}$.

Our assumption allows for such behavior, but rules out a stronger exponential growth.

Assumption 4: Large c expansion of light thermal correlator

Finally we make what is, we believe, a rather mild assumption imposed purely on the light operators, i.e. those with $\Delta < \Delta_c$ as $c \to \infty$. Working on the cylinder, we define the light contribution to the thermal correlator as[6]

$$G_2^{(L)}(\phi, t; \beta) = \frac{e^{\beta c/12}}{Z(\beta)} \sum_L e^{-\beta \Delta_L} \langle L|O(\phi, t)O(0,0)|L\rangle \ , \quad \Delta_L, \Delta_O < \Delta_c \ . \tag{2.3.8}$$

For $\beta > 2\pi$, we perform an asymptotic expansion in $1/\sqrt{c}$ (as in Assumption 2), and then take $\Delta_c \to \infty$ to obtain

$$G_2^{(L)}(\phi, t; \beta) = \sum_{k=0}^{\infty} \frac{1}{c^{k/2}} G_2^{(L,k)}(\phi, t; \beta) \ . \tag{2.3.9}$$

The nontrivial assumption here is the existence of the limit $\Delta_c \to \infty$ for all the coefficient functions $G_2^{(L,k)}(\phi, t; \beta)$; in principle it is possible that the functions appearing in the large c expansion grow with Δ_c, as could potentially occur if the matrix elements $\langle L|O(\phi, t)O(0,0)|L\rangle$ are permitted to grow exponentially in Δ_c for $\Delta_L \sim \Delta_c$.

Given this assumption, the objects $G_2^{(L,k)}(\phi, t; \beta)$ are what one obtains in the bulk computation of the two-point correlator in thermal AdS from Witten diagrams. In such a computation only light fields propagate in the bulk, with the contribution of virtual heavy states assumed to be exponentially suppressed.

[6]We just consider the two-point function here, since that is all we will use, but the generalization is obvious.

2.4 Two-point function analysis

In this section we show that the Euclidean thermal two-point function of a light operator is fixed by data about the light spectrum. Our result will be

$$\langle O(\phi,t)O(0,0)\rangle_\beta \approx \begin{cases} \frac{e^{\beta\frac{c}{12}}}{Z(\beta)}\sum_{A,B\in L} e^{-\beta\Delta_A}e^{t\Delta_{AB}}e^{i\phi J_{AB}}|\langle A|O|B\rangle|^2, & \beta > 2\pi \\ \frac{e^{\beta'\frac{c}{12}}}{Z(\beta)}\left(\frac{2\pi}{\beta}\right)^{2\Delta}\sum_{A,B\in L} e^{-\beta'\Delta_A}e^{\frac{2\pi\phi}{\beta}\Delta_{AB}}e^{i\frac{2\pi t}{\beta}J_{AB}}|\langle A|O|B\rangle|^2, & \beta < 2\pi \end{cases} \tag{2.4.1}$$

where $\approx$ indicates equality up to corrections that are suppressed exponentially in Δ_c, ϵ, or c. The summation variables A and B run over a basis of light states with dimensions Δ_A, Δ_B and spins J_A, J_B. Δ_{AB} stands for $\Delta_A - \Delta_B$ and similarly for J_{AB}. All matrix elements lacking a temperature-indicating subscript are to be evaluated on a cylinder (with circumference 2π) and whenever the position of an operator O is left implicit it is to be understood as $\phi = 0$, $t = 0$.

The important point is that the right hand side of equation (2.4.1) depends only on the dimensions and OPE coefficients of light operators.

The low temperature case of equation (2.4.1) will be established using the assumptions of section 2.3 along with the constraint of modular covariance, which reads

$$\langle O(\phi,t)O(0,0)\rangle_\beta = \left(\frac{2\pi}{\beta}\right)^{2\Delta}\left\langle O(\tfrac{2\pi}{\beta}t,\tfrac{2\pi}{\beta}\phi)O(0,0)\right\rangle_{\beta'}, \quad \beta' = \frac{(2\pi)^2}{\beta}\ . \tag{2.4.2}$$

With the low temperature result in hand, a final application of equation (2.4.2) immediately yields the high temperature result.

The starting point of our analysis is the expression for the two-point function at any temperature obtained from cutting the path integral along two time slices that separate the

operators O and inserting complete sets of states A, B,

$$\langle O(\phi,t)O(0,0)\rangle_\beta = \frac{e^{\beta c/12}}{Z(\beta)} \sum_A \sum_B e^{-\beta\Delta_A} e^{t\Delta_{AB}} e^{i\phi J_{AB}} |\langle A|O|B\rangle|^2 \ . \tag{2.4.3}$$

The right hand side of equation (2.4.3) will sometimes be denoted $G(\phi, t; \beta)$ for brevity.

Given that each state A, B can be light, medium, or heavy, $G(\phi, t; \beta)$ has nine contributions to consider. We will refer to these contributions as $G^{(LL)}, G^{(LM)}, \ldots G^{(MH)}, G^{(HH)}$, where the first superscript refers to A and the second to B. We wish to prove the top case of equation (2.4.1), which states that when $\beta > 2\pi$ the function G is equal to $G^{(LL)}$ up to exponentially small corrections from the other eight contributions. In subsection 2.4.1 we argue from our assumptions that the seven contributions $G^{(Mx)}, G^{(xM)}, G^{(LH)}, G^{(HL)}$ are all small, where x stands for L, M, or H. This leaves $G^{(HH)}$. We then present in subsection 2.4.4 an HKS-like argument that modular covariance demands $G^{(HH)}$ to be small.

2.4.1 Bounding the medium and off-diagonal contributions

In this subsection we use the assumptions about the light spectrum laid out in section 2.3 to argue that many of the contributions to equation (2.4.3) are small.

2.4.2 Medium contributions

The sum of the three quantities $G^{(Mx)}$ is given by

$$G^{(ML)} + G^{(MM)} + G^{(MH)} = \frac{e^{\beta c/12}}{Z(\beta)} \sum_{A\in M} e^{-\beta\Delta_A} \langle A|O(\phi,t)O(0,0)|A\rangle \tag{2.4.4}$$

where we used the fact that B runs over a complete set of states. Assumptions 1 and 3 above bound the size of this sum as follows:

$$\left|G^{(ML)} + G^{(MM)} + G^{(MH)}\right| \leq \frac{e^{\beta c/12}}{Z(\beta)} \int_{\Delta_c}^{\infty} d\Delta\, e^{(2\pi-\beta)\Delta} K\Delta^p \ . \tag{2.4.5}$$

The factor of $e^{2\pi\Delta}$ comes from the upper bound on the density of states in assumption 1. The upper limit of integration has been set to infinity rather than $c/12+\epsilon$, a valid step because doing so only makes the inequality weaker. When $\beta > 2\pi$ the integral is exponentially small at large Δ_c and we conclude that the three contributions[7] $G^{(Mx)}$ are exponentially small in Δ_c.

Exchanging A and B in equation (2.4.3) is equivalent to transforming (ϕ, t) to $(-\phi, \beta - t)$, so we conclude that $G^{(xM)}$ is also small.

2.4.3 Heavy-light contributions

We now argue[8] that the contributions $G^{(LH)}$, $G^{(HL)}$ are suppressed exponentially in c when $\beta > 2\pi$. Because of the symmetry in A, B mentioned above, it is sufficient to focus on $G^{(LH)}$. Setting $\phi = 0$ for the moment, the contribution in question is

$$G^{(LH)} = \frac{e^{\beta c/12}}{Z(\beta)} \sum_{A\in L} \sum_{B\in H} e^{-\beta\Delta_A} e^{(t-t_0)\Delta_{AB}} e^{t_0\Delta_{AB}} \left|\langle A|O|B\rangle\right|^2 \ . \tag{2.4.6}$$

A constant t_0 in the range $0 < t_0 < t$ has been introduced to be used in the next step. Obviously the right hand side of equation (2.4.6) is independent of t_0. The factor $e^{(t-t_0)\Delta_{AB}}$ in the summand above is no larger than $e^{(t-t_0)(\Delta_c - c/12)}$, and since each term in the sum is positive this implies

$$G^{(LH)} \leq e^{(t-t_0)(\Delta_c - c/12)} \frac{e^{\beta c/12}}{Z(\beta)} \sum_{A\in L} \sum_{B\in H} e^{-\beta\Delta_A} e^{t_0\Delta_{AB}} \left|\langle A|O|B\rangle\right|^2 \ . \tag{2.4.7}$$

[7] To proceed from smallness of the left hand side of (2.4.5) to smallness of the three terms individually, we note that when $\phi = 0$ each of the three terms is positive and that taking ϕ nonzero can only decrease each term's absolute value.

[8] A similar argument appears in [53]. Indeed, exponential suppression of $G^{(LH)}$ is a manifestation of their result that the OPE converges exponentially fast.

The inequality only weakens upon extending the sum over $B \in H$ to a sum over all states:

$$G^{(LH)} \leq e^{(t-t_0)(\Delta_c - c/12)} \frac{e^{\beta c/12}}{Z(\beta)} \sum_{A \in L} e^{-\beta \Delta_A} \langle A|O(0,t_0)O(0,0)|A\rangle \ . \tag{2.4.8}$$

The first factor on the right hand side is exponentially small. Meanwhile, the rest of that expression is zeroth-order in c by assumption 4. So equation (2.4.8) tells us the heavy-light contribution is exponentially small in c relative to $e^{\beta c/12}$. The extension to $\phi \neq 0$ is immediate, because each term in equation (2.4.3) only decreases in absolute value upon taking ϕ nonzero. We conclude that $G^{(LH)}$, $G^{(HL)}$ are suppressed exponentially in c.

2.4.4 Heavy-heavy bound from modular covariance

In this subsection, we use modular covariance to show that the contribution to equation (2.4.3) from states A, B that are both heavy is suppressed, at $\beta > 2\pi$, relative to the full sum. The argument, which parallels that of [37], is independent of any assumptions about the CFT spectrum, OPE coefficients, or the size of the central charge. All we require is that ϵ is large enough for the quantity

$$\delta = (\tfrac{\beta}{2\pi})^{2(\Delta+2)} e^{-|\beta - \beta'|\epsilon} \tag{2.4.9}$$

to be small. We will find that $G^{(HH)}$ is suppressed relative to G by a factor of δ.

Modular covariance of equation (2.4.3) leads to an equivalent expression for the two-point function:

$$\langle O(\phi,t)O(0,0)\rangle_\beta = (\tfrac{2\pi}{\beta})^{2\Delta} \frac{e^{\beta' c/12}}{Z(\beta)} \sum_A \sum_B e^{-\beta' \Delta_A} e^{\frac{\beta'}{2\pi}\phi \Delta_{AB}} e^{\frac{2\pi}{\beta} i t J_{AB}} |\ \langle A|O|B\rangle\ |^2. \tag{2.4.10}$$

We will call the right hand side of (2.4.10) $\tilde{G}(\phi, t; \beta)$ just as the right hand side of (2.4.3) was called $G(\phi, t; \beta)$. The left hand sides of those equations are identical so of course $G(\phi, t; \beta) = \tilde{G}(\phi, t; \beta)$. This is the modular crossing equation. We will find that it puts nontrivial

constraints on the matrix elements $\langle A|O|B\rangle$.

We now Fourier expand $G(\phi,t;\beta)$ and $\tilde{G}(\phi,t;\beta)$ as functions of ϕ and t.

$$G(\phi,t;\beta)=\sum_{n=0}^{\infty}\sum_{m=0}^{\infty}G_{nm}\cos(n\phi)\cos(\tfrac{2\pi mt}{\beta})\ , \tag{2.4.11a}$$

$$\tilde{G}(\phi,t;\beta)=\sum_{n=0}^{\infty}\sum_{m=0}^{\infty}\tilde{G}_{nm}\cos(n\phi)\cos(\tfrac{2\pi mt}{\beta})\ . \tag{2.4.11b}$$

Again, the two functions are equal so $G_{nm}=\tilde{G}_{nm}$. Only cosine modes appear because the functions are even under the reflections $\phi\to 2\pi-\phi$ and $t\to\beta-t$. Performing the Fourier transforms term by term inside the sums (2.4.3), (2.4.10) yields

$$G_{nm}=2\beta\frac{e^{\beta c/12}}{Z(\beta)}\sum_{\substack{A,B\\|J_{AB}|=n}}\left(\frac{\Delta_{AB}\left(e^{-\beta\Delta_B}-e^{-\beta\Delta_A}\right)}{\beta^2\Delta_{AB}^2+(2\pi m)^2}\right)|\langle A|O|B\rangle|^2 \tag{2.4.12a}$$

$$\tilde{G}_{nm}=2\beta'\left(\frac{2\pi}{\beta}\right)^{2\Delta}\frac{e^{\beta' c/12}}{Z(\beta)}\sum_{\substack{A,B\\|J_{AB}|=m}}\left(\frac{\Delta_{AB}\left(e^{-\beta'\Delta_B}-e^{-\beta'\Delta_A}\right)}{\beta'^2\Delta_{AB}^2+(2\pi n)^2}\right)|\langle A|O|B\rangle|^2\ . \tag{2.4.12b}$$

When $\Delta_A=\Delta_B$ the summands of (2.4.12a), (2.4.12b) are to be defined via their limits as $\Delta_A\to\Delta_B$, which are finite and nonnegative.

Note that the contribution from any pair of states A,B to either sum (2.4.12a), (2.4.12b) is nonnegative. This fact is central to the argument below, which parallels the original one applied by HKS to the partition function. We begin by separating out the heavy-heavy contribution to each sum (2.4.3),(2.4.10):

$$G(\phi,t;\beta)=G^{(L)}(\phi,t;\beta)+G^{(HH)}(\phi,t;\beta) \tag{2.4.13a}$$

$$\tilde{G}(\phi,t;\beta)=\tilde{G}^{(L)}(\phi,t;\beta)+\tilde{G}^{(HH)}(\phi,t;\beta)\ . \tag{2.4.13b}$$

We define $G^{(HH)}$ to be the contribution to (2.4.3) from states A,B that are both heavy, as above. Meanwhile $G^{(L)}$ is the contribution from all other pairs of states[9]. $\tilde{G}^{(HH)}$, $\tilde{G}^{(L)}$ are

[9]Note that $G^{(L)}$ is distinct from $G^{(LL)}$ (although the conclusion of subsection 2.4.1 is that these functions'

defined in the same way.

The Fourier modes of $G^{(HH)}, \tilde{G}^{(HH)}$ are found by restricting sums (2.4.12) to heavy states:

$$G^{(HH)}_{nm} = 4\beta \sum_{A\in H} \sum_{\substack{B,\,\Delta_B\geq\Delta_A \\ |J_{AB}|=n}} (\tfrac{1}{2})^{\delta_{AB}} \frac{e^{-\beta E_A}}{Z(\beta)} \left(\frac{-\Delta_{AB}\left(1-e^{\beta\Delta_{AB}}\right)}{\beta^2\Delta_{AB}^2 + (2\pi m)^2} \right) |\,\langle A|O|B\rangle\,|^2 \tag{2.4.14a}$$

$$\tilde{G}^{(HH)}_{nm} = 4\beta' (\tfrac{2\pi}{\beta})^{2\Delta} \sum_{A\in H} \sum_{\substack{B,\,\Delta_B\geq\Delta_A \\ |J_{AB}|=n}} (\tfrac{1}{2})^{\delta_{AB}} \frac{e^{-\beta' E_A}}{Z(\beta)} \left(\frac{-\Delta_{AB}\left(1-e^{\beta'\Delta_{AB}}\right)}{\beta'^2\Delta_{AB}^2 + (2\pi n)^2} \right) |\,\langle A|O|B\rangle\,|^2 \ . \tag{2.4.14b}$$

Above we used the symmetry in A, B of equations (2.4.12) to arrange for Δ_A to be less than or equal to Δ_B inside the sum. For proper counting we introduced a factor of $2(1/2)^{\delta_{AB}}$ which is 1 if $A = B$ and 2 otherwise. (There is no loss of generality in assuming B runs over the same basis as A.)

It's important to keep in mind for what follows that $\beta > 2\pi$. Following HKS we note that we can bound the Boltzmann factor in equation (2.4.14a) for $G^{(HH)}_{nm}$ in the following way

$$e^{-\beta E_A} = e^{-(\beta-\beta')E_A} e^{-\beta' E_A} \leq e^{-(\beta-\beta')\epsilon} e^{-\beta' E_A} \ . \tag{2.4.15}$$

This is the step in which it is important that the lightest heavy state has energy ϵ larger than zero. We then use the fact that every term in the sum $G^{(HH)}_{nm}$ is positive to write

$$G^{(HH)}_{nm} \leq 4\beta e^{-(\beta-\beta')\epsilon} \sum_{\substack{A \\ \text{heavy}}} \sum_{\substack{B,\,\Delta_B\geq\Delta_A \\ |J_{AB}|=n}} (\tfrac{1}{2})^{\delta_{AB}} \frac{e^{-\beta' E_A}}{Z(\beta)} \left(\frac{-\Delta_{AB}\left(1-e^{\beta\Delta_{AB}}\right)}{\beta^2\Delta_{AB}^2 + (2\pi n)^2} \right) |\,\langle A|O|B\rangle\,|^2 \ . \tag{2.4.16}$$

difference is small).

The quantity in parentheses in (2.4.16) is bounded by

$$\left(\frac{-\Delta_{AB}\left(1-e^{\beta\Delta_{AB}}\right)}{\beta^2\Delta_{AB}^2+(2\pi n)^2}\right)\leq\left(\frac{\beta}{\beta'}\right)\left(\frac{-\Delta_{AB}\left(1-e^{\beta'\Delta_{AB}}\right)}{\beta'^2(\Delta_{AB}^2+(2\pi n)^2}\right). \tag{2.4.17}$$

To check (2.4.17), first note that the denominator on the left is $\geq$ the one on the right. And second note that the fraction $(1-e^{\beta\Delta_{AB}})/(1-e^{\beta'\Delta_{AB}})$ is an increasing function of $\Delta_{AB}<0$ and so is bounded from above by its limit as that difference goes to zero, which is β/β'. From (2.4.17) it follows that

$$G_{nm}^{(HH)}\leq\tfrac{4\beta^2}{\beta'}e^{-(\beta-\beta')\epsilon}\sum_{A\in H}\sum_{\substack{B,\,\Delta_B\geq\Delta_A\\|J_{AB}|=n}}(\tfrac{1}{2})^{\delta_{AB}}\frac{e^{-\beta'E_A}}{Z(\beta)}\left(\frac{-\Delta_{AB}\left(1-e^{\beta'\Delta_{AB}}\right)}{\beta'^2\Delta_{AB}^2+(2\pi n)^2}\right)|\,\langle A|O|B\rangle\,|^2. \tag{2.4.18}$$

We recognize the right hand side as proportional to $\tilde{G}_{mn}^{(H)}$ and conclude that

$$G_{nm}^{(HH)}\leq\delta\tilde{G}_{mn}^{(HH)} \tag{2.4.19}$$

with δ being the constant defined in equation (2.4.9).

Equation (2.4.19) is analogous to the starting point, equation (2.2.6), of HKS's analysis for the partition function: $G^{(HH)}$, $\tilde{G}^{(HH)}$ and δ play the roles of Z_H, Z'_H and $e^{(\beta'-\beta)\epsilon}$, respectively. From that starting point a clever modular invariance argument (reviewed in section 2.2) showed that the heavy contribution to the low temperature partition function is suppressed relative to the light contribution. In appendix 2.7 we apply the same argument to the two-point function's Fourier modes. The result is

$$G_{nm}^{(HH)}\leq\delta\frac{G_{mn}^{(L)}+\delta G_{nm}^{(L)}}{1-\delta^2}\ . \tag{2.4.20}$$

The right hand side of this result is suppressed by a factor of δ relative to $G_{mn}^{(L)}$ and $G_{nm}^{(L)}$, which are of order unity by the results of section 2.4.1. We conclude that $G_{nm}^{(HH)}$ is

suppressed by δ relative to unity. That this holds for every Fourier mode implies the function $G^{(HH)}(\phi, t; \beta)$ is itself suppressed by a factor of δ. That is, it is exponentially small in the parameter ϵ.

2.4.5 Conclusion of this section

From the results of subsections 2.4.1 and 2.4.4, equation (2.4.1) is established. At $\beta > 2\pi$, the right hand side of that equation is what one computes using Witten diagrams in thermal AdS. To be precise, if one expands the right hand side in powers of $\frac{1}{\sqrt{c}}$ and then takes the limit $\Delta_c \to \infty$ order-by-order one recovers the Witten diagram expansion in powers of $\frac{1}{\sqrt{c}}$. At $\beta < 2\pi$ the same conclusion holds with thermal AdS replaced by a BTZ black hole of the appropriate temperature. This follows from the low temperature statement by bulk modular invariance: The Euclidean BTZ black hole of inverse temperature β is isometric to thermal AdS at inverse temperature β', and the isometry involves exchanging the angular and time coordinates as in equation (2.4.2).

2.5 One-point function

With our two-point function result in hand, we now turn to the one-point function. We first derive an upper bound on the one-point function. We start with the decomposition of the two-point function,

$$\langle O(0, \beta/2) O(0,0) \rangle_\beta = \frac{1}{Z(\beta)} \sum_{A,B} e^{-\frac{\beta}{2}(E_A + E_B)} |\langle A|O|B\rangle|^2 \ . \tag{2.5.1}$$

The right hand side is bounded below by the contribution from $A = B$, hence

$$\langle O(0, \beta/2) O(0,0) \rangle_\beta \geq \frac{1}{Z(\beta)} \sum_{A} e^{-\beta E_A} |\langle A|O|A\rangle|^2 \ . \tag{2.5.2}$$

Now, using the elementary fact that $x^2 \geq 2x - 1$ for real x, we obtain

$$\langle O(0, \beta/2) O(0,0) \rangle_\beta \geq \frac{2}{Z(\beta)} \sum_A e^{-\beta E_A} |\langle A|O|A\rangle| - 1 \ . \tag{2.5.3}$$

(2.5.3) implies a bound on the contribution to the one-point function from any collection of states,

$$\frac{1}{Z(\beta)} \sum_{A \in \psi} e^{-\beta E_A} |\langle A|O|A\rangle| \leq \frac{1 + \langle O(0, \beta/2) O(0,0) \rangle_\beta}{2} \ , \tag{2.5.4}$$

where ψ denotes any subspace of the full Hilbert space. Since $|\langle O \rangle_\beta| \leq \frac{1}{Z(\beta)} \sum_A e^{-\beta E_A} |\langle A|O|A\rangle|$ we also deduce a bound on the full one-point function

$$|\langle O \rangle_\beta| \leq \frac{1 + \langle O(0, \beta/2) O(0,0) \rangle_\beta}{2} \ . \tag{2.5.5}$$

These are exact bounds, valid in any theory for any temperature. For our purposes, the main fact we will use is that since the two-point function is finite in the large c limit, the same is true of the left hand side of (2.5.4).

We now show that for $\beta > 2\pi$ the contributions to the one-point function from medium and heavy states are exponentially suppressed compared to the light state contribution. For the medium state contribution we proceed as in (2.4.5),

$$\begin{aligned} \left| \frac{1}{Z(\beta)} \sum_{A \in M} e^{-\beta E_A} \langle A|O|A\rangle \right| &\leq \frac{1}{Z(\beta)} \sum_{A \in M} e^{-\beta E_A} |\langle A|O|A\rangle| \\ &\leq \frac{e^{\frac{\beta c}{12}}}{Z(\beta)} \int_{\Delta_c}^{\infty} d\Delta e^{(2\pi - \beta)\Delta} K \Delta^p \ . \end{aligned} \tag{2.5.6}$$

For $\beta > 2\pi$ the last expression is exponentially small in Δ_c. For the heavy contribution we

note that

$$\left|\frac{1}{Z(\beta)}\sum_{A\in H} e^{-\beta E_A}\langle A|O|A\rangle\right| \;\leq\; \frac{1}{Z(\beta)}\sum_{A\in H} e^{-\beta E_A}|\langle A|O|A\rangle| \tag{2.5.7}$$

together with (2.5.4) implies that the heavy contribution has a finite large c limit. In particular, this holds for any β sufficiently greater than 2π such that $\delta \ll 1$. But then for any larger β the right hand side is exponentially small in c, since $Z(\beta)^{-1}e^{-\beta E_A}$ is exponentially small for all heavy states.

Since the medium and heavy state contributions are exponentially small, we conclude that

$$\langle O\rangle_\beta \approx \frac{1}{Z(\beta)}\sum_{A\in L} e^{-\beta E_A}\langle A|O|A\rangle \ , \quad \beta > 2\pi \tag{2.5.8}$$

as desired. A modular transformation then gives the high temperature result,

$$\langle O\rangle_\beta \approx \left(\frac{2\pi}{\beta}\right)^{\Delta}\frac{1}{Z(\beta)}\sum_{A\in L} e^{-\frac{4\pi^2}{\beta}E_A}\langle A|O|A\rangle \ , \quad \beta < 2\pi \tag{2.5.9}$$

Since the three-point coefficients $\langle A|O|A\rangle$ of single-trace operators fall off at least as fast as $1/\sqrt{c}$ according to Assumption 2, it follows that the generic one-point function of a single-trace operator is $O(1/\sqrt{c})$. Double-trace operators can have $O(1)$ expectation values, in accord with (2.5.5).

In [45] it was pointed out that modular invariance implies that the one-point function in the high temperature limit behaves as

$$\langle O\rangle_\beta \approx \left(\frac{2\pi}{\beta}\right)^{\Delta}\frac{1}{Z(\beta)}e^{-\frac{4\pi^2}{\beta}E_\chi}\langle \chi|O|\chi\rangle \ , \quad \beta \to 0 \ , \tag{2.5.10}$$

where $|\chi\rangle$ denotes the lightest state such that $\langle\chi|O|\chi\rangle \neq 0$. This results holds for all c. It was further noted that this asymptotic formula for the one-point function has a simple

bulk interpretation in terms of a χ particle winding around the BTZ horizon. What we have shown here is that in a large c theory satisfying our assumptions, the analogous result holds, except now we should sum over all light states winding around the horizon, including multiparticle states. This then yields the one-point function for all $\beta < 2\pi$.

2.6 Discussion

We conclude with a few comments.

Our main CFT result is that, under our assumptions, one and two point correlators of light fields at any temperature are determined entirely by light spectrum data. Translated into bulk gravity language, the statement is that thermal AdS and the BTZ black hole emerge as the universal backgrounds for the computation of thermal one and two-point functions of light operators, and only the propagation of light fields on these backgrounds need be considered. One obvious extension is to generalize to n-point functions of light operators. We anticipate no fundamental obstacles here, although the analysis will become more complicated.

Our result for the thermal two-point function assumes that the time separation is purely Euclidean and is held fixed as $c \to \infty$. Indeed, we expect our results to breakdown if we instead allow for Lorentzian time separations that can grow with c, since in this case we would otherwise violate bounds on the size of such correlators: perturbative Witten diagrams yield a result that decays exponentially to zero at late times, whereas unitarity places a lower bound on the long time average [54]. It would be interesting to explore in detail the regime of validity of our results once we relax the conditions on the time arguments.

It may be instructive to compute correlators in symmetric product orbifold theories as an explicit realization of our assumptions. Such theories are known [37] to saturate the density of states allowed by the HKS analysis, and their correlators admit a $1/\sqrt{c}$ expansion. Of course, such theories, being free, are far from having a bulk description in terms of Einstein gravity (for example, they are not chaotic [55]), but this is the price paid for calculability on

the CFT side. Some related computations were carried out in [56].

It would be very interesting if analogous statements to what we have shown here could be established in higher dimensions. On general grounds we expect a similar result to hold, but it is clear that new issues arise. Namely, modular invariance acts in a more complicated way in higher dimensions, relating CFTs on distinct spaces to one another rather than just changing the temperature [57–60]. The bulk analog of this statement is that the black hole solution — AdS-Schwarzschild — is no longer locally AdS as for BTZ, but depends on the details of the bulk theory, such as the presence of higher derivative terms and so on. The story will thus necessarily be more intricate.

2.7 Appendix: Details of modular crossing analysis

In subsection 2.4.4 we showed that the heavy contributions to the Fourier modes of the two-point function satisfy an inequality (2.4.19), which we repeat here for convenience:

$$G^{(HH)}_{nm} \leq \delta \tilde{G}^{(HH)}_{mn} \ . \tag{2.7.1}$$

The indices n, m are transposed between the left and right hand sides. To treat this complication it is convenient to combine the above relation and its image under $n \leftrightarrow m$ into a single inequality:

$$\begin{pmatrix} G^{(HH)}_{nm} \\ G^{(HH)}_{mn} \end{pmatrix} \leq \begin{pmatrix} 0 & \delta \\ \delta & 0 \end{pmatrix} \begin{pmatrix} \tilde{G}^{(HH)}_{nm} \\ \tilde{G}^{(HH)}_{mn} \end{pmatrix} . \tag{2.7.2}$$

We use a vector inequality such as (2.7.2) to indicate that the comparison holds separately for each component.

Our argument so far has not invoked modular invariance. That is, we have not yet used the fact that $G^{(HH)}_{nm} + G^{(L)}_{nm} = \tilde{G}^{(HH)}_{nm} + \tilde{G}^{(L)}_{nm}$. We use it now. Since $\tilde{G}^{(L)}_{nm}$ is nonnegative, modular invariance implies $G^{(L)}_{nm} \geq \tilde{G}^{(HH)}_{nm} - G^{(HH)}_{nm}$, which in light of equation (2.7.2) implies

$$\begin{pmatrix} G^{(L)}_{nm} \\ G^{(L)}_{mn} \end{pmatrix} \geq \begin{pmatrix} 1 & -\delta \\ -\delta & 1 \end{pmatrix} \begin{pmatrix} \tilde{G}^{(HH)}_{nm} \\ \tilde{G}^{(HH)}_{mn} \end{pmatrix} . \tag{2.7.3}$$

One can multiply both sides of a strict vector inequality by a matrix as long as every element of the matrix is nonnegative. In particular as long as $|\delta| < 1$ we can multiplying both sides of (2.7.3) by the inverse of the matrix on the right hand side. The result is

$$\begin{pmatrix} \tilde{G}^{(HH)}_{nm} \\ \tilde{G}^{(HH)}_{mn} \end{pmatrix} \leq \frac{1}{1-\delta^2} \begin{pmatrix} 1 & \delta \\ \delta & 1 \end{pmatrix} \begin{pmatrix} G^{(L)}_{nm} \\ G^{(L)}_{mn} \end{pmatrix} . \tag{2.7.4}$$

Inequality (2.7.4) is the analog of (2.2.8) in the HKS argument. We now substitute (2.7.4) into the right hand side of the original inequality (2.7.2), a valid step because the matrix there has nonnegative elements, to get

$$\begin{pmatrix} G^{(HH)}_{nm} \\ G^{(HH)}_{mn} \end{pmatrix} \leq \frac{\delta}{1-\delta^2} \begin{pmatrix} \delta & 1 \\ 1 & \delta \end{pmatrix} \begin{pmatrix} G^{(L)}_{nm} \\ G^{(L)}_{mn} \end{pmatrix} . \tag{2.7.5}$$

The above relation is analogous to (2.2.9) in the HKS argument. The upper component is

$$G^{(HH)}_{nm} \leq \delta \frac{G^{(L)}_{mn} + \delta G^{(L)}_{nm}}{1-\delta^2} , \tag{2.7.6}$$

which is equation (2.4.20).

Chapter 3

Localized Excitations from Localized Unitary Operators

Localized unitary operators are basic probes of locality and causality in quantum systems: localized unitary operators create localized excitations in entangled states. Working with an explicit form, we explore properties of these operators in quantum mechanics and quantum field theory. We show that, unlike unitary operators, local non-unitary operators generically create non-local excitations. We present a local picture for quantum systems in which localized experimentalists can only act through localized Hamiltonian deformations, and therefore localized unitary operators. We demonstrate that localized unitary operators model certain quantum quenches exactly. We show how the Reeh-Schlieder theorem follows intuitively from basic properties of entanglement, non-unitary operators, and the local picture. We show that a recent quasi-particle picture for excited-state entanglement entropy in conformal field theories is not universal for all local operators. We prove a causality relation for entanglement entropy and connect our results to the AdS/CFT correspondence.

3.1 Introduction

In this work, we study correlation functions in time-dependent states and in theories with time-dependent Hamiltonians. Our results apply to pure states in quantum mechanics and local quantum field theory. Our primary goal is to detail the universal role of localized unitary operators in creating localized excitations. A brief overview of our results is as follows. Just as every observable is represented by some Hermitian operator, every localized excitation is created by some localized unitary operator. If a localized operator is non-unitary, the excitation it creates is not necessarily localized. For example, a localized unitary operator $e^{i\alpha\mathcal{O}(x)}$ creates a localized excitation while the localized non-unitary operator $e^{\alpha\mathcal{O}(x)}$ does not. Localized experimentalists can only act on states by deforming the Hamiltonian by a localized quantity, $H \to H + H_{loc}(t)$, and this is equivalent to acting with the Heisenberg-picture localized unitary operator $\mathcal{T}\left(e^{i\int dt\mathcal{H}_{loc}(t)}\right)$ on the state. As they create localized excitations, localized unitary operators are tied to basic questions of causality.

This manuscript extends contemporary studies of excited-state entanglement entropy in conformal field theories (CFTs) [61–68]. Our work builds upon the large body of work on localized excitations and real-time perturbation theory (see, for example, [69–79]). In addition to presenting our own results, we reinterpret some well-known results from this body of literature and from quantum information theory that are relevant. We revisit these results to give a coherent picture for the connection between localized unitary operators and localized excitations. We present all results in elementary terms and eschew a complete or axiomatic treatment of the topics discussed. Our purpose is to make contact with modern studies of entanglement entropy in CFT, and a more formal treatment of locality is outside the scope of this work.

While we explore how localized unitary operators create localized excitations, these operators play many other well-known roles in quantum systems. Specific forms of localized unitary operators create squeezed states, coherent states, generalized coherent states, and

implement local gauge transformations [80–84]. Localized unitary operators are also important in large-N and large-dimension limits in quantum mechanics, gauge theories, and the AdS/CFT correspondence.

We now summarize each section. In section 2, we define what we mean by localized and review related concepts. Suppose a Hilbert space $\mathcal{H}$ can be written as a tensor product Hilbert space $\mathcal{H} = \mathcal{H}_1 \otimes \mathcal{H}_2$. An excitation of state $|\Psi\rangle \in \mathcal{H}$ can be represented by acting with some operator $\mathcal{O}_e$ on $|\Psi\rangle$, where $\mathcal{O}_e$ is suitably normalized so that $\mathcal{O}_e|\Psi\rangle$ has unit norm. This excitation is localized in $\mathcal{H}_1$ if

$$\langle\Psi|\mathcal{O}_e^\dagger\mathcal{O}\mathcal{O}_e|\Psi\rangle = \langle\Psi|\mathcal{O}|\Psi\rangle \tag{3.1.1}$$

for all operators $\mathcal{O}$ local in $\mathcal{H}_2$. $\mathcal{O}$ is local in $\mathcal{H}_2$ when $\mathcal{O}$ can be written as

$$\mathcal{O} \equiv \mathbb{I}_1 \times \mathcal{O}_2. \tag{3.1.2}$$

Here $\mathbb{I}_1$ is the identity in $\mathcal{H}_1$ and $\mathcal{O}_2 : \mathcal{H}_2 \to \mathcal{H}_2$. In field theory, $\mathcal{H}_1, \mathcal{H}_2$ can be chosen as the Hilbert spaces of the theory restricted to a subregion A of a Cauchy surface and its complement A^c. An excitation localized to A does not affect correlation functions of operators inserted at points spacelike-separated from all points in A. The familiar local operators $\mathcal{O}(x)$ in field theory are localized to the Hilbert space of every arbitrarily small neighborhood of x. Localized operators can be built from operators that are local in different points or Hilbert spaces. For example, if $f(x)$ has support in region R, smeared operator $\int dx f(x)\mathcal{O}(x)$ is localized in R. We address subtleties involved in defining localization for gauge theories.

In section 3, we review real-time perturbation theory [69, 70]. This perturbation theory gives corrections to correlation functions in time-dependent states perturbatively in a time-dependent interaction Hamiltonian. Perturbation theory for the S-matrix calculates in-out matrix elements $\langle\Psi_{out}|\Psi_{in}\rangle$, while real-time perturbation theory calculates in-in matrix

elements $\langle \Psi_{in} | \mathcal{O}_1 \dots \mathcal{O}_n | \Psi_{in} \rangle$. Real-time perturbation theory makes manifest how localized interaction Hamiltonians create localized excitations.

In section 4, we present a coherent picture for time-dependent operations in quantum mechanics and field theory. We call this picture the local picture of quantum systems. In the local picture, an experimentalist can only alter states through deforming the Hamiltonian. A localized experimentalist can only make localized deformations. The excitations that are natural in the local picture are created by acting with a time-ordered localized unitary operator on a state, for example the Heisenberg-picture operator $\mathcal{T}\left(e^{i\int dt J(t)\mathcal{O}(t)}\right)$. As we show later, the familiar local non-unitary operators of field theory generically create non-localized excitations, so the local picture reveals that local experimentalists cannot act with generic local non-unitary operators.

In section 5, we present results in quantum mechanics. We show how local unitary operators alter entangled states locally, while local non-unitary operators alter entangled states non-locally. Local non-unitary operators can be written as state-dependent non-local unitary operators. In the language of quantum information, non-unitary operators implement non-local quantum gates. Our results explain the Reeh-Schlieder theorem intuitively. The superposition of two local excitations may not be a local excitation itself in entangled states. For instance, the sum of two unitary operators $\mathcal{U}_1 + \mathcal{U}_2$ is not necessarily unitary. We show that the natural way to combine localized excitations created by operators $\mathcal{U}_1, \mathcal{U}_2$ to produce another localized excitation is by acting with the operators in succession: $\mathcal{U}_1\mathcal{U}_2$. This prescription for combining localized excitations follows from the local picture.

In section 6, we move on to quantum field theory, our main focus. We show that localized unitary operators create localized excitations. The reason is as follows. If x, y are spacelike-separated, local operators $\mathcal{O}, \mathcal{O}'$ inserted at x, y commute:

$$[\mathcal{O}(x), \mathcal{O}'(y)] = 0. \tag{3.1.3}$$

It follows immediately that

$$\langle\Psi|e^{i\mathcal{O}(x)}\mathcal{O}'(y)e^{-i\mathcal{O}(x)}|\Psi\rangle = \langle\Psi|\mathcal{O}'(y)|\Psi\rangle\,. \tag{3.1.4}$$

If x, y are not spacelike-separated, then the above equality generically does not hold. For example, in the vacuum of a free real scalar field, the Baker-Campbell-Hausdorff lemma gives

$$\langle 0|e^{i\alpha\phi(x)}\phi(y)e^{-i\alpha\phi(x)}|0\rangle = i\alpha G_R(x-y) + \ldots, \tag{3.1.5}$$

where α can be treated as an expansion parameter and x is restricted to the future of y. The retarded Green's function $G_R(x-y)$ vanishes when $x-y$ is spacelike. More generally, the commutator of operators $\langle[\mathcal{O}(x), \mathcal{O}'(y)]\rangle$ diagnoses causality in field theory, and we see that this commutator is in fact the order α correction to $\langle\mathcal{O}'\rangle$ in the excited state $e^{-i\alpha\mathcal{O}(x)}\,|\Psi\rangle$. We explore the properties of localized unitary operators, including what we call separable and non-separable localized unitary operators. Separable unitary operators like $e^{i(\mathcal{O}(x)+\mathcal{O}(y))}$ create excitations at x, y that are not entangled with each other. Acting with non-separable unitary operators like $e^{i\mathcal{O}(x)\mathcal{O}(y)}$ create excitations at x, y that may be used to violate causality. As such, non-separable unitary operators cannot be applied to states under time evolution in local quantum field theory. We give a criterion to test separability.

We show that local non-unitary operators can create non-local excitations in field theory. We provide examples and show where the intuition that arbitrary local operators create local excitations breaks down. We provide evidence that certain local non-unitary operators do create local excitations and give examples of others that do not.

In section 7, we apply lessons from the previous sections to give new results concerning the entanglement entropy of excited states in field theory. Recently, a compelling quasi-particle picture has emerged from calculations of entanglement entropy in CFTs [61, 63–65, 85]. It has been suggested that local operators create entangled pairs of quasi-particles at their insertion point [64]. We provide evidence that this picture applies to local operators with

definite conformal dimension. It is known that the quasi-particle picture is invalid for certain theories [65,86], and using the example of the operator $e^{\alpha\mathcal{O}(x)}$, we show how this picture fails to extend to all local operators even within theories for which the picture is expected to be accurate. We extend a result in ref. [87] by proving a general causality relation for entanglement entropy.

3.2 Background: Locality in Quantum Systems

We will review locality and causality criteria in quantum mechanics and quantum field theory. Causality in field theory is a statement about the commutators of operators. If spacetime points x, y are spacelike-separated, then any two local operators $\mathcal{O}_1(x), \mathcal{O}_2(y)$ commute.

$$[\mathcal{O}_1(x), \mathcal{O}_2(y)] = 0. \tag{3.2.1}$$

An analogous statement holds if the operators are smeared out over some spacetime region. The vanishing of the commutator for spacelike separation is equivalent to a statement about the branch cuts of all Euclidean correlators that contain $\mathcal{O}_1, \mathcal{O}_2$.

We may state a locality condition based on whether local operations affect observables non-locally. We state a version of this condition first in quantum mechanics. Express the Hilbert space $\mathcal{H}$ of some system as a tensor product Hilbert space $\mathcal{H} = \mathcal{H}_A \otimes \mathcal{H}_B$ of subsystems A, B. First we define local operators.

Definition 1 *The operator $\mathcal{O}(B)$ is local in $\mathcal{H}_B$ when it can be written as*

$$\mathcal{O}(B) \equiv \mathbb{I}_A \otimes \mathcal{O}_B. \tag{3.2.2}$$

Here, $\mathcal{O}_B : \mathcal{H}_B \to \mathcal{H}_B$ and $\mathbb{I}_A$ is the identity in $\mathcal{H}_A$.

As we will show in section 5, acting with operator $\mathcal{O}(B)$ may change the expectation value of some operator $\mathcal{O}(A)$ local in $\mathcal{H}_A$, and therefore some measurement performed by an

experimentalist with access to subsystem A but not B. We define the relevant notions of local and non-local changes in state.

Definition 2 *Suppose operator $\mathcal{O}$ is normalized in a state $|\Psi\rangle$ so that $\langle\Psi|\mathcal{O}^\dagger\mathcal{O}|\Psi\rangle = 1$. Suppose also that there exists an operator $\mathcal{O}(B)$ local in $\mathcal{H}_B$ such that*

$$\langle\Psi|\mathcal{O}^\dagger\mathcal{O}(B)\mathcal{O}|\Psi\rangle \neq \langle\Psi|\mathcal{O}(B)|\Psi\rangle\,. \tag{3.2.3}$$

If for all $\mathcal{O}(A)$ local in $\mathcal{H}_A$,

$$\langle\Psi|\mathcal{O}^\dagger\mathcal{O}(A)\mathcal{O}|\Psi\rangle = \langle\Psi|\mathcal{O}(A)|\Psi\rangle\,, \tag{3.2.4}$$

then $\mathcal{O}$ changes the state $|\Psi\rangle$ locally in $\mathcal{H}_B$. Otherwise, $\mathcal{O}$ changes the state non-locally.

It should be understood that when we assess locality by expectation values of operators, we are considering only operators that correspond to observables. We can also assess locality with the reduced density matrix ρ_A. If acting with $\mathcal{O}$ does not change ρ_A, in other words

$$\rho_A(\mathcal{O}\,|\Psi\rangle) = \rho_A(|\Psi\rangle), \tag{3.2.5}$$

then $\mathcal{O}$ changes the state locally in $\mathcal{H}_B$. Local is a special case of localized. A localized operator is local in more than one Hilbert space.

The definitions we have given for local operators and changes in state apply to field theory. So-called local operators in field theory are local in the quantum-mechanical sense we have defined. Operator $\mathcal{O}(x)$ is local in $\mathcal{H}(x)$, the Hilbert space of the theory restricted to point x. When referring to local operators $\mathcal{O}(x)$, we will refer to the point x as the "insertion point" of $\mathcal{O}$. The insertion points of a Wilson loop are the points along its integration path. An operator inserted at multiple points is non-local. For example $\mathcal{O}(x)\mathcal{O}(y)$ is non-local but localized to x, y.

We define localized excitations in field theories. This definition is the same as definition

1 but we state it using field theory terminology for clarity. First, we define what we mean by an excitation.

Definition 3 *In field theory, we call $\mathcal{O}|\Psi\rangle$ an excitation of the state $|\Psi\rangle$ with operator $\mathcal{O}$.*

The following definition of localized excitations is also known as "strict localization" [72].

Definition 4 *Consider $\mathcal{O}(A)$ inserted in subregion A of a Cauchy surface. The complement of A on the Cauchy surface is subregion B. An operator $\mathcal{O}$ creates an excitation that is localized to B if*

$$\langle\Psi|\mathcal{O}^\dagger\mathcal{O}(A)\mathcal{O}|\Psi\rangle = \langle\Psi|\mathcal{O}(A)|\Psi\rangle \quad \forall \quad \mathcal{O}(A). \tag{3.2.6}$$

The definitions we provided extend in an obvious way to describe operators and excitations localized to a region of spacetime, rather than just a region of a Cauchy surface. A local excitation is an excitation that is localized to a single point. We will sometimes refer to local and non-local excitations of the state in quantum mechanics if we make statements that apply to both quantum mechanics and field theory. Various statements we will make also apply in a natural way to non-localized operators, which are operators inserted in every point in a Cauchy surface.

In gauge theories, we must fix a gauge before checking the above condition, or we may simply work in terms of gauge-invariant operators. We must also fix a gauge in order to use the reduced density matrix ρ_A to diagnose locality as the density matrix is not gauge-invariant. In this work, we will rarely mention these subtleties involved with gauge theories, as our statements can often be extended in an obvious way to these theories.

The ability to change a state through a non-local excitation should not be confused with the inability for localized experimentalists to transmit information between spacelike-separated entangled systems by performing local measurements. We will explain how these two features of locality are different and consistent in section 5.3.

We state the Reeh-Schlieder theorem, a theorem in quantum field theory that is important for understanding locality considerations. Consider the set of all operators $\mathcal{O}(B)$ that are

localized to an open subregion B of a Cauchy surface. These operators generate an algebra $\mathcal{A}(B)$ of the subregion B. The complement of B on the Cauchy surface is B^c. Suppose the Hilbert space of the theory on the full Cauchy surface is $\mathcal{H}$. Consider the vacuum state of some quantum field theory $|\Omega\rangle$. The Reeh-Schlieder theorem is that states $\mathcal{A}(B)\,|\Omega\rangle$ are dense in $\mathcal{H}$ [71]. In other words, one can act with operators that are localized to B to change the state in B^c. Moreover, acting with operators localized in B can prepare a state in B^c that is arbitrarily close to any state in $\mathcal{H}$ even if that state is an excitation localized entirely in B^c. The Reeh-Schlieder theorem is paradoxical if one assumes that any state $\mathcal{O}(B)\,|\Omega\rangle$ in principle represents the action of an experimentalist localized to region B on the state $|\Omega\rangle$. The Reeh-Schlieder theorem holds for states other than the vacuum as well. Standard references to the Reeh-Schlieder theorem, as well as other aspects of locality in algebraic and axiomatic quantum field theory include refs. [88, 89].

3.3 Background: Real-time Perturbation Theory

We review real-time perturbation theory, otherwise known as the in-in formalism [69, 70]. The formalism is called in-in in contrast to perturbation theory for S-matrix elements, which can be called in-out perturbation theory as it calculates transition amplitudes between initial and final states. Real-time perturbation theory calculates correlation functions

$$\langle\Psi|\mathcal{O}_1\dots\mathcal{O}_n|\Psi\rangle \tag{3.3.1}$$

perturbatively in an interaction Hamiltonian with arbitrary time dependence and makes aspects of locality and causality manifest. Beginning with some initial time-independent Hamiltonian H_0 and initial state $|\Psi(t_0)\rangle$, time evolution commences, and an interaction Hamiltonian may be turned on. The calculations proceed purely in Lorentzian signature, but the initial state $|\Psi(t_0)\rangle$ may be prepared in various standard ways including by Euclidean path integral. The real-time formalism is also known as the closed-time or Keldysh formalism

because the same calculation can be performed using a path integral with a closed-time (Keldysh) contour. The real-time formalism is an inherent part of cosmology and AdS/CFT [90–92].

Just as in-out perturbation theory may be obtained from a Euclidean path integral through Wick rotation, real-time perturbation theory may be obtained from the same Euclidean path integral by deforming the purely imaginary-time contour into a closed-time contour. Calculations proceed similarly for in-out and real-time perturbation theory, both in the use of Feynman diagrams and the treatment of divergences.

To illustrate how real-time perturbation theory works, we calculate the expectation value of Heisenberg-picture operator $\mathcal{O}(t, \mathbf{x})$ in a theory with a time-dependent interaction Hamiltonian $H_{\text{int}}(t)$. We work in $(d+1)$-dimensional spacetime throughout this manuscript. In defining the Heisenberg picture, we use reference time t_0. The associated Schrodinger-picture operator defined at time t_0 is $\mathcal{O}(t_0, \mathbf{x})$. The full Hamiltonian is

$$H(t) = H_0 + H_{\text{int}}(t), \tag{3.3.2}$$

where H_0 is time-independent. We use a perturbation that is zero at time t_0:

$$H_{\text{int}}(t_0) = 0. \tag{3.3.3}$$

We now work in the interaction picture, denoting interaction-picture operators with a subscript I. The interaction picture is defined in terms of Schrodinger-picture states and operators as

$$|\Psi_I(t)\rangle = e^{iH_0(t-t_0)} |\Psi(t)\rangle . \tag{3.3.4}$$

$$\mathcal{O}_I(t, \mathbf{x}) = e^{iH_0(t-t_0)} \mathcal{O}(t_0, \mathbf{x}) e^{-iH_0(t-t_0)}. \tag{3.3.5}$$

The interaction Hamiltonian $H_{\text{int}}(t)$ in the interaction picture is $H_I(t)$. As we are working

in real time, time evolution is unitary and preserves the norm of the state, which we choose to be $\langle\Psi(t_0)|\Psi(t_0)\rangle = 1$. The time evolution operator $\mathcal{U}(t,t_0)$ is

$$\mathcal{U}(t,t_0) = \mathcal{T}\left(e^{-i\int_{t_0}^{t} dt' H(t')}\right). \tag{3.3.6}$$

The interaction-picture evolution operator is

$$\mathcal{U}_I(t,t_0) = \mathcal{T}\left(e^{-i\int_{t_0}^{t} dt' H_I(t')}\right) = e^{iH_0(t-t_0)}\mathcal{U}(t,t_0). \tag{3.3.7}$$

We may now calculate $\langle\Psi(t_0)|\mathcal{O}(t,\mathbf{x})|\Psi(t_0)\rangle$ perturbatively in H_I. Explicitly,

$$\begin{aligned}\langle\Psi(t_0)|\mathcal{O}(t,\mathbf{x})|\Psi(t_0)\rangle &= \langle\Psi(t_0)|\mathcal{U}^\dagger(t,t_0)\mathcal{O}(t_0,\mathbf{x})\mathcal{U}(t,t_0)|\Psi(t_0)\rangle \\ &= \langle\Psi(t_0)|\left(\mathcal{U}^\dagger(t,t_0)e^{-iH_0(t-t_0)}\right)\left(e^{iH_0(t-t_0)}\mathcal{O}(t_0,\mathbf{x})e^{-iH_0(t-t_0)}\right) \\ &\qquad \times\left(e^{iH_0(t-t_0)}\mathcal{U}(t,t_0)\right)|\Psi(t_0)\rangle\,.\end{aligned} \tag{3.3.8}$$

Passing into the interaction picture,

$$\langle\Psi(t_0)|\mathcal{O}(t,\mathbf{x})|\Psi(t_0)\rangle = \langle\Psi(t_0)|\mathcal{U}_I^\dagger(t,t_0)\mathcal{O}_I(t,\mathbf{x})\mathcal{U}_I(t,t_0)|\Psi(t_0)\rangle\,. \tag{3.3.9}$$

Expanding in H_I,

$$\begin{aligned}\langle\Psi(t_0)|\mathcal{O}(t,\mathbf{x})|\Psi(t_0)\rangle = \langle\Psi(t_0)|\mathcal{O}(t_0,\mathbf{x})|\Psi(t_0)\rangle &+ i\int_{-\infty}^{t} dt_1\,\langle\Psi(t_0)|[H_I(t_1),\mathcal{O}_I(t,\mathbf{x})]|\Psi(t_0)\rangle \\ &- \int_{-\infty}^{t} dt_1\int_{-\infty}^{t_1} dt_2\,\langle\Psi(t_0)|[H_I(t_2),[H_I(t_1),\mathcal{O}_I(t,\mathbf{x})]]|\Psi(t_0)\rangle + \ldots.\end{aligned} \tag{3.3.10}$$

The all-order expression for real-time perturbation theory is given by Weinberg [91].

$$\langle\Psi(t_0)|\mathcal{O}(t,\mathbf{x})|\Psi(t_0)\rangle = \sum_{N=0}^{\infty} i^N \int_{-\infty}^{t} dt_N \int_{-\infty}^{t_N} dt_{N-1} \ldots \int_{-\infty}^{t_2} dt_1 \times \langle\Psi(t_0)|\left[H_I(t_1),[H_I(t_2),[\ldots[H_I(t_N),\mathcal{O}_I(t,\mathbf{x})]\ldots]\right]|\Psi(t_0)\rangle\,. \tag{3.3.11}$$

The interaction-picture operators are the Heisenberg-picture operators of the unperturbed theory at time t_0.

Real-time perturbation theory makes manifest how turning on a localized interaction creates a localized excitation. Suppose the interaction Hamiltonian is given by some local operator $\mathcal{O}'$ smeared over a spatial region:

$$H_I(t') = \int d^d y f(t',\mathbf{y})\mathcal{O}'_I(t',\mathbf{y}). \tag{3.3.12}$$

The interaction $H_I(t')$ can only change $\langle\mathcal{O}(t,\mathbf{x})\rangle$ if $f(t',\mathbf{y})$ has support on points that are null or time-like separated from the point $(t,\mathbf{x})$. Only the perturbations for which $t' \leq t$ contribute. If $f(t',\mathbf{y})$ has support only at points spacelike-separated from the point $(t,\mathbf{x})$, then

$$[H_I(t'),\mathcal{O}_I(t,\mathbf{x})] = 0. \tag{3.3.13}$$

Each term in (3.3.11) will also vanish for the same reason.

Suppose H_0 is a free Hamiltonian and $|\Psi(t_0)\rangle = |0\rangle$, the vacuum of H_0. At each order in perturbative expansion, the nested commutators will produce various contractions multiplied by an overall retarded Green's function $G_R(x-y)$, which has precisely the correct causality properties. Diagrammatic rules that make retarded Green's functions manifest are discussed in ref. [93]. In practice, one can obtain the different terms in (3.3.11) from different analytic continuations of the appropriate Euclidean correlators. The structure of real-time perturbation theory and the presence of retarded Green's functions parallels a problem in

classical field theory, calculating corrections to the value of a free field perturbatively in a source.

3.4 A Local Picture for Time-Dependent Quantum Systems

We present a coherent picture for time-dependent operations on pure states in quantum systems. We will refer to this picture as the "local picture". This picture is generated by the assumptions that all physical interactions occur through terms in the Hamiltonian, and localized experimentalists deform the Hamiltonian in a localized region. We define the local picture because it unites several different manifestations of locality and causality into one concrete framework. The local picture will provide simple explanations for results in later sections.

We first briefly review the two types of systems we may consider in quantum mechanics. Closed quantum systems are pure states that undergo unitary time evolution. For example, the Hilbert space of a closed quantum system $\mathcal{H}$ may be a tensor-product Hilbert space of a system, experimentalist, and environment:

$$\mathcal{H} = \mathcal{H}_{\text{env}} \otimes \mathcal{H}_{\text{exp}} \otimes \mathcal{H}_{\text{sys}}. \tag{3.4.1}$$

The experimentalist can be described as an observer and an interaction apparatus:

$$\mathcal{H}_{\text{exp}} = \mathcal{H}_{\text{obs}} \otimes \mathcal{H}_{\text{app}}. \tag{3.4.2}$$

Open quantum systems are systems that can be acted upon by some external experimentalist. Pure states of an open quantum system are elements of the Hilbert space $\mathcal{H}_{\text{sys}}$. In closed quantum systems, measurement is described by an interaction term in the Hamiltonian that entangles states between $\mathcal{H}_{\text{exp}}, \mathcal{H}_{\text{sys}}$. This is a unitary process and there is no state collapse. Projecting onto one of the states in $\mathcal{H}_{\text{exp}} \otimes \mathcal{H}_{\text{sys}}$ shows the state that one particular

experimentalist has access to. In an open quantum system, this measurement process is modelled by projection operators that implement the collapse of the state, which is the Copenhagen interpretation of quantum mechanics, together with a re-normalization of the state. In principle, an open quantum system can be obtained from a closed quantum system, and the details of this process are the subject of current research. We will assume this well-known description is valid formally. In short, to describe the measurement process without collapse and state re-normalization, we must use the closed quantum system. To describe operations performed on the state by an external experimentalist and calculate expectation values, the open quantum system is the natural choice.

We now state the local picture, which governs the evolution of the pure state $|\Psi(t_0)\rangle$ of some system prepared at time t_0. Physical operations on the state are described by deformations of the Hamiltonian. Any norm-preserving operation can be treated as a Hamiltonian deformation, but deforming the Hamiltonian by functions of local operators are natural ways to implement physical operations. Localized experimentalists can only deform the Hamiltonian by localized operators, and therefore only act with localized unitary operators on the state. Operators that create non-localized excitations can only be implemented by non-localized experimentalists. Non-localized experimentalists are experimentalists that have access to the entire Cauchy surface, and should not be confused with experimentalists who may depart from the principles of local quantum field theory. We have given the local picture for open quantum systems, but these principles describe closed quantum systems as well.

We give an example that makes the elements of the local picture concrete and shows how they arise. We work in quantum field theory for convenience. The expectation value of operator $\mathcal{O}(\mathbf{x}, t)$ evolves as

$$\langle \mathcal{O}(\mathbf{x}, t) \rangle = \langle \Psi(t_0) | \mathcal{U}^\dagger(t, t_0) \mathcal{O}(\mathbf{x}, t_0) \mathcal{U}(t, t_0) | \Psi(t_0) \rangle \,. \tag{3.4.3}$$

In order to describe the effect of some interaction Hamiltonian H_{int}, we may pass into the

interaction picture. As we reviewed in section 3,

$$\langle\Psi(t_0)|\mathcal{O}(t,\mathbf{x})|\Psi(t_0)\rangle = \langle\Psi(t_0)|\mathcal{U}_I^\dagger(t,t_0)\mathcal{O}_I(t,\mathbf{x})\mathcal{U}_I(t,t_0)|\Psi(t_0)\rangle \tag{3.4.4}$$

The above expresion is equivalent to the following calculation, in the Heisenberg picture defined by evolution from t_0 with Hamiltonian H_0:

$$\begin{aligned}\langle\mathcal{O}(t,\mathbf{x})\rangle &= \langle\Psi_e|\mathcal{O}(t,\mathbf{x})|\Psi_e\rangle\,,\\ |\Psi_e\rangle &\equiv \mathcal{T}\left(e^{-i\int_{t_0}^{t}dt'\mathcal{H}_{int}(t')}\right)|\Psi(t_0)\rangle\,.\end{aligned} \tag{3.4.5}$$

We use $\mathcal{H}_{int}$ to denote H_{int} in the Heisenberg picture. It is therefore natural that localized unitary operators $\mathcal{U}$ of the form

$$\mathcal{U} = \mathcal{T}\left(e^{-i\int_{t_0}^{t}dt'\mathcal{H}_{int}(t')}\right) \tag{3.4.6}$$

create localized excitations, and this follows from real-time perturbation theory. This conclusion is independent of perturbation theory, as we will show in Section 6.

As we have shown, there is a correspondence between excitations of the state and Hamiltonian deformations. We focus on localized unitary operators, but this correspondence holds for non-localized unitary operators and their associated non-localized Hamiltonian deformations in the same way. Localized Hamiltonian deformations take the form of local operators smeared over some compact spacetime region, as in equation (3.3.12), while for non-localized Hamiltonian deformations the smearing function has support on all of spacetime. It is of course not obvious how to find an explicit $\mathcal{H}_{int}$ or unitary operator $\mathcal{U}$ to represent the action of an arbitrary operator $\mathcal{N}\mathcal{O}$ on a state. Here $\mathcal{N}$ is the state-dependent normalization constant $|\mathcal{N}|^2 = 1/\langle\Psi(t_0)|\mathcal{O}^\dagger\mathcal{O}|\Psi(t_0)\rangle$.

We comment on what an experimentalist cannot easily do according to the principle that she may only interact with the system through $\mathcal{H}_{int}$. At any given time, she may only

interact with the state through operators evaluated at that time, and interactions that last for some finite time must be time-ordered. Other operations, while mathematically valid, are not as natural. For example, it is natural to act with the operator $\mathcal{U}_1$ but not $\mathcal{U}_2$:

$$\mathcal{U}_1 = \mathcal{T}\left(e^{-i\int dt\mathcal{O}(t)}\right)$$
$$\mathcal{U}_2 = e^{-i\int dt\mathcal{O}(t)}$$

Calculating correlation functions of operators $\mathcal{O}(t)$ at time t represents experiments conducted at t, and excitation of the state that occur after this time do not contribute. These naturalness conditions for operator excitations follow automatically from the local picture.

The local picture reveals that localized experimentalists cannot act with operators that create non-localized excitations. If the experimentalist is localized to some spacelike region, she can only use $\mathcal{H}_{int}$ also localized in this region, which means acting with unitary operators localized to that same region. These operators create localized excitations. In sections 5 and 6, we will find that local non-unitary operators $\mathcal{N}\mathcal{O}$ can create non-localized excitations, and so a localized experimentalist cannot act with these operators. In fact, if $\mathcal{O}$ creates a non-local excitation, the experimentalist must know the state on the entire Cauchy surface in order to calculate $\mathcal{N}$. Operator $\mathcal{N}\mathcal{O}$ can only be acted on the state by a non-localized experimentalist. An example of such an operator is a normalized projection operator that implements a measurement, but to discuss locality in the context of measurements, one is using a closed quantum system either implicitly or explicitly. Projection operators in an open quantum system are simply models of the process. We will discuss measurements explicitly in a later section.

3.5 Localized Unitary and Non-unitary Operators in Quantum Mechanics

We discuss unitary and non-unitary operators in quantum mechanics. Locality properties of operators depend on whether or not they are unitary. Our conclusions in quantum mechanics apply to quantum field theory as well. For a Hilbert space $\mathcal{H} = \mathcal{H}_1 \otimes \mathcal{H}_2$, we address whether acting with an operator local in $\mathcal{H}_1$ may affect expectation values taken in $\mathcal{H}_2$. In this section, we will use a two-particle system of spin 1/2 particles, where the particles are prepared in product and entangled states. We label the two spin states as $|\pm\rangle$.

Non-unitary operators generically do not preserve the normalization of states, so to represent their action on the state, we must include a normalization factor along with each operator. This normalization factor must be state-dependent, and so in general non-unitary operators are state-dependent. We will refer to these norm-preserving non-unitary operators as non-unitary operators for short.

Consider an operator local in $\mathcal{H}_2$:

$$\mathcal{O} = \mathbb{I}_1 \otimes \mathcal{O}_2. \tag{3.5.1}$$

We will act with $\mathcal{O}$ on different states and calculate the reduced density matrix of particle 1, ρ_1. If ρ_1 changes, $\mathcal{O}$ has changed the state non-locally. Following the examples, we will prove various general results. The proofs are elementary, and we use elementary methods in order to make certain properties explicit.

We will refer to product states and entangled states of, for example, $\mathcal{H}$. A state $|\Psi\rangle \in \mathcal{H}$ is a product state if there exist states $|\Psi_1\rangle \in \mathcal{H}_1, |\Psi_2\rangle \in \mathcal{H}_2$ such that $|\Psi\rangle = |\Psi_1\rangle \otimes |\Psi_2\rangle$. Product states are also known as separable states. A pure state that is not a product state is entangled.

3.5.1 Local operators create local excitations in product states

In this section, we show how both local unitary and non-unitary operators change product states locally. We show an example and then prove this statement. Choose $\mathcal{O}_2$ to be diagonal for convenience:

$$\mathcal{O}_2 = \mathcal{N} \begin{pmatrix} a & 0 \\ 0 & b \end{pmatrix}. \tag{3.5.2}$$

Here, $a, b \in \mathbb{C}$. If a, b are pure phases then $\mathcal{O}_2$ is unitary. Here $\mathcal{N}$ is a normalization factor.

First, consider the product state

$$|\Psi^p\rangle = |+\rangle_1 |-\rangle_2 . \tag{3.5.3}$$

The reduced density matrix ρ_1^p is

$$\rho_1^p = |+\rangle \langle +| . \tag{3.5.4}$$

Acting with $\mathcal{O}$,

$$\mathcal{O} |\Psi^p\rangle = \mathcal{N} |+\rangle_1 (b |-\rangle_2) \equiv |\Psi^{p'}\rangle . \tag{3.5.5}$$

To normalize the state, $|\mathcal{N}|^2 = 1/|b|^2$. The reduced density matrix is unchanged:

$$\rho_1^{p'} = |+\rangle \langle +| . \tag{3.5.6}$$

Acting with $\mathcal{O}$ does not change measurements performed on particle 1 regardless of what values a, b take.

We now prove that all local operators, including non-unitary operators, change product states locally. Consider two Hilbert spaces $\mathcal{H}_{1,2}$ and n orthonormal basis elements $|\psi_{1,2}^n\rangle$. Consider the arbitrary product state $|\Psi_p\rangle \in \mathcal{H}$ with $\mathcal{H} = \mathcal{H}_1 \otimes \mathcal{H}_2$, and an arbitrary norm-

preserving operator $\mathcal{O}$ local in $\mathcal{H}_2$.

$$|\Psi_p\rangle = \sum_i c_1^i \, |\psi_1^i\rangle \sum_j c_2^j \, |\psi_2^j\rangle \, . \tag{3.5.7}$$

The state is normalized:

$$\left(\sum_i |c_1^i|^2 \right) \times \left(\sum_j |c_2^j|^2 \right) = 1. \tag{3.5.8}$$

The reduced density matrix associated with $\mathcal{H}_1$ is

$$\rho_1 = \left(\sum_i c_1^i \, |\psi_1^i\rangle \right) \left(\sum_k c_1^{k*} \, \langle \psi_1^k | \right) \sum_j |c_2^j|^2. \tag{3.5.9}$$

Acting with $\mathcal{O}$ on the state,

$$\mathcal{O} \, |\Psi\rangle = \sum_i c_1^i \, |\psi_1^i\rangle \sum_j d_2^j \, |\psi_2^j\rangle \, , \tag{3.5.10}$$

where the d_2^j are defined by the action of $\mathcal{O}$ on states in $\mathcal{H}_2$ in the chosen basis: $d_2^j \equiv \sum_i \mathcal{O}_{ji} c_2^i$. The normalization condition is

$$\left(\sum_i |c_1^i|^2 \right) \times \left(\sum_j |d_2^j|^2 \right) = 1. \tag{3.5.11}$$

Acting with $\mathcal{O}$ is a unitary operation in $\mathcal{H}_2$:

$$\sum_j |d_2^j|^2 = \sum_j |c_2^j|^2. \tag{3.5.12}$$

We may see that the new reduced density matrix ρ_1' is equal to ρ_1:

$$\begin{aligned}\rho_1' &= \left(\sum_i c_1^i \left|\psi_1^i\right\rangle\right)\left(\sum_k c_1^{k*} \left\langle\psi_1^k\right|\right)\sum_j |d_2^j|^2 \\ &= \left(\sum_i c_1^i \left|\psi_1^i\right\rangle\right)\left(\sum_k c_1^{k*} \left\langle\psi_1^k\right|\right)\sum_j |c_2^j|^2 = \rho_1. \end{aligned} \tag{3.5.13}$$

This concludes the proof.

3.5.2 Locality in entangled states

In entangled states, local unitary operators affect the state locally but local non-unitary operators may affect the state non-locally. As an example, we will act with $\mathcal{O}$ on entangled state $|\Psi_e\rangle$ and find that generically $\mathcal{O}$ will change the state non-locally unless $\mathcal{O}_2$ is unitary.

$$|\Psi^e\rangle = \frac{1}{\sqrt{2}}(|+\rangle_1 |-\rangle_2 - |-\rangle_1 |+\rangle_2). \tag{3.5.14}$$

The reduced density matrix ρ_1^e is

$$\rho_1^e = \frac{1}{2}(|+\rangle\langle+| + |-\rangle\langle-|). \tag{3.5.15}$$

Acting with $\mathcal{O}$ on the state $|\Psi^e\rangle$ gives

$$\mathcal{O}|\Psi^e\rangle = \frac{\mathcal{N}}{\sqrt{2}}(b|+\rangle_1|-\rangle_2 - a|-\rangle_1|+\rangle_2) \equiv |\Psi^{e'}\rangle\,. \tag{3.5.16}$$

The normalization factor satisfies $|\mathcal{N}|^2 = \frac{2}{|a|^2+|b|^2}$. The reduced density matrix is now

$$\rho_1^{e'} = \frac{1}{|a|^2+|b|^2}(|b|^2|+\rangle\langle+| + |a|^2|-\rangle\langle-|). \tag{3.5.17}$$

Acting with $\mathcal{O}$ changes ρ_1^e unless $|a|^2 = |b|^2$, which would make $\mathcal{O}_2$ unitary.

Local operators mix states within $\mathcal{H}_2$, but if these states are coupled with different weights

to states in a different Hilbert space $\mathcal{H}_1$, mixing states within $\mathcal{H}_2$ will generically change the relative weights of the states in $\mathcal{H}_1$. Only local unitary operators mix states in $\mathcal{H}_2$ in the way that leaves the partial trace unchanged.

The action of any non-unitary operator $\mathcal{N}\mathcal{O}$ on a state may by definition be written as a unitary operator $\mathcal{U}$ acting on the state. In the state $|\Psi\rangle$, $|\mathcal{N}|^2 = \langle\Psi|\mathcal{O}^\dagger\mathcal{O}|\Psi\rangle^{-1}$. For every $\mathcal{O}$ and $|\Psi\rangle$ there exists a unitary operator $\mathcal{U}$ such that

$$\mathcal{N}\mathcal{O}\,|\Psi\rangle = \mathcal{U}\,|\Psi\rangle\,. \tag{3.5.18}$$

This equality follows from the fact that acting with $\mathcal{N}\mathcal{O}$ does not change the norm of the state. It follows that this norm-preserving operation on a state can be implemented by acting with some unitary operator $\mathcal{U}$, as the set of all unitary operators is the space of all possible norm-preserving operations on the state. The non-unitary operator $\mathcal{N}\mathcal{O}$ is of course not equal to the corresponding unitary operator $\mathcal{U}$, but their actions on the state $|\Psi\rangle$ are the same. The same $\mathcal{O}$ is represented by different $\mathcal{U}$ on different states $|\Psi\rangle$. If the operator $\mathcal{O}$ changes the state non-locally, $\mathcal{U}$ is non-local. The equivalence between non-unitary and unitary operators acting on the state shows how non-unitary operators may be applied to a state through time evolution. According to the local picture, the unitary operator $\mathcal{U}$ is applied by a non-local experimentalist with access to both systems, as $\mathcal{U}$ is not local in $\mathcal{H}_1$ or $\mathcal{H}_2$ alone.

Let us see an explicit example of the equivalence between non-unitary and unitary operators using the operator $\mathcal{O}$ and state $|\Psi^e\rangle$. We now work in the basis of the full Hilbert space: $(|+\rangle|+\rangle, |+\rangle|-\rangle, |-\rangle|+\rangle, |-\rangle|-\rangle)$ where we have dropped the subscripts $1, 2$. We wish to find a unitary operator $\mathcal{U}$ that satisfies the following:

$$\mathcal{U}\,|\Psi^e\rangle = \mathcal{O}\,|\Psi^e\rangle\,. \tag{3.5.19}$$

Writing this condition in the chosen basis,

$$\mathcal{O}\left|\Psi\right\rangle = \mathcal{N}\frac{1}{\sqrt{2}}\begin{pmatrix}0\\ b\\ -a\\ 0\end{pmatrix} = \mathcal{U}\frac{1}{\sqrt{2}}\begin{pmatrix}0\\ 1\\ -1\\ 0\end{pmatrix} = \mathcal{U}\left|\Psi\right\rangle. \tag{3.5.20}$$

We can now write down a solution. $\mathcal{U}$ rotates components into one another, and may produce an arbitrary phase.

$$\mathcal{U}(\theta,\phi_1,\phi_2) = \begin{pmatrix}1 & 0 & 0 & 0\\ 0 & e^{i\phi_1}\cos\theta & -e^{i\phi_2}\sin\theta & 0\\ 0 & e^{i\phi_1}\sin\theta & e^{i\phi_2}\cos\theta & 0\\ 0 & 0 & 0 & 1\end{pmatrix}. \tag{3.5.21}$$

The above matrix is the product of the rotation matrix with $\mathrm{diag}(1, e^{i\phi_1}, e^{i\phi_2}, 1)$. The relations between the angles and a, b are:

$$e^{i\phi_1}\cos\theta + e^{i\phi_2}\sin\theta = b\mathcal{N} \tag{3.5.22}$$

$$e^{i\phi_1}\sin\theta - e^{i\phi_2}\cos\theta = -a\mathcal{N}. \tag{3.5.23}$$

Elements $a\mathcal{N}, b\mathcal{N}$ have three degrees of freedom: an overall phase, a relative phase, and a relative magnitude. Operator $\mathcal{U}$ has the same three degrees of freedom as well: two phases ϕ_1, ϕ_2, the angle θ that controls the components' magnitudes. The normalization condition $(|a\mathcal{N}|^2 + |b\mathcal{N}|^2)/2 = 1$ is satisfied. We see that the unitary operator $\mathcal{U}$ depends on $\mathcal{O}$ and the state.

We will now show that local unitary operators change entangled states locally and generic local non-unitary operators change entangled states non-locally. This is an elementary property of the partial trace, but we will find a proof in component notation useful. We begin

with an arbitrary entangled state $|\Psi_e\rangle$. We use repeated index summation notation in this proof. Label states in $\mathcal{H}_{1,2}$ by $|\psi_{1,2}\rangle$.

$$|\Psi_e\rangle = C_{ia} |\psi_1^i\rangle |\psi_2^a\rangle . \tag{3.5.24}$$

The normalization condition is $C_{ai}^\dagger C_{ai} = 1$. The reduced density matrix of $\mathcal{H}_1$ is

$$\rho_1 = C_{ia} C_{aj}^\dagger |\psi_1^i\rangle \langle\psi_1^j| . \tag{3.5.25}$$

Now act with an operator $\mathcal{O}$ that is local in $\mathcal{H}_2$ on the state.

$$|\Psi_e\rangle = \mathcal{O}_{ba} C_{ia} |\psi_1^i\rangle |\psi_2^b\rangle . \tag{3.5.26}$$

Assume that $\mathcal{O}$ is normalized to satisfy the normalization condition $C_{di}^\dagger \mathcal{O}_{db}^\dagger \mathcal{O}_{ba} C_{ia} = 1$. If $\mathcal{O}^\dagger = \mathcal{O}^{-1}$ then $\mathcal{O}_{db}^\dagger \mathcal{O}_{ba} = \mathbb{I}_{da}$ and the state's norm is automatically preserved. The new reduced density matrix ρ_1' is

$$\rho_1' = C_{dj}^\dagger \mathcal{O}_{db}^\dagger \mathcal{O}_{ba} C_{ai} |\psi_1^i\rangle \langle\psi_1^j| . \tag{3.5.27}$$

If operator $\mathcal{O}$ is unitary, then $\rho_1' = \rho_1$. If not, the state may change non-locally. In the language of quantum information, non-unitary operators $\mathcal{O}$ implement non-local quantum gates, as $\mathcal{O}$'s action can be represented by a non-local unitary operator.

There are states for which non-unitary operators acting on a subspace do leave ρ_1 unchanged. Suppose that for $a > k$, $C_{ai} = 0$ for every i. To leave ρ_1 unchanged, $(\mathcal{O}^\dagger \mathcal{O})_{db} = \mathbb{I}_{db}$ for $d, b \leq k$ suffices, but this condition not necessary for $d, b > k$. A simple example is if $\mathcal{O}$ is local and unitary in subspace $P \in \mathcal{H}$ but non-unitary in the rest of $\mathcal{H}$: $\mathcal{O}$ will create a local excitation of states in P despite being non-unitary. When the two Hilbert spaces have the same dimensionality, such states require the density matrix to have at least one zero

eigenvalue.

We have not addressed the most general condition for operators to leave entanglement entropy unchanged, which is a weaker condition than leaving ρ_1 unchanged, and an interesting direction for future work. Entanglement entropy is the von Neumann entropy of a reduced density matrix. The entanglement entropy S_1 of the subsystem with Hilbert space $\mathcal{H}_1$ is

$$S_1 = -\text{tr}(\rho_1 \ln \rho_1) \tag{3.5.28}$$

In a pure state, entanglement entropies for the two subsystems must be equal: $S_1 = S_2$. It follows that acting with a local unitary operator on one subsystem or the other does not change S_1, S_2 because the density matrix of the subsystem not acted upon is unchanged.

There can be local non-unitary operators $\mathcal{O}$ that alter a state $|\Psi\rangle$ non-locally, but leave expectation values of operators $\mathcal{O}'$ unchanged. In field theory this condition is sometimes satisfied by the modular Hamiltonian, $\mathcal{O}' = -\ln(\rho_1)$, whose expectation value is entanglement entropy [64]. It would be interesting to investigate this question further in quantum mechanics and field theory to understand the basis of the apparent quasi-particle picture for entanglement entropy.

3.5.3 Causality, non-local state preparation, and Reeh-Schlieder

So far, we have shown how local non-unitary operators act as unitary operators on entangled states, and that these unitary operators must be non-local. According to the local picture, operators that change states non-locally can only be implemented by non-local experimentalists. Experimentalists act with the non-local unitary operators through time evolution. Non-unitary operators are intrinsically non-local in entangled states.

Our results can be viewed another way, motivated by the Reeh-Schlieder theorem in field theory. In a state in $\mathcal{H} = \mathcal{H}_1 \otimes \mathcal{H}_2$ that is entangled between $\mathcal{H}_1, \mathcal{H}_2$, non-unitary operators

$\mathcal{O}$ local in $\mathcal{H}_2$ can prepare states in $\mathcal{H}_1$. We may see how this works for $|\Psi^e\rangle$.

$$|\Psi^e\rangle = \frac{1}{\sqrt{2}}(|+\rangle_1 |-\rangle_2 - |-\rangle_1 |+\rangle_2). \tag{3.5.29}$$

We may use suitably normalized operators $L_\pm, L_z$ acting on particle 2 that are the angular momenta operators for spin 1/2 particles. Ignoring the overall normalizations,

$$\begin{aligned} L_+ |\Psi^e\rangle &= |+\rangle_1 |+\rangle_2 . \\ L_- |\Psi^e\rangle &= |-\rangle_1 |-\rangle_2 . \\ (1 + L_z) |\Psi^e\rangle &= |-\rangle_1 |+\rangle_2 . \\ (1 - L_z) |\Psi^e\rangle &= |+\rangle_1 |-\rangle_2 . \end{aligned} \tag{3.5.30}$$

Our results show that seemingly counter-intuitive features of the Reeh-Schlieder theorem are perfectly straightforward in quantum mechanics. The fact that local non-unitary operators create non-local excitations in entangled states is the origin of the non-local state preparation in the Reeh-Schlieder theorem. The theorem is consistent with causality because local experimentalists act only with local unitary operators, which do not permit non-local state preparation. The example we gave of preparing a state non-locally was used as a quantum-mechanical model for the Reeh-Schlieder theorem in the leading interpretation [75]. Discussions of the Reeh-Schlieder theorem have previously been centered on non-local state preparation through measurements in open quantum systems.

Our conclusions about the non-locality of non-unitary operators may appear to contradict a standard statement of causality for entangled states that allows non-local changes in state, but in fact the two are compatible. Measurements in an open quantum system can be described in the associated closed quantum system by projecting onto an experimentalist-system state with a particular measurement outcome. It is obvious that replacing a superposition of states with one of its constituent states is a non-local change of state, but questions

of locality are more clearly formulated in the closed quantum system, in which it is manifest how measurement does not change states non-locally. These statements are standard, but for completeness we now make them concrete with an explicit example.

Consider an initial state of a closed quantum system with Hilbert space $\mathcal{H} = \mathcal{H}_{\text{exp}} \otimes \mathcal{H}_{\text{sys}}$,

$$|\Psi\rangle = |\Psi^1_{\text{exp}}\rangle \, |\Psi^2_{\text{exp}}\rangle \, (a \, |+\rangle_1 \, |-\rangle_2 - b \, |-\rangle_1 \, |+\rangle_2). \tag{3.5.31}$$

We label the experimentalists by the outcome they observe as $|\Psi_{\text{exp}}(\pm)\rangle$. After experimentalist 2 measures the spin of particle 2, the state is

$$|\Psi\rangle' = |\Psi^1_{\text{exp}}\rangle \, (a \, |\Psi^2_{\text{exp}}(-)\rangle \, |+\rangle_1 \, |-\rangle_2 - b \, |\Psi^2_{\text{exp}}(+)\rangle \, |-\rangle_1 \, |+\rangle_2). \tag{3.5.32}$$

Experimentalist 1 may now measure the spin of particle 1. Once again, this is an interaction that couples experimentalist states to system states. The new state is

$$|\Psi\rangle'' = a \, |\Psi^1_{\text{exp}}(+)\rangle \, |\Psi^2_{\text{exp}}(-)\rangle \, |+\rangle_1 \, |-\rangle_2 - b \, |\Psi^1_{\text{exp}}(-)\rangle \, |\Psi^2_{\text{exp}}(+)\rangle \, |-\rangle_1 \, |+\rangle_2). \tag{3.5.33}$$

We now could project onto various states to determine what each experimentalist measures. However, tracing out experimentalist 2 and particle 2, the reduced density matrix $\rho_{\text{exp}_1 \otimes \text{sys}_1}$ for experimentalist 1 and particle 1 is

$$\rho_{\text{exp}_1 \otimes \text{sys}_1} = |a|^2 \left(|\Psi^1_{\text{exp}}(+)\rangle \, |+\rangle \, \langle +| \, \langle \Psi^1_{\text{exp}}(+)| \right) + |b|^2 \left(|\Psi^1_{\text{exp}}(-)\rangle \, |-\rangle \, \langle -| \, \langle \Psi^1_{\text{exp}}(-)| \right). \tag{3.5.34}$$

The reduced density matrix is unchanged by the measurement that experimentalist 2 performed. The unitary operator that implements experimentalist 2's measurement is localized to $\mathcal{H}^2_{\text{sys}} \otimes \mathcal{H}^2_{\text{exp}}$, and so it does not change $\rho_{\text{exp}_1 \otimes \text{sys}_1}$.

3.5.4 Superpositions of localized excitations

In entangled states, the superposition of two localized excitations is generically not itself a localized excitation. One can represent each localized excitation as a localized unitary operator acting on some reference state. The sum of two unitary operators need not be unitary, and so their superposition need not create a localized excitation. For example, by adding two unitary matrices of the form $\mathrm{diag}(e^{i\phi_1}, e^{i\phi_2})$, we may change the magnitude of the sum's diagonal entries. The non-locality of the superposition measures a kind of interference between the two unitary operators. We can state the general condition for which the superposition of localized excitations implemented by $\mathcal{U}_1, \mathcal{U}_2$ must itself be a localized excitation in entangled states.

$$\mathcal{U}_1\mathcal{U}_2^\dagger + \mathcal{U}_2\mathcal{U}_1^\dagger = 0 \tag{3.5.35}$$

We will not explore this condition. It follows that a local experimentalist cannot superimpose two local excitations of an entangled state. The condition for superpositions of local unitary operators to be local has been addressed on a more formal level [73].

There is a natural way to combine local excitations without superposition. Acting with two localized unitary operators on the same state creates a localized excitation. For example, the operator $\mathcal{U}_1\mathcal{U}_2$ creates an excitation localized to the same Hilbert spaces in which $\mathcal{U}_1, \mathcal{U}_2$ are localized. In the local picture, these two operators should be time-ordered: $\mathcal{T}(\mathcal{U}_1\mathcal{U}_2)$. This method of combining local excitations is natural in the local picture, as it corresponds to an interaction that occurs in two subsystems: $\mathcal{T}\left(e^{i(\mathcal{O}_1+\mathcal{O}_2)}\right)$ and is implemented by turning on sources for both $\mathcal{O}_1$ and $\mathcal{O}_2$. We will elaborate on this point in a later section when we discuss separable and non-separable localized unitary operators.

Superpositions of local unitary operators create non-local excitations, which are associated more naturally with non-unitary operators. This relationship between unitary and non-unitary operators can be viewed from another direction. Non-unitary operators can be written as superpositions of unitary operators. Acting with a non-unitary operator is

equivalent to superimposing states formed by acting with unitary operators. As is standard, any operator $\mathcal{O}$ can be written as a linear combination of an Hermitian operator H_+ and anti-Hermitian operator H_-.

$$\mathcal{O} = H_+ + H_-. \tag{3.5.36}$$

$$H_\pm = \frac{1}{2}(\mathcal{O} \pm \mathcal{O}^\dagger). \tag{3.5.37}$$

In fact, H_- can be written in terms of a Hermitian operator H'_+ simply: $H'_+ = iH_-$. We now show that any Hermitian operator can be written in terms of a unitary operator and its adjoint, subject to a certain condition. Suppose the spectrum of some Hermitian operator H is bounded from above and below. This is not always the case for the Hamiltonian, but this is true for many other operators, especially those relevant in systems with a finite number of spins. There exists λ which is at least as large as H's largest-magnitude eigenvalue, but finite. Operator H is given by

$$H = \frac{1}{2|\lambda|}(U + U^\dagger). \tag{3.5.38}$$

To prove this, first suppose H is diagonal. Its entries are its eigenvalues, which are real. We may choose $U = \mathrm{diag}(e^{i\phi_1}, e^{i\phi_2}, \ldots)$.

$$U + U^\dagger = \mathrm{diag}(2\cos(\phi_1), 2\cos(\phi_2), \ldots). \tag{3.5.39}$$

One may then choose each ϕ_i to match each eigenvalue in H. Hermitian matrices are diagonalized by unitary matrices, so we may use unitary V to produce any other Hermitian operator from H that has the same eigenvalues:

$$VHV^\dagger = \frac{1}{2|\lambda|}(VUV^\dagger + VU^\dagger V^\dagger) \tag{3.5.40}$$

$$\equiv \frac{1}{2|\lambda|}(U' + U'^\dagger). \tag{3.5.41}$$

Note that U' is also unitary. This concludes the proof.

3.6 Localized Unitary and Non-unitary Operators in Quantum Field Theory

We now turn to field theory and our main result: localized unitary operators create localized excitations, while more familiar local non-unitary operators generically create non-local excitations. We explore the properties of these operators. As generic states in field theory are entangled over spatial regions, field theory is often the study of operators in entangled states. The properties we found in section 5 will apply in field theory as well. An initial investigation into the locality of certain local unitary operators was conducted in the context of free field theory, and our work extends this investigation [72].

3.6.1 Localized unitary operators create localized excitations

In a $(d+1)$-dimensional theory, we give a general form for time-ordered localized unitary operators $\mathcal{U}$, or localized unitary operators for short. This form arises naturally in the local picture. Foliate the spacetime by Cauchy surfaces and define a timelike coordinate that parameterizes motion across these surfaces. For any given foliation, all operators of the following form are localized unitary operators:

$$\mathcal{U} = \mathcal{T}\left(e^{-i\sum_n\left(\prod_{\{i_n\}}\int_{R_{i_n}} d^{d+1}x_{i_n}\right)J_n(x_1,x_2,\ldots,x_{i_n})\left(\prod_{\{i_n\}}\mathcal{O}_{i_n}(x_{i_n})\right)}\right). \tag{3.6.1}$$

For each n, there is a set denoted by $\{i_n\}$ which specifies the source function J_n and operators $\mathcal{O}_{i_n}(x_{i_n})$ appearing in the product. Functions J_n can have dimensions and include a small expansion parameter. The term in the exponent multiplying i is Hermitian. Unitary operators can always be placed in exponential form but the expression we present is simply the general time-ordered exponential of products and sums of localized operators with smearing functions. Operators $\mathcal{O}(x_{i_n})$ need not be local in space but must be local in time,

and we have labelled operators $\mathcal{O}_{i_n}$ by their insertion points schematically.

R_{i_n} is defined as the spacetime region in which the smearing function $J_n(x_1, \ldots, x_{i_n})$ is non-zero. The localized unitary operator $\mathcal{U}$ creates an excitation localized to spacetime region $R = \cup_{i_n} R_{i_n}$. Correlators of operators inserted at spacelike separation from all points in R do not change. Consider $\langle \mathcal{O}(y) \rangle$ in an excited state formed by $\mathcal{U}$. If y is spacelike-separated from all points in R,

$$\langle \Psi | \mathcal{U}^\dagger \mathcal{O}(y) \mathcal{U} | \Psi \rangle = \langle \Psi | \mathcal{U}^\dagger \mathcal{U} \mathcal{O}(y) | \Psi \rangle = \langle \Psi | \mathcal{O}(y) | \Psi \rangle \,. \tag{3.6.2}$$

If y is not spacelike from all of R, the above equality may not hold. While we may find it convenient to use perturbation theory to calculate correlators in this state, this result is true non-perturbatively, and follows from (3.2.1).

There is an operator-excited state correspondence for subregions. For every Hermitian operator $\mathcal{O}$ inserted in a subregion A of a Cauchy surface, there is an excited state whose excitation is localized to A and is given by acting $e^{i\mathcal{O}}$ on the original state.

Just as $\mathcal{H}_{int}$ is not normal ordered, the operators in the exponent of $\mathcal{U}$ are not normal-ordered. Correlators in this state will generically diverge. Treating $\mathcal{H}_{int}$ as a perturbative correction, calculating correlators in a state created by $\mathcal{U}$ amounts to a calculation in real-time perturbation theory, and the divergences are treated using standard methods.

A simple example of a local unitary operator is

$$\mathcal{U}(x) = e^{-i\alpha \mathcal{O}(x)}, \quad \mathcal{O}^\dagger(x) = \mathcal{O}(x). \tag{3.6.3}$$

The parameter α can be chosen to be $\alpha \equiv \alpha' \epsilon$, where α' may have dimensions and the dimensionless parameter ϵ may be taken small. Exciting a state with this operator is equivalent to introducing the interaction

$$\int \mathcal{H}_{int} = \alpha \int d^{d+1}x' \delta^{d+1}(x' - x) \mathcal{O}(x'). \tag{3.6.4}$$

The first-order correction to $\langle \mathcal{O}(y) \rangle$ is a familiar quantity in time-dependent systems, the commutator.

$$\langle \Psi | \mathcal{U}^\dagger(x) \mathcal{O}(y) \mathcal{U}(x) | \Psi \rangle = \langle \Psi | \mathcal{O}(y) | \Psi \rangle - i\alpha \langle \Psi | [\mathcal{O}(y), \mathcal{O}(x)] | \Psi \rangle + \dots . \tag{3.6.5}$$

Conversely, calculations of the commutator of two operators are also the first-order correction to the one-point function in an excited state. In general, the correspondence between localized unitary operators and Hamiltonian deformations is

$$\begin{gathered} \mathcal{U} = \mathcal{T}\left(e^{-i\sum_n \left(\prod_{\{i_n\}} \int_{R_{i_n}} d^{d+1}x_{i_n}\right) J_n(x_1,x_2,\dots,x_{i_n}) \left(\prod_{\{i_n\}} \mathcal{O}_{i_n}(x_{i_n})\right)} \right) \\ \updownarrow \\ \int \mathcal{H}_{int} = \sum_n \left(\prod_{\{i_n\}} \int_{R_{i_n}} d^{d+1}x_{i_n} \right) J_n(x_1, x_2, \dots, x_{i_n}) \left(\prod_{\{i_n\}} \mathcal{O}_{i_n}(x_{i_n}) \right) . \end{gathered} \tag{3.6.6}$$

This correspondence is clear from the interaction picture and section 4.

Deformations of the Hamiltonian cannot always be represented by localized unitary operators acting on states. For example, if $\mathcal{H}_{int}$ has not turned off at the time operators are inserted, the calculation of an unequal-time correlator will involve insertions of operators $e^{-i\int^t \mathcal{H}_{int}}$ between operators inserted at different times. Also, the time t should not be taken later than the latest time at which the operators in the correlation function are inserted. These rules follow from the interaction picture.

In gauge theories, it is natural to restrict the operators in the exponent of a localized unitary operator to be gauge invariant. For example, the operator $\mathcal{U}(x) = e^{iF^2(x)}$ with $F_{\mu\nu}(x)$ being the field strength tensor of a gauge theory creates a local excitation. Not all quantities diagnose locality well in gauge theories. For example, entanglement entropy is not a gauge-invariant measure, but relative entropy and mutual information are free of ambiguities associated with the gauge theories, and so may prove useful [94–96].

Localized excitations can change conserved quantities. For example, a localized excitation

created by $\mathcal{U}(x)$ will generically change the total energy $\langle \int d^d y T^{00}(y) \rangle$. The energy added by $\mathcal{U}(x)$ is injected at x and can spread within the forward lightcone of x. The amount by which a localized unitary operator changes a conserved quantity is a property of both the operator and the state. It has been argued that localized excitations of fixed particle number are of limited applicability [72, 77, 78, 97].

We may also prepare a localized excitation by sending in an "ingoing excitation" rather than by deforming the Hamiltonian. So far, we have described how to create a localized excitation by applying a localized unitary operator $\mathcal{U}$ to some state $|\Psi\rangle$. Applying this operator can change conserved quantities. The same localized excitation can be prepared by beginning with some initial state and evolving time. Conserved quantities will not change in this case. The initial state $|\Psi(t_0)\rangle$ that encodes the ingoing excitation is found by evolving the state $\mathcal{U}(x)\,|\Psi\rangle$ backwards in time. Here, $\mathcal{U}(t, t_0)$ is the time evolution operator and $\mathcal{U}(x)$ is a local unitary operator inserted at spacetime point $x = (t, \mathbf{x})$.

$$|\Psi(t_0)\rangle = \mathcal{U}(t_0, t)\mathcal{U}(x)\,|\Psi\rangle\,. \tag{3.6.7}$$

Even in an interacting field theory in an arbitrary number of dimensions, the ingoing excitation must be a pulse that leaves no imprint on the state as it passes through a spacetime region, because the regions it passes through are causally connected to points that are spacelike-separated from x. While such excitations are familiar in classical theories, in quantum field theories they can require extensive fine-tuning, and may not be possible in practice.

The dynamics of entanglement at different scales within a local excitation can be investigated through the time-dependence of entanglement density [98]. This investigation may be useful in the AdS/CFT correspondence through the Hubeny-Rangamani-Takayanagi conjecture, and as part of the entanglement tsunami picture [86, 99–101].

3.6.2 Separable vs. non-separable localized unitary operators

There are two qualitatively different types of excitations created by localized unitary operators, separable and non-separable. We explore their properties. We use the labels separable and non-separable for reasons which will become clear.

We have stated a general form for useful localized unitary operators is

$$\mathcal{U} = \mathcal{T}\left(e^{-i\sum_n \left(\prod_{\{i_n\}} \int_{R_{i_n}} d^{d+1}x_{i_n}\right) J_n(x_1,x_2,\ldots,x_{i_n}) \left(\prod_{\{i_n\}} \mathcal{O}_{i_n}(x_{i_n})\right)}\right).$$

Separable unitary operators $\mathcal{U}$ create separable excitations, and take the form

$$\mathcal{U} = \mathcal{T}\left(e^{-i\sum_n \int_{R_n} d^{d+1}x_n J_n(x_n)\mathcal{O}_n(x_n)}\right). \tag{3.6.8}$$

Non-separable unitary operators contain products of operators in the exponent that are inserted at different points. For example, consider separable and non-separable local unitary operators $\mathcal{U}_s, \mathcal{U}_{ns}$, with

$$\mathcal{U}_s = e^{-i(\mathcal{O}(x)+\mathcal{O}(y))}. \tag{3.6.9}$$

$$\mathcal{U}_{ns} = e^{-i\mathcal{O}(x)\mathcal{O}(y)}. \tag{3.6.10}$$

Points x, y are spacelike-separated and so time-ordering has no effect for these two operators. We require that $\mathcal{O}^\dagger = \mathcal{O}$. Operator $\mathcal{U}_s$ can be separated into the product of two local unitary operators while $\mathcal{U}_{ns}$ cannot. This will become obvious shortly.

We can understand separable and non-separable unitary operators through their quantum-mechanical analogs. Consider an entangled state of two spin 1/2 particles. A separable operator is $\mathcal{U}_s = e^{-i(S_z^1+S_z^2)}$, which amounts to acting with a local unitary operator on each particle. Separable operators are the natural way to concatenate local excitations of a system. A non-separable operator is $\mathcal{U}_{ns} = e^{-iS_z^1 \otimes S_z^2}$. This is equivalent to turning on a spin-spin

coupling between the two systems. Separable operators represent interaction of an external system with the state and non-separable operators represent the coupling of two subsystems. In the local picture, separable operators are implemented by a non-local experimentalist.

Separable unitary operators represent uncorrelated localized excitations while non-separable unitary operators represent correlated excitations. We will explore this statement in field theory. If two excitations are correlated, correlators affected by one excitation will also depend on the value of the field at the location of the second excitation. Consider the expectation value of operator $\mathcal{O}(z)$ which is altered by the excitation at x but not y. Suppose z and x are timelike-separated and z is in the future of x. Point z is spacelike-separated from y. For the separable operator,

$$\langle\Psi|\mathcal{U}_s^\dagger(x,y)\mathcal{O}(z)\mathcal{U}_s(x,y)|\Psi\rangle = \langle\Psi|e^{i\mathcal{O}(x)}\mathcal{O}(z)e^{-i\mathcal{O}(x)}|\Psi\rangle\,. \tag{3.6.11}$$

For the non-separable operator,

$$\begin{aligned}\langle\Psi|\mathcal{U}_{ns}^\dagger(x,y)\mathcal{O}(z)\mathcal{U}_{ns}(x,y)|\Psi\rangle &= \langle\Psi|\mathcal{O}(z) + i[\mathcal{O}(x)\mathcal{O}(y),\mathcal{O}(z)] + \ldots|\Psi\rangle \\ &= \langle\Psi|\mathcal{O}(z) + i\mathcal{O}(y)[\mathcal{O}(x),\mathcal{O}(z)] + \ldots|\Psi\rangle\,. \end{aligned}\tag{3.6.12}$$

Both separable and non-separable unitary operators create localized excitations, just as $\mathcal{U}_s, \mathcal{U}_{ns}$ change the state only in the forward lightcones of their insertion points x, y. With $\mathcal{U}_{ns}$, the correction to $\langle\mathcal{O}(z)\rangle$ depends on an operator $\mathcal{O}(y)$ inserted at spacelike separation. Just as in quantum mechanics, the non-separable operator has coupled the state at x and y.

We can understand what this coupling entails. If we first alter the state at y with another local excitation, we will affect $\langle\mathcal{O}(z)\rangle$ only when the next excitation is non-separable. Create this first excitation with a local unitary operator $\mathcal{U}(y')$ where y' and y are timelike-separated but y' is spacelike-separated from x and z. Point y' is earlier in time than y. The operator $\mathcal{U}(y')$ when acted alone changes the state at y, but not x or z. The expectation value $\langle\mathcal{O}(z)\rangle$

does not change for the separable excitation:

$$\begin{aligned}\langle\Psi|\mathcal{U}^\dagger(y')\mathcal{U}_s^\dagger(x,y)\mathcal{O}(z)\mathcal{U}_s(x,y)\mathcal{U}(y')|\Psi\rangle &= \langle\Psi|e^{i\mathcal{O}(x)}\mathcal{O}(z)e^{-i\mathcal{O}(x)}e^{i\mathcal{O}(y')}e^{i\mathcal{O}(y)}e^{-i\mathcal{O}(y)}e^{-i\mathcal{O}(y')}|\Psi\rangle \\ &= \langle\Psi|e^{i\mathcal{O}(x)}\mathcal{O}(z)e^{-i\mathcal{O}(x)}|\Psi\rangle\,. \end{aligned} \tag{3.6.13}$$

The expectation value $\langle\mathcal{O}(z)\rangle$ does change for the non-separable excitation:

$$\begin{aligned}\langle\Psi|\mathcal{U}^\dagger(y')\mathcal{U}_{ns}^\dagger(x,y)\mathcal{O}(z)\mathcal{U}_{ns}(x,y)\mathcal{U}(y')|\Psi\rangle &= \langle\Psi|\mathcal{U}^\dagger(y')(\mathcal{O}(z)+i\mathcal{O}(y)[\mathcal{O}(x),\mathcal{O}(z)]+\ldots)\mathcal{U}(y')|\Psi\rangle \\ &= \langle\Psi|\mathcal{O}(z)+i\mathcal{U}^\dagger(y')\mathcal{O}(y)\mathcal{U}(y')[\mathcal{O}(x),\mathcal{O}(z)]+\ldots|\Psi\rangle\end{aligned}$$

As y and y' are timelike-separated, the above expectation value of an operator at z has changed in response to an excitation at y' which is spacelike-separated from z.

The behavior we have identified for non-separable excitations violates the causality properties of local quantum field theory at the time the operator acts. Measurements at z are affected by a local excitation at y', which was spacelike-separated from z. This violation of causality is no surprise, as acting with $\mathcal{U}_{ns}$ corresponds to turning on an interaction $\mathcal{O}(x)\mathcal{O}(y)$ in the Hamiltonian, which couples the field at spacelike-separated points. This term is not allowed in the Hamiltonian of a local quantum field theory. Even a non-local experimentalist in the closed system cannot act with this operator as long as the theory that describes the experimentalist and system are both local quantum field theories. We conclude that there is a restriction on localized operators and excitations in local quantum field theories: the operators and excitations must be separable. Separability can be tested using the criteria we have used in this section.

Separable unitary operators localized to two different regions of a Cauchy surface do not change the entanglement entropy of those regions, as the operators can be expressed as the product of unitary operators, each local in a different subregion. For example, $\mathcal{U}_s(x,y)$ does not change the entanglement entropy of region A or B for $x\in A, y\in B$.

3.6.3 Noteworthy quantities as localized unitary operators

We give examples of familiar quantities that are localized unitary operators. Squeezed states, coherent states, generalized coherent states are examples of excitations that can be created by localized unitary operators, and their interpretations are well-understood [80–83]. In a free $(d+1)$-dimensional field theory, a coherent state is (cf. [102])

$$|\Psi_c(\pi_c(\mathbf{x}), \phi_c(\mathbf{x}))\rangle = e^{i\int d^d x \pi_c(\mathbf{x})\hat{\phi}(\mathbf{x}) - \phi_c(\mathbf{x})\hat{\pi}(\mathbf{x})} |0\rangle . \tag{3.6.14}$$

The state is labelled by its expectation values

$$\langle \Psi_c(\pi_c(\mathbf{x}), \phi_c(\mathbf{x}))|\phi(\mathbf{y})|\Psi_c(\pi_c(\mathbf{x}), \phi_c(\mathbf{x}))\rangle = \phi_c(\mathbf{y}). \tag{3.6.15}$$

$$\langle \Psi_c(\pi_c(\mathbf{x}), \phi_c(\mathbf{x}))|\pi(\mathbf{y})|\Psi_c(\pi_c(\mathbf{x}), \phi_c(\mathbf{x}))\rangle = \pi_c(\mathbf{y}). \tag{3.6.16}$$

A coherent state is a localized excitation when both $\phi_c(\mathbf{x}), \pi_c(\mathbf{x})$ have compact support. Generalized coherent states are analogous constructions for arbitrary Lie groups [103] and also create localized excitations.

Path-ordered exponentials can be localized unitary operators for certain choices of path. If the path is nowhere spacelike, then the path ordering is a time ordering. If the path is everywhere spacelike, then the operator creates an excitation at a single time. Wilson loops with spacelike integration paths are examples of these operators, and they create flux tubes along their path.

Localized unitary operators model certain quantum quenches exactly. Quantum quenches are abrupt changes in the Hamiltonian. For instance, the coefficient $\lambda(x)$ of some operator $\mathcal{O}(x)$ in the Hamiltonian may change suddenly. If the state was the ground state of the Hamiltonian, the state after the quench is an excited state of the new Hamiltonian. In global quenches, $\lambda(x)$ is constant in space. In inhomogeneous quenches, $\lambda(x)$ varies in space. Two different types of quenches go by the name "local quenches". One type of local quench

involves preparing two different states in half the space, joining them, and evolving with time [104, 105]. Another type of local quench is given by changing $\lambda(x)$ at one spacetime point [61, 62, 64]. We give the localized unitary operators that describe this second type of local quench. Global and inhomogeneous quenches are described in a similar way, although the corresponding unitary operators are fully non-localized. In a $(d+1)$-dimensional field theory,

$$\text{Global quench}: \ \mathcal{U} = e^{-i\int d^d x \mathcal{O}(x)}. \tag{3.6.17}$$

$$\text{Inhomogeneous quench}: \ \mathcal{U} = e^{-i\int d^d x f(x)\mathcal{O}(x)}. \tag{3.6.18}$$

$$\text{Local quench}: \ \mathcal{U} = e^{-i\mathcal{O}(x)}. \tag{3.6.19}$$

Motivated by the properties of non-separable unitary operators, we see that non-separable operators model a "non-separable quantum quench"

$$\text{Non-separable quench}: \ \mathcal{U} = e^{-i\mathcal{O}(x)\mathcal{O}(y)}. \tag{3.6.20}$$

Introducing a small parameter α in the exponent to control the strength of the quench, the first, second, and third-order corrections to operator expectation values are straightforward to calculate in CFTs as they often involve two, three, and four-point functions.

3.6.4 Localized non-unitary operators do not always create localized excitations

In this section, we show that the familiar local operators in field theory do not always create localized excitations. While this may seem counter-intuitive, locality in field theory is enforced through commutators, and expectation values in states $\mathcal{O}|\Psi\rangle$ do not involve any commutators with $\mathcal{O}$. Moreover, the statement that two operators commute at spacelike separation is not a statement about expectation values in the state created by acting with one

of those operators. In section 5, we showed that localized finite-norm operators generically create non-localized excitations. An operator $\mathcal{O}$ has a finite norm if $\mathcal{O}\left|\Psi\right\rangle$ has a finite norm for all normalized states $\left|\Psi\right\rangle$. A related conclusion is that local non-unitary operators do not always model a local quench exactly. Infinite-norm operators will be treated more carefully, and we give a specific infinite-norm operator that creates a non-local excitation.

We first address an intuition that is sometimes held about local operators creating local excitations. Consider a real scalar field in $(3+1)$ dimensions. We may ask about the interpretation of the state

$$\phi(\mathbf{x})\left|0\right\rangle = \int \frac{d^3p}{(2\pi)^3}\frac{1}{2E_{\mathbf{p}}}e^{-i\mathbf{p}\cdot\mathbf{x}}\left|\mathbf{p}\right\rangle. \tag{3.6.21}$$

We will paraphrase the interpretation of this state given in a well-known field theory textbook [106]. For small (non-relativistic) $\mathbf{p}$, $E_{\mathbf{p}}$ is approximately constant, and in this case $\phi(\mathbf{x})\left|0\right\rangle$ approaches the non-relativistic expression for a position eigenstate $\left|\mathbf{x}\right\rangle$ in basis $\left|\mathbf{p}\right\rangle$. To quote the authors, "we will therefore put forward the same interpretation, and claim that the operator $\phi(\mathbf{x})$, acting on the vacuum, creates a particle at position $\mathbf{x}$." Moreover, this interpretation is corroborated by calculating

$$\left\langle 0\right|\phi(\mathbf{x})\left|\mathbf{p}\right\rangle = \left\langle 0\right|\int \frac{d^3p'}{(2\pi)^3}\frac{1}{\sqrt{2E_{\mathbf{p}'}}}\left(a_{\mathbf{p}'}e^{i\mathbf{p}'\cdot\mathbf{x}} + a^{\dagger}_{\mathbf{p}'}e^{-i\mathbf{p}'\cdot\mathbf{x}}\right)\sqrt{2E_{\mathbf{p}}}a^{\dagger}_{\mathbf{p}}\left|0\right\rangle \tag{3.6.22}$$

$$= e^{i\mathbf{p}\cdot\mathbf{x}}. \tag{3.6.23}$$

This is the same as the inner product $\left\langle\mathbf{x}\right|\left.\mathbf{p}\right\rangle$ in non-relativistic quantum mechanics. We may perform another check to learn that the analogy with quantum mechanics is only valid in the non-relativistic limit.

$$\text{QM}: \quad \left\langle\mathbf{x}\right|\left.\mathbf{y}\right\rangle = \delta^{(3)}(\mathbf{x}-\mathbf{y}) \tag{3.6.24}$$

$$\text{QFT}: \quad \left\langle 0\right|\phi(\mathbf{x})\phi(\mathbf{y})\left|0\right\rangle = \int \frac{d^3p}{(2\pi)^3}\frac{e^{i\mathbf{p}\cdot(\mathbf{x}-\mathbf{y})}}{2E_{\mathbf{p}}} = D(\mathbf{x}-\mathbf{y}). \tag{3.6.25}$$

In the non-relativistic approximation, $E_{\mathbf{p}}$ is approximately constant, and both expressions are delta functions. The authors of course never make an erroneous claim, for example that $\phi(\mathbf{x})$ creates a particle only at $\mathbf{x}$ but nowhere else. In fact, particles themselves are approximate notions, and it has been shown that localizing a finite number of particles in a single region is in tension with causality [72, 77, 97]. We have reproduced a textbook argument here to make explicit what considerations and terminology may lead one to the incorrect intuition that if a field theory operator is local it creates a local excitation.

In field theory, the Dirac orthogonality condition does not diagnose locality as we have defined it. The condition that the inner product between two states $\langle 0|\phi(x)\phi(y)|0\rangle = D(x-y)$ grows small as the separation between x, y grows large is known as asymptotic locality [107]. We have seen how localized unitary operators create localized excitations, and even localized unitary operators are not Dirac orthogonal. Consider operators of the form $\mathcal{U} = e^{-i\mathcal{O}}$:

$$\langle\Psi|\mathcal{U}^\dagger(y)\mathcal{U}(x)|\Psi\rangle = \langle\Psi|\Psi\rangle + i\,\langle\Psi|\mathcal{O}(y) - \mathcal{O}(x)|\Psi\rangle + \dots \tag{3.6.26}$$

The failure of local excitations in field theory to obey the Dirac orthogonality condition illustrates that not all quantum-mechanical measures of locality are useful measures in field theory.

Our discussion of the Reeh-Schlieder theorem in section 5.3 applies to field theory as well. The Reeh-Schlieder theorem is a consequence of local non-unitary operators acting in entangled states. It is widely accepted that the source of Reeh-Schlieder theorem in field theory is the entanglement between spatial regions [75]. To make the connection with our quantum-mechanical explanation of the Reeh-Schlieder theorem, we should consider finite-norm operators in field theory localized to some region. Local operators generically have infinite norm, and must be smeared over some region to have finite norm. Just as in quantum mechanics, these finite-norm non-unitary operators may be localized, but they create the non-localized excitations described by the Reeh-Schlieder theorem.

Some local infinite-norm operators create non-localized excitations. For example, con-

sider the infinite-norm operator

$$\mathcal{O}_e = e^{\alpha\mathcal{O}(x)}. \tag{3.6.27}$$

Here, α is real and $\mathcal{O}$ is Hermitian. Consider how the expectation value of some operator in the vacuum $\langle 0|\mathcal{O}'|0\rangle$ changes in the excited state $\mathcal{O}_e|0\rangle$. To first order in α this excitation does not change the state's norm as $\langle 0|\mathcal{O}(x)|0\rangle = 0$. So, for the first-order calculation, we do not have to regulate the operator. The expectation value to first order is therefore

$$\langle 0|\mathcal{O}_e(x)\mathcal{O}'(y)\mathcal{O}_e(x)|0\rangle \approx \langle 0|\mathcal{O}'|0\rangle + \alpha\langle 0|\{\mathcal{O}(x),\mathcal{O}'(y)\}|0\rangle + \dots \tag{3.6.28}$$

The anticommutator of two operators does not vanish for spacelike separations and so this local infinite-norm operator creates a non-localized excitation.

3.6.5 Certain local non-unitary operators create local excitations

While not all infinite-norm local operators create local excitations, we show some which do. The locality of these operators comes from the singularity structure of the infinite-norm states they create. This is in contrast to unitary operators, which obtain their locality through operator commutators. To calculate correlators in excitations created by infinite-norm operators, we must first regulate the norm. One way to regulate is to dampen the high-energy modes, which is equivalent to inserting the operator at complex time [64, 108]:

$$e^{-\delta H}\mathcal{O}(x)|0\rangle = \mathcal{O}(x - i\delta)|0\rangle. \tag{3.6.29}$$

We have used the shorthand $x \pm i\delta \equiv (t \pm i\delta, \mathbf{x})$. Expectation values are taken with the limit $\delta \to 0$.

As a simple example of an expectation value in an infinite-norm state, we consider the two-point function $\langle\phi(x)\phi(y)\rangle$ of a free scalar field in state $\phi(z)|0\rangle$, and we work in $d+1 > 2$ spacetime dimensions. We will find that $\phi(z)$ creates a local excitation at z. Suppose x, y

are spacelike-separated from z. This way the $\delta \to 0$ limit can be taken without crossing any branch cuts in complex time, and so including the state normalization factor,

$$\begin{aligned}\langle\phi(x)\phi(y)\rangle &\equiv \frac{\langle 0|\phi(z+i\delta)\phi(x)\phi(y)\phi(z-i\delta)|0\rangle}{\langle 0|\phi(z+i\delta)\phi(z-i\delta)|0\rangle} \\ &= \frac{D(z+i\delta,x)D(y,z-i\delta)+D(z+i\delta,y)D(x,z-i\delta)}{D(z+i\delta,z-i\delta)}+D(x,y). \end{aligned} \tag{3.6.30}$$

Here, $D(x-y)=\langle 0|\phi(x)\phi(y)|0\rangle$. The two-point function is unchanged by the excitation in comparison to its vacuum expectation value, as only the $\phi(z+i\delta)\phi(z-i\delta)$ contraction in the numerator has the same divergence as the denominator in the $\delta \to 0$ limit, as long as x, y are spacelike-separated from z:

$$\lim_{\delta\to 0}\langle\phi(x)\phi(y)\rangle = D(x,y). \tag{3.6.31}$$

The same conclusion holds for an n-point function in this state. The infinite-norm local operator $\phi(z)$ creates a local excitation at z even though it is not unitary.

In general CFTs, we can prove the same behavior we saw in the free scalar case, that a non-unitary infinite-norm local operator with definite conformal dimension creates a local excitation. When calculating a correlation function in the state $\mathcal{O}(x-i\delta)\,|\Psi\rangle$, the OPE between $\mathcal{O}$ and $\mathcal{O}^\dagger$ may be used when x is spacelike separated from the locations of the other operators in the correlation function. When $|\Psi\rangle$ is a conformally-invariant state, for example the vacuum, the identity dominates the OPE in the $\delta \to 0$ limit, and the correlator is unaffected by the excitation created by $\mathcal{O}$. We will see an explicit example of this process in section 7.2. This argument applies when $\mathcal{O}$ has definite non-zero conformal dimension. For example, this excludes the operator ϕ of the free scalar in $(1+1)$ dimensions, which has conformal dimension zero and creates an excitation that is not asymptotically local [107].

Explicitly, for x spacelike-separated from all y_i,

$$\begin{aligned}\langle \mathcal{O}(y_1)\mathcal{O}(y_2)\dots\mathcal{O}(y_n)\rangle &\equiv \frac{\langle\Psi|\mathcal{O}^\dagger(x+i\delta)\mathcal{O}(y_1)\mathcal{O}(y_2)\dots\mathcal{O}(y_n)\mathcal{O}(x-i\delta)|\Psi\rangle}{\langle\Psi|\mathcal{O}^\dagger(x+i\delta)\mathcal{O}(x-i\delta)|\Psi\rangle} \\ &= \sum_{\Delta_k,s_k} \frac{\langle\Psi|\left[C_{\mathcal{O}^\dagger\mathcal{O}\mathcal{O}_k}\frac{\mathcal{O}_k(x+i\delta)}{(2i\delta)^{2\Delta-\Delta_k}}\right]\mathcal{O}(y_1)\mathcal{O}(y_2)\dots\mathcal{O}(y_n)|\Psi\rangle}{\langle\Psi|\mathcal{O}^\dagger(x+i\delta)\mathcal{O}(x-i\delta)|\Psi\rangle}. \end{aligned} \tag{3.6.32}$$

The sum is over all operators $\mathcal{O}_k$, which we have indexed by dimension Δ_k and spin s_k, and the $C_{\mathcal{O}^\dagger\mathcal{O}\mathcal{O}_k}$ are theory-dependent coefficients. If $\mathcal{O}_k$ is a primary operator, then $C_{\mathcal{O}^\dagger\mathcal{O}\mathcal{O}_k}$ is the three-point coefficient.

As the state $|\Psi\rangle$ is conformally invariant, $\langle\Psi|\mathcal{O}_p|\Psi\rangle = 0$ for all local primary operators $\mathcal{O}_p$. Therefore, $\mathcal{O}^\dagger\mathcal{O}$ must contain the identity in its OPE in order for the two-point function in this state, $\langle\Psi|\mathcal{O}^\dagger(x+i\delta)\mathcal{O}(x-i\delta)|\Psi\rangle$, to be non-zero. We will assume the identity is present in this OPE. It follows that only the identity's contribution to the OPE in the numerator of (3.6.32) survives the $\delta\to 0$ limit.

$$\begin{aligned}\langle \mathcal{O}(y_1)\mathcal{O}(y_2)\dots\mathcal{O}(y_n)\rangle &= \sum_{\Delta_k,s_k} \frac{\langle\Psi|\left[C_{\mathcal{O}^\dagger\mathcal{O}\mathcal{O}_k}\frac{\mathcal{O}_k(x+i\delta)}{(2i\delta)^{2\Delta-\Delta_k}}\right]\mathcal{O}(y_1)\mathcal{O}(y_2)\dots\mathcal{O}(y_n)|\Psi\rangle}{\langle\Psi|\mathcal{O}^\dagger(x+i\delta)\mathcal{O}(x-i\delta)|\Psi\rangle} \\ &= \sum_{\Delta_k,s_k} \frac{\langle\Psi|\left[C_{\mathcal{O}^\dagger\mathcal{O}\mathcal{O}_k}\frac{\mathcal{O}_k(x+i\delta)}{(2i\delta)^{2\Delta-\Delta_k}}\right]\mathcal{O}(y_1)\mathcal{O}(y_2)\dots\mathcal{O}(y_n)|\Psi\rangle}{(2i\delta)^{-2\Delta}} \\ &\xrightarrow{\delta\to 0} \langle\Psi|\mathcal{O}(y_1)\mathcal{O}(y_2)\dots\mathcal{O}(y_n)|\Psi\rangle\,. \end{aligned} \tag{3.6.33}$$

Even if the field theory is not a CFT, an argument similar to (3.6.33) shows that $\mathcal{O}(x)$ creates local excitations if we assume a certain short-distance factorization. The only non-zero contribution to a correlator evaluated a state created by $\mathcal{O}(x-i\delta)$ comes from the $\delta\to 0$ contribution. If x is spacelike from the insertion points of all the other operators, then the $\delta\to 0$ limit does not cross any branch cut of the complex-time correlator. If, in a particular state of a field theory, the correlator factorizes on the $\delta\to 0$ singularity, then $\mathcal{O}(x)$ creates

a local excitation, and the argument proceeds similar to the CFT case:

$$\frac{\langle \mathcal{O}^\dagger(x+i\delta)\mathcal{O}(y_1)\mathcal{O}(y_2)\dots\mathcal{O}(y_n)\mathcal{O}(x-i\delta)\rangle}{\langle \mathcal{O}^\dagger(x+i\delta)\mathcal{O}(x-i\delta)\rangle} \xrightarrow{\delta\to 0} \frac{\langle \mathcal{O}^\dagger(x+i\delta)\mathcal{O}(x-i\delta)\rangle \langle \mathcal{O}(y_1)\mathcal{O}(y_2)\dots\mathcal{O}(y_n)\rangle}{\langle \mathcal{O}^\dagger(x+i\delta)\mathcal{O}(x-i\delta)\rangle}$$
$$= \langle \mathcal{O}(y_1)\mathcal{O}(y_2)\dots\mathcal{O}(y_n)\rangle\,, \quad y_i - x \text{ spacelike.} \tag{3.6.34}$$

Strictly speaking, local operators themselves are only operator-valued distributions. While certain infinite-norm operators may create local excitations, these operators must be smeared with some test function to create a physical excitation with finite norm. But once the non-unitary operator has finite norm, the finite-norm excitation will generically not be localized to the region of smearing. As such, the conclusions drawn from the locality properties of infinite-norm operators must be treated with care, as they may not extend to the operators' smeared counterparts.

3.7 Entanglement Entropy in Excited States

Entanglement entropy has recently emerged as a useful probe of excited-state dynamics in $(1+1)$-dimensional conformal field theories. A compelling quasi-particle picture has been proposed for local operators, wherein generic local operators create local excitations that can be interpreted as entangled pairs of quasi-particles [64]. In this section, we revisit the results in the literature and show how, while some infinite-norm operators create local excitations that may admit a quasi-particle description, entanglement and Renyi entropies change non-locally for other infinite-norm operators, and so the quasi-particle picture is not universal for all local operators. It is known that the quasi-particle picture fails for some theories [65, 86], and we show its failure in theories in which the picture is expected to be accurate. We show the results in the literature are consistent with evidence we have presented that local operators with definite conformal dimensions create local excitations. We also prove a causality relation for entanglement entropy.

3.7.1 Causal properties of entanglement entropy

The details of how localized excitations are implemented by localized unitary operators motivate a general causality condition for entanglement entropy in quantum field theories. The condition applies to pure states. Our result extends the result proved in ref. [87]. This earlier result makes use of the fact that, for a localized excitation within domain of dependence $\mathcal{D}(A)$ of subregion A of a Cauchy surface, one can always find a Cauchy surface A' of $\mathcal{D}(A)$ such that the state on A' is unaffected by the excitation. The excitation's support R is in the future of A' and to the past of A. As a reminder, the domain of dependence is defined as the region $\mathcal{D}(A)$ that, if an inextendible curve that is nowhere spacelike passes through the region, then this curve must intersect A. The domain of dependence $\mathcal{D}(A') = \mathcal{D}(A)$. The reduced density matrices on A, A' are unitarily related and so the entanglement entropy does not change.

However, having a Cauchy surface A' that is unaffected by the excitation is not a necessary condition. For example, no such A' exists for local excitations prepared by ingoing excitations, yet these excitations still do not change entanglement entropy. We provide a proof that does not rely on the existence of A', but on the properties of the excitation regardless of how it was prepared.

Consider a quantum field theory in some pure state $|\Psi\rangle$. We choose a purely spatial surface at time t as a Cauchy surface for simplicity. Divide the spatial surface into two regions A, B with reduced density matrices ρ_A, ρ_B. Consider an excitation localized within A at time t. This excitation can be created by acting with a unitary operator $\mathcal{U}(A)$ localized in A. This localized excitation does not change ρ_B. The entanglement entropy S_B of region B therefore does not change either. As the state $|\Psi\rangle$ is pure, $S_A = S_B$, and so S_A does not change. If the perturbation is localized within B, the excitation does not change ρ_A or S_A.

Only when the excitation is localized to a region that is causally connected to both A and B will these arguments fail. In this case, the entanglement entropy may change.

The complement of $\mathcal{D}(A) \cup \mathcal{D}(B)$ to the past of t is precisely the correct region. This region includes its boundary, which consists of null rays. We recover the causality condition of ref. [87]. Some excitations with support in both A and B can leave the entanglement entropy unchanged. As we showed in section 6.2, the excitations created by separable unitary operators accomplish this.

3.7.2 Entanglement entropy calculations with infinite-norm operators

In light of our conclusions that some infinite-norm local operators can create non-localized excitations, the results of recent entanglement entropy calculations may seem surprising. We show how these calculations are consistent with our results.

Calculations of entanglement entropy in excited states created by infinite-norm operators have shown that Renyi and entanglement entropies change only when the operator insertion is null or timelike to the subregion [61–68]. States of the form $\mathcal{O}(x)\,|0\rangle$ were considered in (1+1)-dimensional CFTs. It was suggested that the jumps in entanglement entropy reveals a local quasi-particle picture. In this picture, a local operator creates quasi-particle pairs that propagate at the speed of light from the operator's insertion point. Entanglement entropy changes only when one member of the pair is inside the subregion, but not both members.

The $(1 + 1)$-dimensional calculations we address use the replica trick to calculate entanglement entropy. In the replica trick, entanglement entropy of interval A is calculated from the replicated density matrix $\mathrm{tr}\rho_A^n$, and conveniently given by correlators with twist operators Φ_n [109, 110]. The path integral for a field ϕ on an n-sheeted Riemann surface is given by a path integral for fields ϕ_i living on $\mathbb{C}$ with certain boundary conditions relating the ϕ_i. These boundary conditions can be represented by inserting twist operators at the endpoints of the interval. Twist operators are primary. Correlators are taken in the theory with the n fields ϕ_i. For details, see ref. [111].

We consider a single interval A with endpoints u, v. The replica trick for excited states

has been established [61–64]. Take $\mathcal{O}$ to be an operator creating an excited state. For example, one such operator could be $\mathcal{O}(x) = \prod_i^n \phi_i(x)$. Renyi entropies are calculated from

$$\mathrm{Tr}(\rho_A^n) = \frac{\langle 0|\mathcal{O}^\dagger(x+i\delta)\Phi_n(u)\bar{\Phi}_n(v)\mathcal{O}(x-i\delta)|0\rangle}{\langle 0|\mathcal{O}^\dagger(x+i\delta)\mathcal{O}(x-i\delta)|0\rangle}. \tag{3.7.1}$$

The normalization is such that $\mathrm{Tr}(\rho_A^n) = 1$ for $n = 1$. Entanglement entropy is calculated from the Renyi entropy. In generic excited states, when the Renyi entropy changes, the entanglement entropy will change as well.

Suppose $\mathcal{O}$ is an operator with definite conformal dimension. If x is spacelike-separated from u, v, we can use the $\mathcal{O}(x+i\delta)\mathcal{O}^\dagger(x-i\delta)$ OPE to understand what happens in the limit $\delta \to 0$. For finite δ the excitation created by $\mathcal{O}$ has a finite-norm and can be non-local. Indeed, entanglement entropy changes at spacelike separations for finite δ [61–64]. The leading contribution to the OPE for small δ is from the identity operator, and we showed in (3.6.33) how this implies the locality of certain operator excitations. We will revisit and provide context for this statement shortly, comparing it to the result in ref. [66] to understand when the leading contribution to the full correlator comes from the identity and when it can come from the full identity block. For small δ,

$$\mathrm{Tr}(\rho_A^n) = \frac{\langle 0|\mathcal{O}^\dagger(x+i\delta)\mathcal{O}(x-i\delta)|0\rangle \langle 0|\Phi_n(u)\bar{\Phi}_n(v)|0\rangle + \text{subleading}}{\langle 0|\mathcal{O}^\dagger(x+i\delta)\mathcal{O}(x-i\delta)|0\rangle}. \tag{3.7.2}$$

For $\delta \to 0$,

$$\mathrm{Tr}(\rho_A^n) = \langle 0|\Phi_n(u)\bar{\Phi}_n(v)|0\rangle . \tag{3.7.3}$$

The excitation created by $\mathcal{O}$ does not affect the Renyi entropy. This argument was also given in section 6.5.

As x becomes null-separated from u or v, the OPE of $\mathcal{O}^\dagger(x+i\delta)\mathcal{O}(x-i\delta)$ is not convergent because the twist operators are within what would be the neighborhood of convergence. In ref. [66], the authors instead consider the vacuum block approximation to the four-point func-

tion, which is valid under certain assumptions and in a particular limit. They observe that this function has a certain branch cut, that when performing the continuation to real time, causes the entanglement entropy to pick up an additional contribution when the excitation is not spacelike-separated from the subregion. This is an example of how the entanglement entropy changes when the subregion becomes null and timelike to x.

Our statement that for spacelike-separations the identity operator and not also its descendants dominates the correlation function as $\delta \to 0$ is consistent with the recent calculations in ref. [66] of Renyi and entanglement entropies in the presence of a local operator excitation of the vacuum. In the $\delta \to 0$ limit, their expression for $\mathrm{Tr}(\rho_A^n)$ reduces to the two-point function of twist operators in the vacuum as long as the excitation is spacelike-separated from the interval. The Renyi entropy is therefore unchanged by the excitation, just as we found in (3.7.3). In the expression for the vacuum conformal block used in ref. [66], $\delta \to 0$ is the $z \to 1$ limit. The leading divergence in the vacuum block corresponds to exchanging the identity, while all divergences subleading in $z-1$ correspond to exchanging descendants of the identity. As $\delta \to 0$, only the leading divergence to the vacuum block gives a non-zero contribution to the correlator. Only when the excitation is not spacelike-separated from the interval does $\bar{z}$ pass to its second sheet, and the branch cut in the conformal block causes the Renyi entropy to change.

The argument we have given that infinite-norm local operators create local excitations fails when $\mathcal{O}$ does not have a definite scaling dimension. As an example, instead excite the vacuum with the operator

$$\mathcal{O}_e = \prod_i^n e^{\alpha \mathcal{O}_i(z)} \tag{3.7.4}$$

Here α is real and contains a small dimensionless parameter. For simplicity, take $\mathcal{O}_i = \mathcal{O}_i^\dagger$. To first order in α,

$$\mathcal{O}_e = 1 + \alpha \sum_i^n \mathcal{O}_n(z) \equiv 1 + \alpha \mathcal{O}(z). \tag{3.7.5}$$

We denote $\sum_i^n \mathcal{O}_n(z) = \mathcal{O}(z)$ for short. Notice that this operator does not change the

state's norm to first order in α. The correction to the Renyi entropy is proportional to $\langle 0| \left\{\mathcal{O}(z), \Phi_n(u)\bar{\Phi}_n(v)\right\} |0\rangle$, and unless the three-point function vanishes, the anti-commutator generically is not zero for z spacelike-separated from u, v. For an explicit example, choose $\mathcal{O} = \sum_i^n T_n(z)$, the stress tensor. The anticommutator is known [109]. This calculation may be performed with the entanglement first law. Alternatively, replace $\mathcal{O}_i(z)$ with a non-local operator $\mathcal{O}_i(z_1)\mathcal{O}_i(z_2)$ to see a case in which the Renyi entropy will be non-zero.

The argument we gave that uses the OPE to show that Renyi and entanglement entropies change in response to a local excitation does not apply to $\mathcal{O}_e$. For example, to first order in α, the four-point function is a three-point function involving one $\mathcal{O}$, and so there is no $\mathcal{O}\mathcal{O}$ OPE to take. Said another way, as the OPE $\mathcal{O}_e(z+i\delta)\mathcal{O}_e(z-i\delta)$ contains no divergence to first order in α, the contribution of the identity operator to the OPE does not determine the correlator's behavior. While we must introduce a regulator δ for the state's infinite norm, we need not introduce δ if we are working to first order in α.

The calculations we have shown are consistent with our arguments in section 6.5, as operators $\mathcal{O}$ which have definite conformal dimension change entanglement entropy only when $\mathcal{O}$ is in causal contact with the interval.

We have shown the quasi-particle picture does not describe excitations created by all local operators, but we have provided evidence that operators with definite conformal dimension have a quasi-particle interpretation for certain conformal field theories. Others have demonstrated that the quasi-particle picture is invalid for some field theories [65, 86]. The quasi-particle picture remains a compelling description of certain excitations in certain theories, and understanding its origin may reveal important properties of entanglement entropy.

3.8 Discussion

In this work, we have shown how localized unitary operators are fundamental building blocks of time-dependent quantum systems in entangled states. Localized unitary operators create localized excitations. We have detailed various features of localized unitary operators,

including their locality properties, their behavior under superposition, and the difference between separable and non-separable unitary operators. We found that non-separable unitary operators, and their associated non-separable localized excitations, are in conflict with the principles of local quantum field theory. We gave a criterion to test for separability.

We have shown how, unlike local unitary operators, local non-unitary operators can create non-local excitations in entangled states. As a reminder, generic states in field theory are entangled over spatial regions. Local non-unitary operators are state-dependent and can have infinite norm. We provided an example of an infinite-norm local non-unitary operator that creates a non-local excitation. We gave arguments that suggest that certain infinite-norm local non-unitary operators do create local excitations. However, these operators must be smeared to have finite norm, and the resulting finite-norm operators can create fully non-localized excitations. Consequently, one must be careful when drawing conclusions about locality properties based on those of infinite-norm local operators. In practice, however, correlators in excited states created by a non-unitary operator $\mathcal{O}(x)$ can be simpler to calculate than correlators in excited states created by a unitary operator $e^{i\alpha\mathcal{O}(x)}$, which can involve perturbation theory in α and a treatment of divergences.

We defined a local picture for quantum systems that unifies several different manifestations of locality and causality into a simple description. The local picture follows naturally from real-time perturbation theory and the definitions of open and closed quantum systems. According to the local picture, experimentalists can only act through deforming the Hamiltonian, and localized experimentalists can only deform the Hamiltonian locally. Localized unitary operators are central features of the local picture. Deforming the Hamiltonian in a localized region is equivalent to acting with a localized unitary operator on the state, and this operator will create a localized excitation. Generic non-unitary operators create non-localized excitations, so in order to act with these operators on the state, the experimentalist must be fully non-localized herself.

Using the local picture and our analysis of unitary and non-unitary operators, we dis-

tilled more formal results in algebraic quantum field theory into elementary statements in quantum mechanics, and demonstrated their underlying mechanisms. We showed how the non-local state preparation described by the Reeh-Schlieder theorem comes from the fact that local non-unitary operators create non-localized excitations in entangled states. The local picture makes clear how the Reeh-Schlieder theorem is intuitive and consistent with causality. Localized experimentalists can only create localized excitations, and so cannot act with the local non-unitary operators that create non-localized excitations.

We applied our results to entanglement entropy in field theory. We used properties of localized excitations to prove a causality condition for entanglement entropy that extends an earlier result [87]. Our proof applies to separable excitations and states prepared with ingoing excitations. We addressed recent calculations of entanglement entropy in $(1+1)$-dimensional conformal field theories [61–64, 66], and provided evidence that the locality properties demonstrated by these calculations are only properties of operators with definite conformal dimension. We showed consistency between these calculations and our conclusions about the locality of operator excitations. We provided an example of a local non-unitary operator that changes entanglement non-locally. While the quasi-particle picture is known to fail in certain theories [65,86], we concluded that the quasi-particle picture does not describe excitations created by all local operators in theories in which the picture is expected to hold. Understanding whether the picture applies to all localized excitations may provide insights into entanglement entropy.

We connect our results to the AdS/CFT correspondence in the limit in which the bulk is semiclassical. Non-normalizable modes of bulk fields ϕ with dual CFT operators $\mathcal{O}$ are turned on at the boundary by acting with the localized unitary operators $\mathcal{T}\left(e^{-i\int d^{d+1}x\phi_0(x)\mathcal{O}(x)}\right)$ in the CFT. An excitation of the CFT on a Cauchy surface $\mathcal{S}$ is associated with a bulk excitation in $\mathcal{Q}_\mathcal{S} \cup \mathcal{S}$, where the causal shadow $\mathcal{Q}_\mathcal{S}$ is the set of points spacelike-separated from all points in $\mathcal{S}$. This is because the region $\mathcal{Q}_\mathcal{S} \cup \mathcal{S}$ is the union of all possible bulk Cauchy surfaces which intersect the boundary at $\mathcal{S}$, and there is generically no preferred way

to choose one of these Cauchy surfaces for the bulk theory. Work on operator reconstruction is fully compatible with the fact that local non-unitary operators generically create non-localized excited states. For instance, for every local Hermitian operator $\mathcal{O}(x)$ there is a unitary operator $e^{i\alpha\mathcal{O}(x)}$ which creates a local excitation at x. Recent work sheds light on these considerations through a bulk exploration of the Reeh-Schlieder theorem [112, 113]. Recall that unlike unitary operators, non-unitary operators are state-dependent operators. State-dependent operators in AdS/CFT have been explored in detail [114–117].

We expect that our results, along with our elementary treatment of related discussions in diverse branches of the literature will help clarify investigations into locality, causality, entanglement entropy, and the AdS/CFT duality in the future.

Chapter 4

Entanglement Entropy with a Time-dependent Hamiltonian

The time evolution of entanglement tracks how information propagates in interacting quantum systems. We study entanglement entropy in CFT_2 with a time-dependent Hamiltonian. We perturb by operators with time-dependent source functions and use the replica trick to calculate higher order corrections to entanglement entropy. At first order, we compute the correction due to a metric perturbation in AdS_3/CFT_2 and find agreement on both sides of the duality. Past first order, we find evidence of a universal structure of entanglement propagation to all orders. The central feature is that interactions entangle unentangled excitations. Entanglement propagates according to "entanglement diagrams," proposed structures that are motivated by accessory spacetime diagrams for real-time perturbation theory. To illustrate the mechanisms involved, we compute higher-order corrections to free fermion entanglement entropy. We identify an unentangled operator, one which does not change the entanglement entropy to any order. Then, we introduce an interaction and find it changes entanglement entropy by entangling the unentangled excitations. The entanglement propagates in line with our conjecture. We compute several entanglement diagrams. We provide tools to simplify the computation of loop entanglement diagrams, which probe UV effects in

entanglement propagation in CFT and holography.

4.1 Introduction

Entanglement is a fundamental feature of quantum field theory. The program of studying entanglement and other information-theoretic quantities in field theory has recently led to new understanding of the well-known holographic correspondence between gravitational theories in anti-de Sitter spacetimes (AdS) and large-N strongly-coupled conformal field theories (CFTs). The AdS/CFT correspondence provides a route towards understanding quantum gravitational effects through their dual CFT description, and aspects of strongly coupled field theories through their dual AdS solutions [118]. Basic entries in the AdS/CFT dictionary involve information-theoretic quantities, including quantum error correction, complexity, mutual information, and relative entropy [119–123]. The black hole information loss paradox is intimately tied to questions of entanglement across the horizon [124, 125].

We will focus on entanglement entropy in this work. A significant body of evidence suggests that surface area in AdS calculates the entanglement entropy of CFT subregions, see for example [100, 101, 126, 127]. CFT entanglement entropy can also be used to derive bulk equations of motion [128]. We investigate the time-dependence of entanglement entropy in CFTs. We work in $1+1$ dimensions, in which global conformal symmetry is enhanced to Virasoro symmetry, providing greater control over the system in question. We study time-dependent perturbations of vacuum entanglement entropy of a single interval in a CFT and apply our results to the $\mathrm{AdS}_3/\mathrm{CFT}_2$ correspondence.

The time evolution of entanglement entropy in excited states has been well-studied, see for example [61, 63–66, 85, 129, 130]. Excited states can also be created by a time-dependent Hamiltonian, and the two setups are related but distinct [2]. Excited states have been used to model quantum quenches, wherein the Hamiltonian changes abruptly and the state is no longer a vacuum of the new Hamiltonian [66, 131]. Studies of entanglement with time-dependent Hamiltonians have also focused on quantum quenches

[104, 105, 108, 132–134]. General features of Hamiltonian perturbations by local operators have been explored [135, 136] and a study of their time-dependence has been initiated [137]. In [137], the first law was used to calculate the change in entanglement entropy to first order in J due to the Hamiltonian perturbation $J(x,t)\mathcal{O}(x)$ for operators $\mathcal{O}$ in the free scalar and fermion theories in various spacetime dimensions. Their CFT results agreed with that of the Hubeny-Rangamani-Takayanagi prescription (HRT) in the bulk, the covariant generalization of the Ryu-Takayanagi prescription (RT) for computing CFT entanglement entropy through extremal surface area.

We will now summarize this manuscript for the reader's convenience. In this work, we study corrections to vacuum entanglement entropy of a single interval A due to Hamiltonian perturbations of the form $J(x,t)\mathcal{O}(x)$. For illustrative purposes, the source function $J(x,t)$ is localized in spacetime, but our methods apply for general source functions. Our primary CFT tool is the replica trick.

In 4.2, we provide background on the analytic continuation of correlators from Euclidean to Lorentzian signature in position space and the replica trick.

In 4.3, we warm up with first-order Euclidean computations. We consider an infinitesimal Weyl transformation, equivalent to choosing $\mathcal{O} = \mathrm{Tr}(T)$, and compute the change in entanglement entropy with the replica trick and a proper length cutoff procedure. As expected, entanglement entropy changes only at the location of $\mathcal{O}$, the only place conformal symmetry is broken. Using a bulk diffeomorphism that implements the CFT metric transformation, we compute the change in the Ryu-Takayanagi surface area and find agreement with the CFT result. The Euclidean entanglement entropy changes only due to the perturbation at the entangling surface ∂A, as in the CFT.

In 4.4, we work in Lorentzian signature and perform a metric perturbation equivalent to choosing $\mathcal{O}(z) = T(z)$. Computing the entanglement entropy in the CFT using the replica trick and the entanglement first law give the same result, and we identify a non-trivial causality property that the modular Hamiltonian obeys but does not make manifest.

We compute the change in entanglement entropy in the bulk using the corresponding AdS_3 solution and find agreement with the CFT result. The bulk geodesic integral reduces to the CFT first law integral. We conclude that the perturbation changes physics at the entangling surface, just as in the Euclidean case.

Shifting gears, we move to higher orders in perturbation theory. Here, we find evidence of a universal structure of entanglement propagation to all orders: interactions entangle unentangled excitations according to entanglement diagrams.

In 4.5, we make the precise conjecture. For operators $\mathcal{O}$ that do not change entanglement entropy to any order in J, certain interactions $\lambda\mathcal{O}_\lambda$ in the Hamiltonian entangle these excitations. Entanglement changes only when a non-trivial "entanglement diagram" can be drawn of the process, depicting entanglement propagating through a web of interactions. See figure 4.1 for an example. Entanglement diagrams are position-space diagrams associated with the computation of entanglement entropy in real-time perturbation theory, with rules specific to entanglement propagation. However, even in the case of perturbation about a free field theory, entanglement diagrams are not the standard spacetime Feynman diagrams built from Wick contractions of the elementary fields. Instead, lines and vertices in entanglement diagrams are built from operators that serve as building blocks of entanglement in that theory. We provide a procedure to identify these operators.

Entanglement diagrams explicitly differentiate between two mechanisms of entanglement: entanglement due to interactions between excitations, and entanglement due to pre-existing background state correlations. We develop a diagrammatic method of organizing and streamlining real-time perturbation theory computations that makes causality properties manifest.

In 4.6, we perform calculations that provide evidence for the conjecture in 4.5. We use explicit twist operators in the bosonized free fermion theory to compute perturbative corrections to entanglement entropy, as in for example [138]. In the free fermion theory, the natural entanglement diagrams are the position-space Feynman diagrams associated with real-time perturbation theory, but in which lines are Wick contractions of the free boson

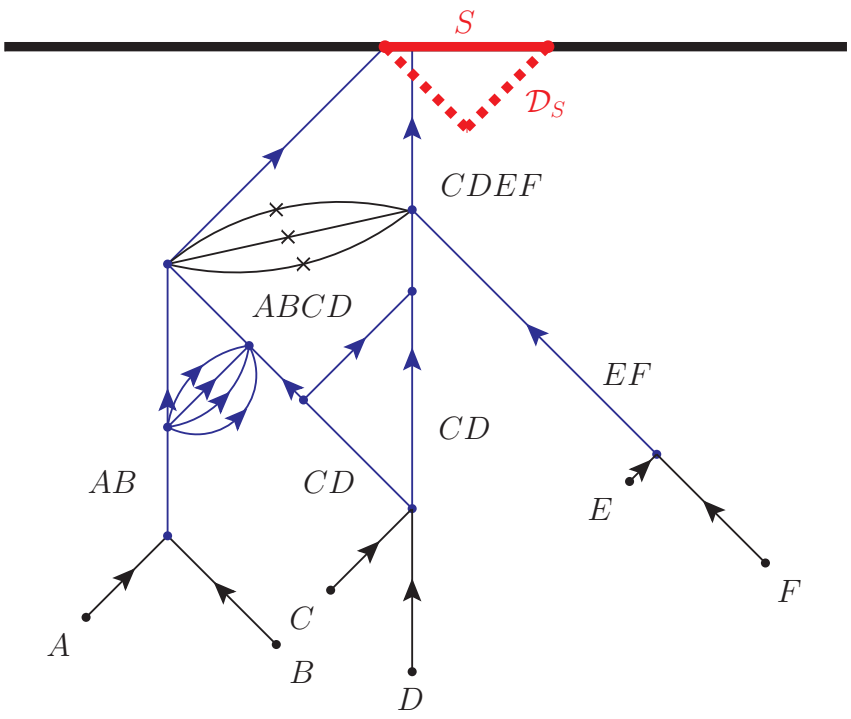

Figure 4.1: A sample spacetime entanglement diagram for subsystem S. $\mathcal{D}_s$ is the domain of dependence of S. $A - F$ label incoming unentangled excitations, which interactions subsequently entangle as labeled.

ϕ rather than the free fermion $\psi = e^{i\phi}$. We identify an unentangled operator $\mathcal{O} = \partial\phi$, the spin 1 current, that does not change entanglement entropy to any order. Then, we compute entanglement entropy in the presence of the cubic interaction $\mathcal{O}_\lambda = (\partial\phi)^3$, the spin-three current. Entanglement entropy changes at order $J^2\lambda^2$, and entanglement propagates according to the associated entanglement diagrams. We compute all $J^2\lambda^2$ diagrams. The computation manifests various features of the conjecture in Section 6, for instance that processes that would contribute to a generic correlator are prohibited entanglement entropy corrections according to the entanglement diagram rules. The free fermion is an elementary, tractable testing ground for features of entanglement propagation to high loop order.

Our goal is to make locality and causality manifest and so we express the lightcone divergences in position space rather than momentum space. Divergences can be addressed using methods in [139]. We consider irrelevant, marginal, and relevant $\mathcal{O}_\lambda$, and we expect that the

entanglement structure we find is independent of operator dimension. All expectation values are taken in the vacuum unless otherwise specified, and beginning in 4.4, we omit overall numerical factors that play no role in our results.

4.2 Background

4.2.1 Analytic continuation to Lorentzian signature

We review the procedure of analytically continuing correlators from Euclidean to Lorentzian signature, connecting the $i\epsilon$ prescription that is transparent in free field theory to the more general contour prescription discussed in [85].

We begin with the $i\epsilon$ prescription for obtaining Lorentzian two-point functions in free field theory. We will use the free scalar field in $d+1$ dimensions as an example and use the mostly minus signature. Just as in the Feynman prescription, we may begin with the Euclidean Green's function

$$\mathcal{G}(x) = \int_{\mathcal{C}} d^{d+1}p \frac{e^{-i(p^0(\pm i\epsilon)-\mathbf{p}\cdot\mathbf{x})}}{(p^0)^2 - (\mathbf{p})^2 - m^2}, \tag{4.2.1}$$

with contour $\mathcal{C}$ for p^0 chosen along the imaginary axis. Notice that if Euclidean time ϵ is continued to Lorentzian time in the integrand, the integral will diverge unless the contour is rotated. Choosing $-i\epsilon$ allows us to close the contour in the $p^0 > 0$ half of the plane, enclosing the $E_p = \sqrt{(\mathbf{p})^2 + m^2}$ pole. At this point, ϵ is analytically continued so that $-i\epsilon \to t - i\epsilon$, which amounts to increasing t to its non-zero Lorentzian value. Taking the $\epsilon \to 0$ limit, we obtain the Lorentzian two-point function $\langle 0|\phi(x)\phi(0)|0\rangle$. Using the $i\epsilon$ value instead gives $\langle 0|\phi(0)\phi(x)|0\rangle$. In the spacelike region $x^2 < 0$, choosing either $\pm i\epsilon$ will give the same result. In this case, the operators commute just as in the Euclidean correlator [88, 89].

Now we examine the $i\epsilon$ prescription in position space. Correlators are multivalued in complex time and the $i\epsilon$ prescription indicates the direction from which we approach branch

cuts in the correlator when we continue from complex to real time. Consider a spinless operator $\mathcal{O}$ of dimension Δ in a CFT as an example. In the spacelike region $x^2 < 0$,

$$\langle 0|\mathcal{O}(x)\mathcal{O}(0)|0\rangle = \frac{1}{(-x^2)^\Delta}. \tag{4.2.2}$$

When $-x^2 > 0$, choosing $\pm i\epsilon$ gives the same result because there is no branch cut in this region. When $-x^2$ crosses zero, choosing $\pm i\epsilon$ must give different results. We may orient the branch cut of $(-x^2)^{-\Delta}$ along the negative real axis of $-x^2$. To obtain the correlator for timelike separation, we must analytically continue the spacelike expression.

$$\langle \mathcal{O}(\mathbf{x}, t \pm i\epsilon)\mathcal{O}(0)\rangle = \frac{1}{((|\mathbf{x}| + t \pm i\epsilon)(|\mathbf{x}| - t \mp i\epsilon))^\Delta} \approx \frac{1}{(\mathbf{x}^2 - t^2 \mp i\epsilon \ \mathrm{sgn}(t))^\Delta}. \tag{4.2.3}$$

The quantity $\langle \mathcal{O}(\mathbf{x}, t \pm i\epsilon)\mathcal{O}(0)\rangle$ denotes the continuation of the Euclidean two-point function to complex time, and so the operator ordering of this expression is meaningless except in the limit $\epsilon \to 0$. Moving $\mathcal{O}(x)$ through the future f or past p lightcone of $\mathcal{O}(0)$ corresponds to t crossing $\pm|\mathbf{x}|$, which is equivalently fixed by $\mathrm{sgn}(t)$. This choice is separate from the choice of $\pm i\epsilon$ that gives the two different operator orderings. The timelike two-point function in the two kinematic regions $t > |\mathbf{x}|$ and $t < -|\mathbf{x}|$ is

$$\begin{aligned} \langle \mathcal{O}(\mathbf{x}, t \pm i\epsilon)\mathcal{O}(0)\rangle_f &= \frac{1}{(t^2 - \mathbf{x}^2)^\Delta} e^{\pm \pi \Delta i}, \\ \langle \mathcal{O}(\mathbf{x}, t \pm i\epsilon)\mathcal{O}(0)\rangle_p &= \frac{1}{(t^2 - \mathbf{x}^2)^\Delta} e^{\mp \pi \Delta i}. \end{aligned} \tag{4.2.4}$$

The $i\epsilon$ prescription is precisely what chooses the branch cut of the two-point function when the argument becomes negative. There is an unphysical choice of overall normalization. Here we have chosen $e^{\pm i\pi}$ to parameterize the two directions of approaching the branch cut, but in general we may choose $e^{\alpha i}, e^{\beta i}$ for any $|\alpha - \beta| = 2\pi$. A common choice is $\alpha = 0, \beta = 2\pi$.

Having addressed the two-point function, we summarize the rules for obtaining the n-point correlator in which all operators are timelike separated from one another. The

Lorentzian correlator

$$\langle \mathcal{O}_1(x_1)\mathcal{O}_2(x_2)\mathcal{O}_3(x_3)\dots\rangle \tag{4.2.5}$$

corresponds to the continuation $t_i \to t_i - i\epsilon_i$ with $\epsilon_1 > \epsilon_2 > \epsilon_3 \dots > 0$ of the Euclidean correlator in the limit of $\epsilon_1 \to 0$ [88,89,140–142]. Moving $\mathcal{O}_i(x_i)$ past $\mathcal{O}_j(x_j)$ in the correlator amounts to reversing the sign of $\epsilon_i - \epsilon_j$, which as we have seen amounts to approaching the branch cut in $x_i - x_j$ from the opposite direction, as in (4.2.4). It is equivalent to view the $i\epsilon$ prescription of approaching branch cuts as the complex time path of analytic continuation passing through different sheets of the correlator before reaching the real axis [85]. The location of the singularities can be different on different sheets of the correlator. See [85] for a detailed explanation of this contour prescription.

Now, we address the null singularities of correlators. Correlators can have delta-function lightcone singularities that require a generalization of the $i\epsilon$ prescription. We review the lightcone singularity of the $3+1$ dimensional free scalar two-point function, as in for example [143], and then provide its generalization to all dimensions. To our knowledge this generalization has not been stated in position space in the literature, so we justify the result in detail.

We begin by calculating the spacelike two-point function $D(x)$ in $d+1$ dimensions. We will omit most numerical prefactors. Performing the p^0 integral,

$$D(x) = \int d^d p \frac{1}{E_p} e^{\mp i E_p t + i\mathbf{p}\cdot\mathbf{x}}, \qquad E_p = |\mathbf{p}|. \tag{4.2.6}$$

The $\pm$ signs specify the pole $\pm E_p$ enclosed. With $r \equiv |\mathbf{p}|$, we can integrate over the angular directions. The lightcone divergence comes from the large r behavior of $D(x)$, which is

$$D(x) = \frac{1}{|\mathbf{x}|} \int_0^\infty dr r^{d-3} \left(e^{-ir(\pm t - |\mathbf{x}|)} - e^{-ir(\pm t + |\mathbf{x}|)} \right). \tag{4.2.7}$$

In the familiar case of $d = 3$ [143, 144], the quantity (4.2.7) is

$$D(x) = \frac{1}{|\mathbf{x}|}(\delta(\pm t - |\mathbf{x}|) - \delta(\pm t + |\mathbf{x}|)) = \delta(t^2 - |\mathbf{x}|^2) = \delta(x^2). \tag{4.2.8}$$

We could have obtained this divergence by analytically continuing the Euclidean two-point function instead. For $t > 0$,

$$\lim_{\epsilon \to 0} D(\mathbf{x}, t \pm i\epsilon) = \lim_{\epsilon \to 0} \frac{1}{x^2 \mp i\epsilon} = \pm i\pi\delta(x^2) + \text{p.v.} \left(\frac{1}{-x^2} \right), \tag{4.2.9}$$

where p.v. denotes the Cauchy principal value. We will omit the principal value designation from now on, but it is understood to be present and can be restored easily. For higher dimensions, (4.2.7) becomes

$$D(x) = \frac{1}{|\mathbf{x}|}\partial_t^{d-3} \int dr \left(e^{-ir(\pm t - |\mathbf{x}|)} - e^{-ir(\pm t + |\mathbf{x}|)} \right) = \partial_t^{d-3}\delta(x^2). \tag{4.2.10}$$

Using

$$\lim_{\epsilon \to 0} \frac{1}{(s \pm i\epsilon)^n} = \frac{(-1)^{n-1}}{(n-1)!}\partial_s^{n-1} \lim_{\epsilon \to 0} \frac{1}{s \pm i\epsilon}, \tag{4.2.11}$$

and (4.2.4), we can write the full CFT two-point function of $\mathcal{O}$ in general dimensions by analytically continuing the position-space Euclidean correlator.

$$\begin{aligned} \text{Spacelike} \quad x^2 < 0 : \quad & \langle \mathcal{O}(x)\mathcal{O}(0) \rangle = \langle \mathcal{O}(0)\mathcal{O}(x) \rangle = \frac{1}{(-x^2)^\Delta}. \\ \text{Timelike, null} \quad x^2 \geq 0 : \quad & \langle \mathcal{O}(x)\mathcal{O}(0) \rangle = \langle \mathcal{O}(\mathbf{x}, t - i\epsilon)\mathcal{O}(0) \rangle , \\ & \langle \mathcal{O}(0)\mathcal{O}(x) \rangle = \langle \mathcal{O}(\mathbf{x}, t + i\epsilon)\mathcal{O}(0) \rangle , \end{aligned} \tag{4.2.12}$$

where for $x^2 \geq 0$,

$$\langle \mathcal{O}(\mathbf{x}, t \pm i\epsilon)\mathcal{O}(0)\rangle_f = \pm \frac{(-1)^{\Delta-1}}{(\Delta-1)!} \cdot i\pi \partial_{x_f}^{\Delta-1}\delta(x^2) + \frac{1}{(x^2)^\Delta} e^{\pm\pi\Delta i},$$
$$\langle \mathcal{O}(\mathbf{x}, t \pm i\epsilon)\mathcal{O}(0)\rangle_p = \mp \frac{(-1)^{\Delta-1}}{(\Delta-1)!} \cdot i\pi \partial_{x_p}^{\Delta-1}\delta(x^2) + \frac{1}{(x^2)^\Delta} e^{\mp\pi\Delta i}. \tag{4.2.13}$$

The lightcone coordinates $x_f = |\mathbf{x}| - t$ and $x_p = |\mathbf{x}| + t$. The prescription (4.2.13) matches the $3+1$ dimensional free-scalar result of [144].

We have discussed correlators of bosonic operators, but there is an additional negative sign involved in computing fermionic correlators through analytic continuation. Taking $t_z \to t_z - i\epsilon$ in the two-point function $\langle 0|\psi(z)\psi^*(w)|0\rangle$ at timelike separation produces $1/(z-w)$, but to obtain the other ordering one must take $t_z \to t_z + i\epsilon$ and also anticommute the fermions, obtaining $\langle 0|\psi^*(w)\psi(z)|0\rangle = -1/(z-w)$. In even spacetime dimensions, the commutator of free scalars and anticommutator of free fermions have support only on the lightcone while the anticommutator of scalars and commutator of scalars have support everywhere inside the lightcone. However, this is reversed in odd spacetime dimensions, leading to what is known as a violation of Huygen's principle in odd dimensions [145].

4.2.2 Entanglement entropy from the replica trick

Our main tool in this work will be the replica trick, a useful method of calculating entanglement entropy in $1+1$ dimensional CFTs. We will briefly review the replica trick here, but for a more complete review, see for example [109, 111]. The entanglement entropy S_A of subsystem A can be computed as $S_A = -\partial_{n=1}\mathrm{tr}(\rho_A)^n$, where ρ_A is the reduced density matrix of A. The quantity $\mathrm{tr}\rho_A^n$ can be computed from an n-sheeted Riemann surface,

$$\mathrm{tr}\rho_A^n = \frac{Z_n(A)}{(Z_1)^n}, \tag{4.2.14}$$

where $Z_n(A)$ is the partition function of the theory on an n-sheeted Riemann surface. The surface is formed by joining n copies of the plane along cuts located at A on each sheet. The theory on the Riemann surface can be mapped to n copies of the theory on the plane with local twist operators that impose the correct boundary conditions upon the n species of replica fields. $\mathrm{tr}\rho_A^n$ is proportional to the expectation value of these twist operators [109]. The twist operator $\Phi_n(u)$ and anti-twist operator $\bar{\Phi}_n(v)$ are inserted when the subsystem A is the interval (u, v), the case we consider. We use the twist operator normalization fixed by $\langle \Phi_n(u)\bar{\Phi}_n(v)\rangle = 1/(u-v)^{2\Delta_\Phi}$, where the scaling dimension $\Delta_\Phi = \frac{c}{12}(n - \frac{1}{n})$ and c is the central charge of the theory.

The action of the twist operators is apparent in their diagonalizing basis. Labeling the n replica fields on the plane as ϕ_l, the diagonalizing replica fields $\tilde{\phi}_k$ are

$$\tilde{\phi}_k = \sum_{l=0}^{n-1} e^{2\pi i l \frac{k}{n}} \phi_l, \qquad k = 0, 1, \ldots, n-1. \tag{4.2.15}$$

Moving the ϕ_l around the twist operator $\Phi_n(u)$ takes $\phi_l \to \phi_{l\pm1}$, and is equivalent to multiplying $\tilde{\phi}_k$ by $e^{2\pi i k/n}$. Moving around the anti-twist $\bar{\Phi}_n(v)$ produces a factor of $e^{-2\pi i k/n}$. Deforming the Lagrangian $\mathcal{L}$ of the original theory by ϕ^m corresponds to deforming the replicated Lagrangian $\mathcal{L}_n$ by $\sum_l (\phi_l)^m$, and

$$\sum_{l=1}^{n} (\phi_l)^m = \delta_{0,\sum k_i} \tilde{\phi}_{k_1} \tilde{\phi}_{k_2} \ldots \tilde{\phi}_{k_m}, \tag{4.2.16}$$

up to an overall n-dependent normalization factor. For bilinears, $\sum_l \phi_l \phi_l = \sum \tilde{\phi}_k \tilde{\phi}_{-k}$.

The free fermion theory provides an explicit realization of the twist operators through bosonization. Details of the setup not provided here can be found in [138, 146–148]. In bosonization, the holomorphic and anti-holomorphic fermions are written in terms of a free scalar as follows:

$$\psi(z) = e^{i\phi(z)}, \qquad \bar{\psi}(\bar{z}) = e^{i\bar{\phi}(\bar{z})}, \tag{4.2.17}$$

where $\langle\phi(z)\phi(w)\rangle = -\ln(z-w)$ and similarly for $\bar{\phi}$. Here $\phi, \bar{\phi}$ are real.

Under cyclic permutation of ψ_l, the fermion on the last sheet must be identified with the first fermion up to a negative sign that depends on whether n is even or odd, as ψ_l can always be redefined to eliminate all but a possible overall sign change under this operation [147]. The diagonalizing replica fields $\tilde{\psi}_k$ are

$$\tilde{\psi}_k = \sum_{l=0}^{n-1} e^{2\pi i l \frac{k}{n}} \psi_l, \qquad k = -1/2(n-1), -1/2(n-1)+1, \ldots, 1/2(n-1). \tag{4.2.18}$$

The inverse transformation is

$$\psi_l = \frac{1}{n} \sum_k e^{-i2\pi l \frac{k}{n}} \tilde{\psi}_k. \tag{4.2.19}$$

We will be using fermion bilinears in this work, for which $\sum_l \psi_l \psi_l^* = \sum \tilde{\psi}_k \tilde{\psi}_k^*$. The twist operators for the free fermion are

$$\begin{aligned} \Phi_n(z,\bar{z}) &= \prod_k e^{i\frac{k}{n}(\phi_k(z) - \bar{\phi}_k(\bar{z}))}, \\ \bar{\Phi}_n(z,\bar{z}) &= \prod_k e^{-i\frac{k}{n}(\phi_k(z) - \bar{\phi}_k(\bar{z}))}. \end{aligned} \tag{4.2.20}$$

The operator $e^{i\alpha\phi(z)}$ has conformal dimension $\frac{1}{2}\alpha^2$, consistent with the normalization of $\langle\phi(z)\phi(w)\rangle$.

We will use the normal-ordered product of twist operators. Notice that this operator is a neutral product of vertex operators. For interval A between $(u,\bar{u})$ and $(v,\bar{v})$,

$$N(\Phi_n(u,\bar{u})\bar{\Phi}_n(v,\bar{v})) =: \exp\left(\sum_k i\frac{k}{n}\left[\phi_k(u) - \bar{\phi}_k(\bar{u}) - \phi_k(v) + \bar{\phi}_k(\bar{v})\right]\right) Z_0(n), \tag{4.2.21}$$

where $Z_0(n)$ is the n-sheeted partition function for the vacuum [147]. $Z_0(1) = 1$ and $-\partial_n|_{n=1} Z_0(n) = S_A$, the entanglement entropy of the interval in the vacuum. The factor $Z_0(n)$ will not contribute to any of our entanglement entropy calculations, so we will omit it. We will sometimes use the notation $\Phi_n(u,\bar{u}) = \Phi_n(u)$ for compactness.

4.3 First order metric perturbation: Euclidean AdS_3/CFT_2

In this section we work in Euclidean AdS_3/CFT_2 and compute the perturbative correction to the vacuum entanglement entropy, which is

$$S_A = \frac{c}{3} \ln \left(\frac{u-v}{\epsilon} \right), \tag{4.3.1}$$

to first order in a metric perturbation. Here, ϵ is a UV cutoff. We consider an infinitesimal Weyl transformation as our metric perturbation:

$$g'_{\mu\nu} = \delta_{\mu\nu} + \omega(x)\delta_{\mu\nu}, \qquad \omega(x) \ll 1. \tag{4.3.2}$$

We compute the change in entanglement entropy using the replica trick in the CFT and find that the correction depends only on the metric perturbation at the interval's endpoints, which is expected as perturbation by the trace of the stress tensor preserves conformal symmetry wherever $\omega(x) = 0$. Next, we compute the change in entanglement entropy as the change in a proper-length cutoff and find agreement with the replica trick result. Using the Ryu-Takayanagi prescription, we compute the first-order correction in AdS_3 and reproduce the CFT result. Our ultimate goal is to work in Lorentzian signature, and this Euclidean computation will mirror features of later Lorentzian calculations.

4.3.1 CFT_2: Replica trick

We begin by using the replica trick. The quantity $\mathrm{tr}\rho_A^n$ changes under an infinitesimal Weyl transformation as

$$\delta \mathrm{tr}\rho_A^n = -\frac{1}{2} \int d^2x \frac{\langle \Phi_n(u)\bar{\Phi}_n(v) T^\mu_\mu(x) \rangle \, \omega(x)}{\langle \Phi_n(u)\bar{\Phi}_n(v) \rangle}. \tag{4.3.3}$$

We have used the stress tensor normalization such that for an infinitesimal diffeomorphism that acts as $g'_{\mu\nu} = g_{\mu\nu} + \delta g_{\mu\nu}$, the action changes as $\delta S = -\frac{1}{2}\int T^{\mu\nu}\delta g_{\mu\nu}$. Using the Ward

identity,

$$T^{\mu}_{\mu}(x)\Phi_n(u)\bar{\Phi}_n(v) = -\delta(x-u)\Delta_{\Phi}\Phi_n(u)\bar{\Phi}_n(v) - \delta(x-v)\Delta_{\Phi}\Phi_n(u)\bar{\Phi}_n(v). \tag{4.3.4}$$

We therefore have

$$\delta \mathrm{tr}\rho_A^n = \frac{c}{24}\left(n - \frac{1}{n}\right)(\omega(u) + \omega(v)), \tag{4.3.5}$$

and the change in entanglement entropy

$$\delta S_A = \frac{c}{12}(\omega(u) + \omega(v)). \tag{4.3.6}$$

Only the Weyl transformation at the endpoints changes the entanglement entropy to this order.

4.3.2 CFT$_2$: Proper length cutoff

We can view the change in entanglement entropy as a change in the coordinate length UV cutoff ϵ defined by a proper length ϵ_p that is held fixed under the infinitesimal Weyl transformation. After the Weyl transformation, the coordinate length cutoff ϵ associated with u for example is

$$\epsilon = \int_u^{u\pm\epsilon_p} ds' = \int_u^{u\pm\epsilon_p} \sqrt{e^{\omega}dx^2} \approx \int_u^{u\pm\epsilon_p} \left(1 + \frac{1}{2}\omega(x)\right) dx. \tag{4.3.7}$$

Assuming $(\epsilon_p)^n \frac{d^n}{dx^n}\omega(x) \ll 1$ for $n \geq 1$, we can expand $\omega(x)$ about u and neglect all but the leading term $\omega(u)$. Therefore,

$$\epsilon = \left(1 + \frac{1}{2}\omega(u)\right)\epsilon_p. \tag{4.3.8}$$

We remind the reader that we have the freedom to choose two distinct UV cutoffs, one associated with each endpoint [110]. Choosing two cutoffs $\epsilon_p(u), \epsilon_p(v)$ is equivalent to replacing

ϵ_p by $\sqrt{\epsilon_p(u)\epsilon_p(v)}$ in the vacuum result with a single cutoff.

$$S_A = \frac{c}{6}\left(\ln\left(\frac{u-v}{\epsilon_p(u)}\right) + \ln\left(\frac{u-v}{\epsilon_p(v)}\right)\right). \tag{4.3.9}$$

Using (4.3.8),

$$S_A + \delta S_A \approx \frac{c}{3}\ln\left(\frac{u-v}{\epsilon}\right) + \frac{c}{12}(\omega(u)+\omega(v)), \tag{4.3.10}$$

in agreement with (4.3.6).

4.3.3 AdS_3: Ryu-Takayanagi

For a holographic CFT_2, the Ryu-Takayanagi prescription can be used to calculate the change in entanglement entropy in the dual AdS_3. In AdS_3, we can implement the infinitesimal boundary Weyl transformation through a bulk diffeomorphism. We work in the Poincare patch of AdS_3 and use the Fefferman-Graham coordinates for the metric near the boundary.

$$ds^2 = d\eta^2 + e^{2\eta/l}dzd\bar{z}, \tag{4.3.11}$$

where $\eta \to \infty$ corresponds to the boundary of AdS_3 and l is the AdS radius. In an asymptotically AdS_3 spacetime, the CFT_2 metric and expectation value of the CFT_2 stress tensor can be read off from the form

$$ds^2 = d\eta^2 + e^{2\eta/l}g^{(0)}_{ij}dz^i dz^j + g^{(2)}_{ij}dx^i dx^j. \tag{4.3.12}$$

The term $g^{(0)}_{ij}$ is the CFT_2 metric and $g^{(2)}_{ij}$ is proportional to the expectation value of the boundary stress tensor [149].

Precisely speaking, conformal transformations of the CFT are a conformal coordinate transformation followed by a Weyl transformation to remove the conformal factor. By modifying the bulk diffeomorphism that produces this boundary conformal transformation [149],

we can find the diffeomorphism that will implement only the boundary Weyl transformation. We work in (anti) holomorphic coordinates $z, \bar{z}$ with $z = x + i\tau, \bar{z} = x - i\tau$. Consider the infinitesimal Weyl parameter

$$\omega = (\epsilon + \bar{\epsilon})/l, \tag{4.3.13}$$

where $\omega \ll 1$. ϵ/l will be the small parameter in the bulk. The diffeomorphism that produces the infinitesimal boundary Weyl transformation is

$$z \to z + \frac{1}{2} l\bar{\epsilon}' e^{-2\eta/l}, \qquad \bar{z} \to \bar{z} + \frac{1}{2} l\epsilon' e^{-2\eta/l}, \qquad \eta \to \eta + \frac{1}{2}(\epsilon + \bar{\epsilon}), \tag{4.3.14}$$

where the primes denote (anti)holomorphic derivatives. To first order in $\epsilon, \bar{\epsilon}$,

$$ds^2 = d\eta^2 + e^{2\eta/l}\left(1 + (\epsilon + \bar{\epsilon})/l\right) dzd\bar{z} + \frac{1}{2} l(\epsilon'' + \bar{\epsilon}'')dzd\bar{z}. \tag{4.3.15}$$

It will be convenient to work in Poincare coordinates, with the radial coordinate $\rho = le^{-\eta/l}$. The transformation (4.3.14) in Poincare coordinates is

$$z \to z + \frac{\rho^2}{2l}\bar{\epsilon}', \qquad \bar{z} \to \bar{z} + \frac{\rho^2}{2l}\epsilon', \qquad \rho \to \rho\left(1 - \frac{\epsilon + \bar{\epsilon}}{2l}\right). \tag{4.3.16}$$

Converting back to coordinates x, τ, the transformation (4.3.14) is

$$x \to x + \frac{\rho^2}{4l}(\bar{\epsilon}' + \epsilon'), \quad \tau \to \tau + \frac{\rho^2}{4il}(\bar{\epsilon}' - \epsilon'), \quad \rho \to \rho\left(1 - \frac{\epsilon + \bar{\epsilon}}{2l}\right). \tag{4.3.17}$$

According to the Ryu-Takayanagi prescription, the geodesic distance between boundary points $x = u, x = v$ computes entanglement entropy. As (4.3.17) is simply a diffeomorphism, the geodesic distance between two points on the boundary will take the same form before and after the diffeomorphism. The change in length will arise from applying the diffeomorphism to the geodesic length expression.

We will review the geodesic length computation. Consider a $\tau = 0$ geodesic without loss

of generality. The boundary cutoff surface is at $\rho = \delta \ll l, r$, where δ is related to the CFT cutoff and $r = v - u$. Geodesics in Euclidean AdS_3 are semi-circles. We parametrize the semi-circle centered at $x = a, \rho = 0$ and with radius r as

$$\rho = r \sin\theta, \qquad x = a + r\cos\theta. \tag{4.3.18}$$

Integrating from $x = a + r$ to $x = a - r$, the geodesic length L is

$$L = \int ds = \int_0^\pi d\theta \frac{l}{\sin\theta} = l \ln\left(\tan\left(\frac{\theta}{2}\right)\right)\Big|_{\delta/r}^{\pi-\delta/r} \approx l\ln(2r/\delta) + l\ln(2r/\delta). \tag{4.3.19}$$

The regulated endpoints of the interval, $(x, \rho) = (a \pm r, \delta)$, transform to first order in the δ, ϵ as follows, where we denote spatial dependence of $\epsilon, \bar{\epsilon}$ with $[\ldots]$:

$$(a \pm r, \delta) \to \left(a \pm r, \delta\left(1 - \frac{\epsilon[a \pm r] + \bar{\epsilon}[a \pm r]}{2l}\right)\right). \tag{4.3.20}$$

The geodesic length is therefore

$$L = l\ln\left(\frac{2r}{\delta\left(1 - \frac{\epsilon[a-r]+\bar{\epsilon}[a-r]}{2l}\right)}\right) + l\ln\left(\frac{2r}{\delta\left(1 - \frac{\epsilon[a+r]+\bar{\epsilon}[a+r]}{2l}\right)}\right). \tag{4.3.21}$$

This is the transformed geodesic length. We now use the Ryu-Takayanagi prescription $S_A = \text{Area}_{min}/4G_N$ and the Brown-Henneaux relation $c = \frac{3l}{2G_N}$ [101, 150] and find

$$\delta S_A = \frac{c}{12}(\omega(u) + \omega(v)), \tag{4.3.22}$$

in agreement with the CFT_2 result (4.3.6). The bulk computation resembles the proper-length CFT computation in that the transformation of the cutoff led to the change in entanglement entropy (4.3.10). There is no fundamental obstacle to extending (4.3.22) to higher orders in ω: the diffeomorphism that produces the finite Weyl transformation of the bound-

ary is known [151], and correlators of twist operators with stress tensor insertions are fixed by Ward identities.

4.4 First order metric perturbation: Lorentzian AdS_3/CFT_2

In this section, we will calculate the first-order change in entanglement entropy due to a metric perturbation. From this point on, we will work entirely in Lorentzian signature. We will view the corresponding Hamiltonian perturbation by the stress tensor as creating an excited state. The two descriptions are entirely equivalent [2]. We consider the excited state $U|0\rangle$ with

$$U = \mathcal{T}\left(e^{-i\int d^2y g(y^\mu)T(y_-)}\right), \tag{4.4.1}$$

where $y_\pm$ are lightcone coordinates. Our notation in this section is $y_- = y - t_y$ with $y^\mu = (t_y, y)$. The function $g(y^\mu) \equiv g(t_y, y)$ is bounded and contains a small dimensionless parameter so that the first order correction in g to correlation functions dominates for small value of this parameter. To first order in g, time ordering will not be relevant. Acting with the operator in (4.4.1) is equivalent to perturbing the metric by $\delta g_{--} = g(y^\mu)$. We compute entanglement entropy of a constant-time interval A at a time t_x when the source has turned off: $g(t_x, y) = 0$ for all y. At this point the Hamiltonian is once again equal to the unperturbed Hamiltonian, but the state is no longer the vacuum of that Hamiltonian. We choose $t_x = 0$ for convenience.

The first order correction to entanglement entropy is found by calculating the entanglement entropy in the state $(1 - i\lambda T(y_-))|0\rangle$ to first order in λ and then integrating this quantity $\mathcal{I}_\lambda$ against g:

$$\delta S_A = \int d^2y g(y^\mu)\mathcal{I}_\lambda(y^\mu). \tag{4.4.2}$$

Agreement between CFT and bulk methods occurs for the kernel of the perturbation $\mathcal{I}_\lambda$ as expected. Non-analyticity of g in time poses no fundamental obstacle to defining or implementing the replica trick, and our calculation demonstrates this perturbatively. In the

CFT, we will use the entanglement first law and the replica trick and find agreement. A basic causality property of entanglement entropy, that excitations localized to the causal domain of A cannot change the entanglement entropy S_A, is not manifest in the modular Hamiltonian. However, this property holds nevertheless, and imposes constraints on the modular Hamiltonian. In the bulk we will use the Hubeny-Rangamani-Takayanagi proposal and reproduce the CFT result. Finally, we will integrate $\mathcal{I}_\lambda$ and provide an interpretation for the change in entanglement entropy as a changing of the physics at the cutoff (entangling) surface.

4.4.1 $\mathbf{CFT_2}$: Entanglement First Law

We will compute the correction to the entanglement entropy using the entanglement first law [129]. The first-order correction δS_A is

$$\delta S_A = \int d^2y g(y^\mu) \int_A dx f(x) \langle 0|[T_{--}(y_-), T_{00}(x)]|0\rangle \tag{4.4.3}$$

For the interval A, $f(x) = (x-u)(x-v)/(u-v)$. The commutator $\langle 0|[T_{--}(y_-), T_{00}(x)]|0\rangle$ is fixed by conformal invariance.

$$\langle T_{--}(x,t)T_{00}(0)\rangle = \frac{1}{(x-t)^4}, \tag{4.4.4}$$

where we have omitted the overall factor of c. The commutator has support only on the lightcone, as seen from (4.2.13).

$$\langle [T_{--}(x,t), T_{00}(0)]\rangle = \partial_x^3 \delta(x-t). \tag{4.4.5}$$

The correction to entanglement entropy (4.4.3) is

$$\mathcal{I}_\lambda = \int_{\partial A} dx f(x) \partial_x^3 \delta(x_- - y_-) \tag{4.4.6}$$

From this expression, it naively seems that entanglement entropy can change when the perturbation is within the causal domain $\mathcal{D}_A$ of A, violating a well-known causality property of entanglement entropy [2, 87]. $\mathcal{D}_A$ is defined as the region through which no timelike geodesic can intersect without also passing through A. In the present case, $\mathcal{D}_A$ is the causal diamond of A. Integrating by parts,

$$\mathcal{I}_\lambda = -f'(x)\partial_x\delta(x_- - y_-)\Big|_{\partial A} + f''(x)\delta(x_- - y_-)\Big|_{\partial A}, \tag{4.4.7}$$

where primes denote spatial derivatives. We have used that $f(x)$ is zero for $x \in \partial A$, the boundary of the interval, which is necessary for the modular flow to vanish at ∂A. If we restored the overall numerical factors we have omitted, we would find that the i in the commutator multiplies the i coming from the perturbation to give a real result.

We have also used that $f'''(x) = 0$ for $x \in A$. We had no reason *a priori* to require $f'''(x) = 0$, but notice that if this were not true, entanglement entropy would change due to an excitation localized entirely within $\mathcal{D}_A$. We see that simple causality considerations restrict the form of $f(x)$. This argument applies only in two dimensions, but the same $f(x)$ appears in higher-dimensional modular Hamiltonians, and so can be viewed as a constraint on the modular Hamiltonian. This argument applies whenever the modular Hamiltonian is given by an integral over the stress tensor over any spacelike surface with the same boundary as A. Showing that $f'''(x) = 0$ for $x \in A$ follows from some basic principle would be illuminating. In general, this property holds for the vacuum modular Hamiltonian defined by choosing any Cauchy surface for $\mathcal{D}_A$. Substituting for $f(x)$, we have

$$\mathcal{I}_\lambda = -\partial_y(\delta(v - y_-) + \delta(u - y_-)) + \frac{2}{u - v}(\delta(v - y_-) - \delta(u - y_-)). \tag{4.4.8}$$

While the perturbation we have shown is right-moving, a general metric perturbation can change the entanglement entropy when null-separated from the interval's endpoints.

4.4.2 CFT_2: Replica Trick

We compute $\mathcal{I}_\lambda$ using the replica trick [109] in Lorentzian signature. In Euclidean signature, the expectation value of $T(y_-)$ on the n-sheeted Riemann surface is

$$\langle T(y_-)\rangle_{\mathcal{R}_n} = \frac{\langle T(y_-)\Phi_n(u)\bar{\Phi}_n(v)\rangle}{\langle \Phi_n(u)\bar{\Phi}_n(v)\rangle} = \frac{c}{24}(n-1/n)\frac{(u-v)^2}{(y_--u)^2(y_--v)^2}. \tag{4.4.9}$$

Acting with $-\partial_{n=1}$,

$$\partial_n|_{n\to 1}\,\langle T(y_-)\rangle_{\mathcal{R}_n} = \frac{c}{12}\frac{(u-v)^2}{(y_--u)^2(y_--v)^2} \tag{4.4.10}$$

We will assume that we can use the replica trick to calculate the change in entanglement entropy by treating the twist operators as well-defined local operators purely in Lorentzian signature. Using standard real-time perturbation theory implies that corrections to their expectation value will involve computing their commutators with Hamiltonian perturbations. This assumption is the natural sibling of the assumption made in order to compute excited-state entanglement entropy using twist operator insertions [66].

Our assumption should not be confused with assuming a purely-Lorentzian definition of the twist operators. The twist operators are ordinarily defined by imposing boundary conditions that lead to a Euclidean n-sheeted Riemann surface - moving a diagonalizing replica field ϕ_n on sheet n around the twist operator in Euclidean signature exchanges the field for one on another sheet: $\phi_n \to \phi_{n\pm1}$. Calculations for non-zero Lorentzian time are performed first in Euclidean time and then analytically continued. This procedure is equivalent to using the Schwinger-Keldysh contour. See [127] for further discussion of this point. Performing real-time perturbation theory, however, is equivalent to instead using the closed-time (Keldysh) contour and treating the twist operators as well-defined operators in some Lorentzian-signature quantum field theory. See refs. [2, 91] for a review. While in Lorentzian signature the replica trick is well-defined and twist operators can be identified by their fractional lightcone singularities in correlators, there is no obvious method of defining

the twist operators without recourse to complex time.

According to our assumption,

$$\mathcal{I}_\lambda = -\partial_{n=1} \frac{\langle 0|[T(y_-), \Phi_n(u)\bar{\Phi}_n(v)]|0\rangle}{\langle 0|\Phi_n(u)\bar{\Phi}_n(v)|0\rangle}. \tag{4.4.11}$$

We must analytically continue

$$\mathcal{I}_\lambda = \left[\frac{1}{(y_- - u)^2} - \frac{2}{(u-v)(y_- - u)} + \frac{1}{(y_- - v)^2} + \frac{2}{(u-v)(y_- - v)}\right]_{t_y \pm i\epsilon}. \tag{4.4.12}$$

Using (4.2.13),

$$\mathcal{I}_\lambda = -\partial_y(\delta(v - y_-) + \delta(u - y_-)) + \frac{2}{u-v}(\delta(v - y_-) - \delta(u - y_-)). \tag{4.4.13}$$

This agrees with the first law result (4.4.8).

4.4.3 AdS_3: Hubeny-Rangamani-Takayanagi

We compute the change to entanglement entropy using the HRT proposal. We first use a bulk diffeomorphism to implement the boundary metric perturbation in analogy to the Euclidean case. Next, we directly compute the geodesic length and find agreement between the two methods and with the CFT result.

In general dimensions, we would need to check that the bulk metric sourced by our metric perturbation at the cutoff surface has a boundary stress tensor expectation value that agrees with the CFT value. However, in pure AdS_3, the solution for the bulk metric with a flat boundary CFT metric $g^{(0)}_{\mu\nu} = \eta_{\mu\nu}$ is known exactly. For $\langle T_{z\bar{z}}\rangle = \langle T_{\bar{z}z}\rangle = 0$,

$$ds^2 = l^2\left(L_+ dx_+^2 + L_- dx_-^2 - \frac{1}{2}\rho^2 L_+ L_- dx_+ dx_- - 2\frac{1}{\rho^2} dx_+ dx_- + \frac{d\rho^2}{\rho^2}\right), \tag{4.4.14}$$

where $L_\pm \propto \langle T_{\pm\pm}\rangle$ [149, 152]. By solving Einstein's equations in the bulk or using the CFT

stress tensor two-point function, one can show that perturbations of $g_{\pm\pm}$ are accompanied by a non-zero Weyl anomaly, $\langle T_{\pm\mp}\rangle \neq 0$ [153]. However, after the perturbation has turned off, $\langle T_{\pm\mp}\rangle = 0$ and (4.4.14) applies. It is this regime we are considering.

As in the Euclidean case, we may calculate the change in the HRT surface length by finding the diffeomorphism that reproduces the correct boundary stress tensor expectation values. We will label the boundary lightcone coordinates as $z, \bar{z}$ so the parallels to the Euclidean case are clear. The small parameter $\epsilon(z, \bar{z})$ is dimensionless and corresponds to the metric perturbation $\delta g_{zz} = \epsilon(z, \bar{z})\delta_{zz}$. We assume ϵ has compact spacetime support. The diffeomorphism that reproduces $\langle T(z)\rangle = \partial_z^3 \delta(z - z_s)$ is

$$\eta \to \eta + \epsilon l^2 \partial_z \delta(z - z_s), \qquad z \to z - \epsilon 2l\delta(z - z_s), \qquad \bar{z} \to \bar{z} + \epsilon l^3 e^{-2\eta/l}\partial_z^2 \delta(z - z_s). \quad (4.4.15)$$

As expected, once the source turns off, the bulk metric can be obtained by a diffeomorphism that implements a boundary conformal transformation. The metric becomes

$$ds^2 = d\eta^2 + e^{2\eta/l} dz d\bar{z} + \epsilon l^3 \partial_z^3 \delta(z - z_s) dz dz. \quad (4.4.16)$$

We use the diffeomorphism (4.4.15) to compute the change in entanglement entropy. To first order in the cutoff δ the extremal surface area changes as

$$\begin{aligned} S_A \to S_A &+ \frac{c}{3} \ln\left(1 + \epsilon \frac{l}{u - v}\left(\delta(v - z_s) - \delta(u - z_s)\right)\right) \\ &- \frac{c}{6}\left(\ln(1 - \epsilon l \partial_u \delta(u - z_s)) + \ln(1 - \epsilon l \partial_v \delta(v - z_s))\right). \end{aligned} \quad (4.4.17)$$

Omitting overall factors and using $z_s = y_-$,

$$\mathcal{I}_\lambda = -\partial_y(\delta(v - y_-)) + \delta(u - y_-)) + \frac{2}{u - v}(\delta(v - y_-) - \delta(u - y_-)). \quad (4.4.18)$$

This agrees with the CFT result (4.4.8).

A related but distinct computation was performed in [154]. The method of finding a diffeomorphism to reproduce the AdS_3 metric corresponding to a stress tensor perturbation was used to model the time-dependent entanglement entropy of a pulse in a CFT [154]. In this case the pulse produced a finite expectation value for the boundary stress tensor at all times, while in our case, the stress tensor expectation value turns on at some finite time. The two setups are physically different: in [154], the state of the dual CFT being modeled was a mixed state, as the pulse changed the entanglement entropy when its location on the boundary was inside $\mathcal{D}_A$. In contrast, the perturbation we consider is a pure-state perturbation and, as we have seen, does not change the entanglement entropy when the perturbation is within $\mathcal{D}_A$.

We will now reproduce the AdS_3 result through directly computing the geodesic length in the background (4.4.16). Interestingly, the integral naturally takes the same form as the entanglement first law. To first order in the metric perturbation, the extremal surface does not change. The extremal surface is a geodesic parameterized by θ as $x = \frac{v+u}{2} - \frac{v-u}{2}\cos\theta, \theta \in [0, \pi]$. With $r = (v-u)/2$, the geodesic is parameterized by $\rho = r\sin\theta$. The new extremal length $\mathcal{L}'$ in terms of the original length $\mathcal{L}$ is

$$\mathcal{L}' = \mathcal{L} + \frac{1}{2}\int d\theta \frac{\partial_z^3 \delta(z-z_s)\,(r\sin\theta)^2}{\sqrt{\frac{1}{(r\sin\theta)^2}\left((r\cos\theta)^2 + (r\sin\theta)^2\right)}} = \mathcal{L} + \frac{1}{2}r^2\int d\theta (\sin\theta)^3 \partial_z^3 \delta(z-z_s). \quad (4.4.19)$$

Here, $\frac{d}{dz} = \frac{1}{r\sin\theta}\frac{d}{d\theta}$. This derivative is singular at the endpoints $\theta = 0, \pi$ as expected. We can rewrite this integral in a more familiar form. Substituting back for x and using

$$dx = -r\sin\theta d\theta, \qquad r^2\sin^2\theta = -(x-u)(x-v), \quad (4.4.20)$$

we can rewrite the integral as an integral over boundary coordinate x.

$$\mathcal{I}_\lambda = \int dx \frac{(x-u)(x-v)}{(u-v)} \partial_x^3 \delta(z-z_s). \quad (4.4.21)$$

We have demonstrated agreement with the the CFT first law result (4.4.3) and therefore (4.4.8). It would be interesting to extend this to higher order and include matter to obtain higher-order integral expressions for holographic CFT entanglement entropy. By subtracting the contributions from the perturbation to the state, which are known from standard real-time perturbation theory, this procedure would algorithmically calculate the corrections to the expectation value of the modular Hamiltonian for holographic CFTs.

4.4.4 Integrating the perturbation and interpretation

In this section we integrate $\mathcal{I}_\lambda$ against g and discuss the result. As g has compact support, boundary terms arising in integration by parts are zero. We restore the factor of c we had omitted.

$$\delta S_A = c \int dy_+ \left[\partial_v g(v, y_+) + \partial_u g(u, y_+) + \frac{2}{u - v} \left(g(v, y_+) \delta(v - y_-) - g(u, y_+) \delta(u - y_-) \right) \right]. \tag{4.4.22}$$

We have used the notation $g = g(y_-, y_+)$. The entanglement entropy depends only on g along the lightcones of u, v.

The ∂g term is independent of interval length but zero if g is constant on the lightcone. In the Lorentzian bulk computation, this term arises from changing the cutoff. This interpretation of the result in the CFT is consistent with the ∂g term, as we expect changes in entanglement entropy due to changing the cutoffs at u, v to be additive and independent of the interval length $v - u$. When g changes across the lightcone, that is $\partial_v g(v, y_+) \neq 0$, the relationship between the inner and outer cutoff surfaces changes.

In contrast, the g term changes entanglement entropy even when g is constant across the lightcone. We interpret the g term as arising from correlations of the background state (the vacuum) between different locations on the entangling surface. This interpretation is consistent with the g term, whose contribution decays as $1/(v - u)$ and if g is constant, the change in entanglement entropy along u's lightcone precisely cancels that from v's lightcone.

In the bulk calculation, this term comes from transforming the interval length.

Entanglement entropy obeys the causality properties of an operator localized to the entanglement surface. While there are well-known ambiguities in associating entanglement entropy with an observable located at the entangling surface, these ambiguities can arise from gauge invariance [94]. It would be interesting to examine whether these issues arise in computing corrections due to time-dependent perturbations. The causality structure of these corrections depends only on Lorentz-invariant quantities, and so perhaps these causal properties provide a gauge-invariant probe of the physics at the entangling surface.

The result (4.4.22) is valid even when $g(t_y, y)$ is not analytic in time. As previously discussed, Lorentzian-time calculations of entanglement entropy that use the replica trick begin with all operators at zero Lorentzian time and then the result is analytically continued. One may wonder whether this procedure is fundamentally limited, inapplicable when features of the excitation are not analytic in time, for example, discontinuities in the excitation or, in the bulk description, the metric. Perturbatively, however, we see that the computation does proceed by analytic continuation. We do not anticipate that non-analyticity in time poses a fundamental obstruction to implementing the replica trick.

4.5 A conjecture: interactions entangle excitations

The higher-order computations we will perform shortly provide evidence for the conjecture that interactions entangle excitations. In this section we will develop a convenient diagrammatic tool for performing computations in real-time perturbation theory, detail our conjecture, and provide motivation. The content in this section uses real-time perturbation theory [69, 70]. For a recent review, see [2, 91]. In real-time perturbation theory, the time contour in the path integral is never complex.

4.5.1 Diagrammatic rules for real-time perturbation theory

We develop a diagrammatic approach to real-time perturbation theory in order to simplify computations and make basic causality properties manifest. This approach applies to perturbations about a free field theory.

Consider computing corrections to the expectation value of an operator $\mathcal{O}$ due to turning on sources for operators A, B, C. We will consider a local operator $\mathcal{O}$ as an example. Spacetime Feynman diagrams describe the various contributions to the integrand at each order, as a function of operator locations $x_A, x_B, x_C, x_{\mathcal{O}}$. In Euclidean AdS/CFT, these diagrams are Witten diagrams. Suppose the contribution we are interested in comes from the commutator $[A, [B, [C, \mathcal{O}]]]]$. The spacetime diagram will be ordered with $t_{\mathcal{O}} > t_C > t_B > t_A$, which also determines whether operators cross future or past lightcones of other operators when continued to Lorentzian signature. The procedure we give accounts for that sign. The only non-zero contribution to the commutator comes from fully connected contractions.

In a spacetime diagram, lines that correspond to Wick contractions between operators at spacelike-separated points are labeled separated, as in figure 4.2. We call these lines spacelike lines for short, and similarly for timelike and null cases. Factor the spacelike contractions $\langle E \rangle_s$ out of the Euclidean integrand $\langle E \rangle$, as they will not affect the causal structure of the quantity $\langle E_c \rangle$ we use to compute the commutator: $\langle E \rangle = \langle E \rangle_s \langle E \rangle_c$. The time-ordering and corresponding commutator can be read off from the spacetime diagram. Begin by continuing $\langle E \rangle_c$ to Lorentzian time with the following operator ordering:

$$\langle L \rangle_c^{(1)} = \langle ABC\mathcal{O} \rangle \tag{4.5.1}$$

using (4.2.13). Now beginning from $\mathcal{O}$ in the diagram and descending, subtract the continuation corresponding to reversing the $i\epsilon$ associated with each vertex passed. This is nothing more than computing the commutator beginning with $[C, \mathcal{O}]$ and working outwards. Explic-

itly,

$$\langle L\rangle_c^{(2)} = \langle L\rangle_c^{(1)} - \langle L\rangle_c^{(1)}\,|_{\epsilon_{\mathcal{O}C}\to-\epsilon_{\mathcal{O}C}} = \langle AB[C,\mathcal{O}]\rangle\,. \tag{4.5.2}$$

Moving past B,

$$\langle L\rangle_c^{(3)} = \langle L\rangle_c^{(2)} - \langle L\rangle_c^{(2)}\,|_{\epsilon_{\mathcal{O}B},\epsilon_{CB}\to-\epsilon_{\mathcal{O}B},-\epsilon_{CB}} = \langle A[B,[C,\mathcal{O}]\rangle\,. \tag{4.5.3}$$

Another iteration produces the full Lorentzian commutator

$$\langle L\rangle_c^{(4)} = [A,[B,[C,\mathcal{O}]]]. \tag{4.5.4}$$

This procedure is illustrated in figure 4.2.

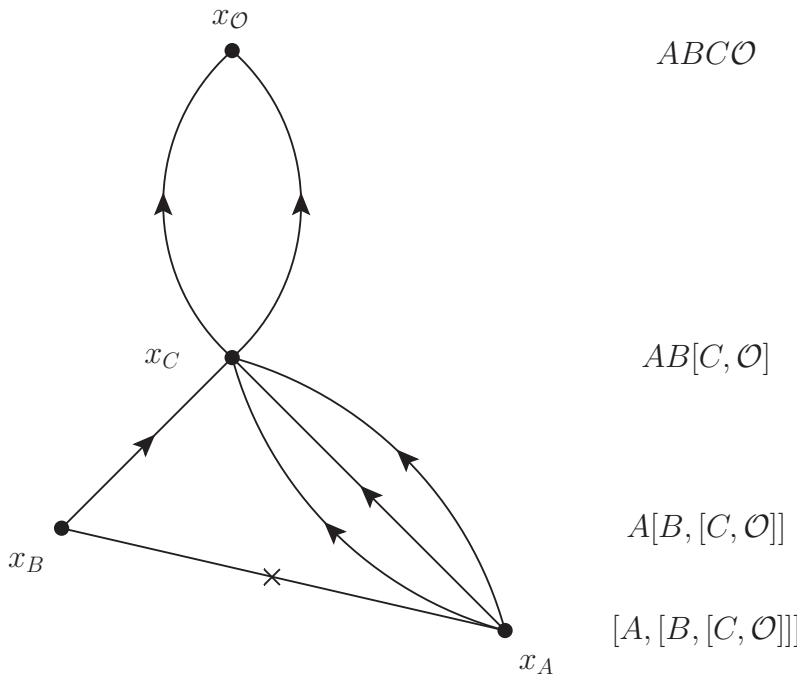

Figure 4.2: A sample diagram for real-time perturbation theory. We have chosen conventions to make the diagram less visually confusing. When a loop is between null-separated points, we draw only one of the lines null. Some lines therefore may appear spacelike, but it is understood that only the lines labeled with $\times$ are spacelike.

Other than the rules we have described, the rules for building integrands from diagrams

are the standard position-space Feynman rules. In the in-out perturbation theory used for scattering amplitudes, disconnected contractions cancel due to their exponentiation, while here the presence of disconnected contractions makes the whole diagram zero due when the commutators are computed.

Causality properties are manifest in the diagrammatic formulation. Information cannot be transmitted along spacelike lines, but these lines contribute to the perturbative result according to the correlations in the background state. This can be seen in the simple case of the correction to the two-point function given by $[\phi^2(x), [\phi^2(y), \phi(z)\phi(w)]]$. When integrating, spacelike lines can become null or timelike, becoming propagators and carrying information. Non-zero diagrams must be fully-connected to $\mathcal{O}$ once all spacelike lines are cut. From the cutting rule, it follows that every operator insertion must be connected to an operator in its future by at least one null or timelike line. Otherwise, this operator will commute with all operators in its future and the diagram will be zero.

4.5.2 The conjecture

In this section we make a conjecture about entanglement propagation in field theory. Consider a Lagrangian of a quantum field theory in $d+1$ dimensions somewhere along its RG flow, written schematically as

$$\mathcal{L} = \mathcal{L}_0 + J(t)\mathcal{O} + \lambda\mathcal{O}_\lambda. \tag{4.5.5}$$

Assume the initial state $|\Psi\rangle$ is time independent for simplicity.

Consider the entanglement entropy S of subregion A at a time t by which the source has turned off: $J(t) = 0$. S can be expanded in J, λ.

$$S = \sum_{m,n=0} S_{m,n} J^m \lambda^n, \tag{4.5.6}$$

where $S_{0,0}$ is the entanglement entropy in state $|\Psi\rangle$. Suppose that there exists at least one local operator $\mathcal{O}$ such that

$$S_{m,0} = 0. \tag{4.5.7}$$

Operators $\mathcal{O}$ create unentangled excitations and serve as building blocks for entangled states in that theory. We refer to these operators as unentangled operators, and all others as entangled operators. There generically exists a set of entangled operators $\mathcal{O}_\lambda$ that change the entanglement entropy in the presence of these unentangled excitations:

$$S_{m,n>0} \neq 0. \tag{4.5.8}$$

When $\mathcal{L}_0$ is a free action, $\mathcal{O}_\lambda$ can sometimes be built from normal-ordered products of $\mathcal{O}$. One can think of $\mathcal{O}_\lambda$ as interactions necessary to entangle unentangled excitations created by $\mathcal{O}$, and which themselves must be entangled operators.

$S_{m,n>0} \neq 0$ only when one can draw spacetime "entanglement diagrams" to determine for which n, interactions $\mathcal{O}_\lambda$, and kinematic regions $S_{m,n>0} \neq 0$ is allowed. See figure 4.3 for a simple example. Entanglement diagrams are zero when the same diagram interpreted as a spacetime Feynman diagram would be zero according to the properties explained in 4.5.1.

When $\mathcal{L}_0$ is a free Lagrangian, it is possible but not necessary that entanglement diagrams reduce to the spacetime Feynman diagrams associated with real-time perturbation theory, and the lines are Wick contractions of free fields [1].

In interacting conformal field theories, one may identify vertices as follows: for example, in the $S_{3,1}$ correction, the $\mathcal{O}_\lambda$ serves as a cubic vertex for the three operators $\mathcal{O}$ in the associated entanglement diagram when

$$\langle\Psi|\mathcal{O}\mathcal{O}\mathcal{O}\mathcal{O}_\lambda|\Psi\rangle \neq 0. \tag{4.5.9}$$

[1] In the following section, we will see that this occurs for a special case, the bosonized free fermion. In this case, the contractions occur between the bosons, whose relationship to the fermions is inherently non-local.

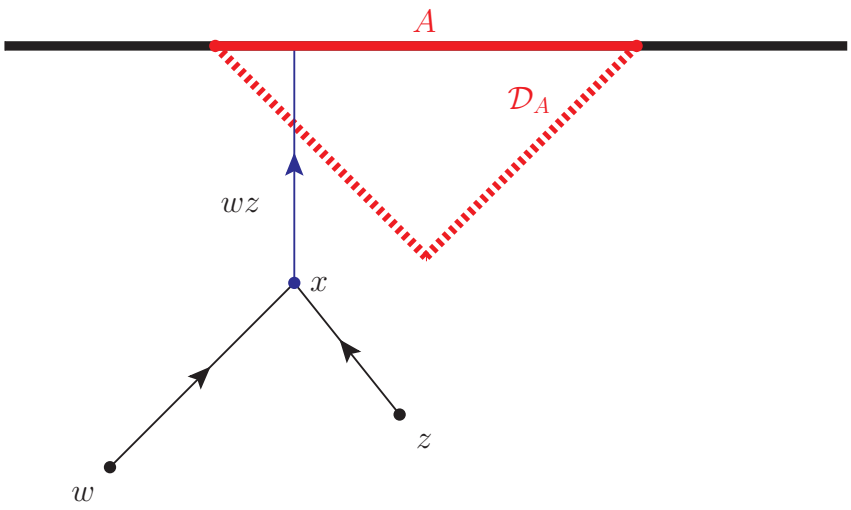

Figure 4.3: An entanglement diagram for a non-zero $S_{2,1}$ process in $1+1$ dimensions in which propagation occurs only along null rays. Entanglement entropy of a subregion A obeys the causality properties of a non-local operator $\mathcal{O}_A$ with support within $\mathcal{D}_A$, and this diagram corresponds to the commutator $[\mathcal{O}(w), [\mathcal{O}(z), [\mathcal{O}_\lambda(x), \mathcal{O}_A]]]$. The line labeled with z, w is the flow of entanglement of unentangled excitations. If we want to keep track of the flow of all entanglement, we would also include the label x. We may also keep track of background state entanglement across spacelike lines.

One consequence [2] is that in large-N field theories in which $\mathcal{O}, \mathcal{O}_\lambda$ are single-trace primaries whose dimensions are held fixed as $N \to \infty$, $\mathcal{O}_\lambda$ serves as an m-point vertex for m odd to order N^0. At order $1/N$, m can be even or odd. By inserting projectors $\sum_i |\psi_i\rangle \langle\psi_i|$ into (4.5.9), each entanglement diagram line can be decomposed into a sum over contributions from different states $|\psi_i\rangle$. This is equivalent to inserting the identity along Cauchy surfaces between each operator in the entanglement diagram. Not all exchanged states lead to a non-zero entanglement diagram; as a trivial example, the exchange of the vacuum state $|0\rangle$ along every line will produce no change in entanglement entropy. In $1+1$ dimensions, the state-operator correspondence allows us to identify the exchanged states $|\psi_i\rangle$ with those created by local operators. While the notions of generalized contractions and vertices we have discussed depend on the system, entanglement diagrams always chart causality and the flow of entanglement consistent with real-time perturbation theory.

[2] This follows from large-N factorization of generalized free fields.

Entanglement diagrams obey the following rules, which are particular to entanglement propagation. At least one timelike or null line must end on the subregion A. All $\mathcal{O}_\lambda, \mathcal{O}$ insertions must remain outside the outside $\mathcal{D}_A$[3]. Entanglement diagrams obey an additional cutting rule over for example spacetime Feynman diagrams. Upon cutting all lines that end on A, every remaining connected subdiagram must contain at least one operator that is itself entangled. As a corollary, turning on sources for different unentangled operators does not produce entanglement.

Entanglement diagrams distill two kinds of entanglement: entanglement due to excitations interacting and entanglement due to correlations in the background state. Entanglement cannot propagate along spacelike lines, but correlations in the state $|\Psi\rangle$ will cause excitations to be correlated [4]. One can label diagrams according to the propagation of background state entanglement.

$\mathcal{O}_\lambda$ can entangle excitations that are themselves entangled, but not entangled with each other. This is the more common case, as generic operators are entangled. In this case, $S_{m,0} \neq 0$ but entanglement diagrams still dictate when $S_{m,n} \neq 0$ is allowed and govern the flow of entanglement. We have formulated this section in terms of unentangled excitations, but our statements apply to processes which contain only entangled excitations.

4.5.3 Motivation and evidence

Similar entanglement structure has been found in excited state entanglement entropy computations [2, 61, 63–65, 85]. Working with the free scalar, [64] showed that entanglement entropy in state $e^{i\alpha\phi}|0\rangle$ is equal to that of the vacuum, but in the state $\left(e^{i\alpha\phi} + e^{-i\alpha\phi}\right)|0\rangle$ jumps by $\log(2)$, precisely what is expected from a single entangled pair. The authors put forward a compelling quasi-particle picture, including a discussion of entangled operators. Here, the additional entanglement arose from interactions between the pair of excitations

[3] This fact follows from basic entanglement entropy causality [2, 87].

[4] As discussed in 4.5.1, the existence of these two types of correlations is not specific to entanglement entropy, but is a general feature of field theory.

that occurred in preparing the entangled state. In processes with a time-dependent Hamiltonian, the entanglement will arise from interactions for the same reason. We expect the notion of entangled operators creating entangled states to parallel our conjecture for time-dependent Hamiltonians. We have only explored perturbations about the vacuum, but one can perform similar perturbative computations in excited states.

In this work, we consider $\mathcal{L}_0$ for free and holographic field theories and $|\Psi\rangle = |0\rangle$. Our results in 4.6 will provide evidence for the conjecture in 4.5.2. We consider localized excitations to make the mechanisms physically transparent. Without a general method to compute field theory entanglement entropy, it is unclear how to prove the statements in 4.5.2 that we have not already shown follow from basic properties of entanglement and causality. While entanglement entropy is not itself a physical observable, it is determined by ρ_A, and all observable properties of ρ_A are fixed according to the expectation values of operators localized to $\mathcal{D}_A$, which themselves change according to standard real-time perturbation theory.

4.6 Higher order perturbation theory: the free fermion

The computations in this section demonstrate the mechanisms that we conjecture in 4.5.2. Even in the absence of excitations, deforming a CFT by some operator will change its vacuum entanglement entropy. This can be seen from the Euclidean perturbation theory and has been well studied. How this happens is clear: deforming the CFT changes the vacuum state. Here, we will perform computations that reveal a different mechanism: separately from changing the vacuum state of the theory, interactions change entanglement entropy by entangling excitations.

We calculate higher-order corrections to entanglement entropy in the free $1+1$ dimensional fermion using the replica trick. The twist operators for the free fermion are known explicitly and so the result can be computed exactly, with causality properties manifest at every step. We compute several entanglement diagrams built from the following chiral

operators:

$$J = \sum_k \partial\phi_k, \qquad T = \sum_k (\partial\phi_k)^2, \qquad W = \sum_k (\partial\phi_k)^3, \tag{4.6.1}$$

with $k = -1/2(n-1), -1/2(n-1)+1, \ldots, 1/2(n-1)$. These operators are the spin 1, 2, and 3 currents respectively, which are built from bilinears of fermion fields, schematically $:\psi\partial^m\psi^*:$ with $m = 0, 1, 2$ [138, 155].

4.6.1 Warmup: metric perturbation

To understand basic features of fermionic calculations of entanglement entropy, we warm up by reproducing the first-order change in entanglement entropy due to a metric perturbation (4.4.13). Using (4.2.21),

$$\langle 0|T(z)\Phi_n(u)\bar{\Phi}_n(v)|0\rangle = \sum_k \frac{-k^2}{n^2} \langle 0| :(\partial\phi_k)^2(z)::(\phi_k(u)-\phi_k(v))^2: |0\rangle \,. \tag{4.6.2}$$

The singularity structure of (4.4.13) is apparent even before acting with $-\partial_{n=1}$ to obtain entanglement entropy.

$$\langle 0|T(z)\Phi(u)\bar{\Phi}_n(v)|0\rangle = \sum_k \frac{-k^2}{n^2}\left(\frac{1}{(z-u)^2} + \frac{1}{(z-v)^2} + \frac{2}{(u-v)(z-v)} - \frac{2}{(u-v)(z-u)}\right). \tag{4.6.3}$$

The remaining steps lead to (4.4.13).

4.6.2 J creates unentangled excitations

We will compute entanglement entropy due to perturbations in J with a time-dependent source. Without loss of generality, we will suppose v is spacelike-separated from all sources to simplify the expressions unless specified otherwise. At first order in $J(z)$, entanglement

entropy does not change. The Euclidean integrand is

$$\mathcal{I}_J^E(z) = \sum_k \frac{k}{n} \langle 0|\partial\phi_k(z)\phi_k(u)|0\rangle = \sum_k \frac{k}{n}\frac{1}{z-u}. \tag{4.6.4}$$

Performing the sum over k, we see $\mathcal{I}_J = 0$, as expected for a primary operator. The second-order correction comes from

$$\mathcal{I}_{J^2}^E(w,z) = \sum_{k_1,k_2,k_3,k_4} \langle 0|\partial\phi_{k_1}(w)\partial\phi_{k_2}(z) : \frac{k_3}{n}\phi_{k_3}(u)\frac{k_4}{n}\phi_{k_4}(u) : |0\rangle . \tag{4.6.5}$$

Performing the sum over k_3, k_4 gives zero in any connected correlator above. All higher-order corrections will be zero for the same reason, which is that J is linear in $\partial\phi$. J therefore creates an unentangled excitation as defined in 4.5.2. J is indeed a non-trivial excitation, as it does change correlators of fermions on the plane.

4.6.3 Adding an interaction W entangles J excitations

We introduce a cubic interaction W and observe how this entangles two unentangled J excitations. To $\mathcal{O}(J^2W)$,

$$\mathcal{I}_{J^2W}^E(w,z,x) = \sum_{k_1,k_2,k_3} \langle 0|\partial\phi_{k_1}(w)\partial\phi_{k_2}(z) : (\partial\phi_{k_3})^3(x) :: e^{\sum_{k_4} i\frac{k_4}{n}\phi_{k_4}(u)} : |0\rangle . \tag{4.6.6}$$

All connected contractions are zero because they involve a sum over an odd power of k_i. Non-zero correlators require an even number of ϕ operators within the correlator with twist operators. At $\mathcal{O}(J^2W^2)$,

$$\begin{aligned}\mathcal{I}_{J^2W^2}^E(w,z,x,y) = \sum_{k_1,k_2,k_3,k_4} &\langle 0|\,\partial\phi_{k_1}(w)\partial\phi_{k_2}(z) \\ &\times : (\partial\phi_{k_3})^3(x) :: (\partial\phi_{k_4})^3(y) :: e^{\sum_{k_5} i\frac{k_5}{n}\phi_{k_5}(u)} : |0\rangle .\end{aligned} \tag{4.6.7}$$

Not all contractions contribute to entanglement entropy. All terms with a single contraction between $\phi(w)$ or $\phi(z)$ with $\phi(u)$ are zero upon summing over k_i. This is true to all orders in J, W, consistent with the cutting rule for entanglement diagrams, as J represents an unentangled excitation. This conjectured cutting rule is non-trivial and specific to entanglement entropy: in computing corrections to generic correlators instead of entanglement entropy, these contractions would not be zero. If all lines ending on A are cut and the diagram D factorizes into $D_{ent}D_{unent}$, which is the product of a diagram that changes the entanglement entropy on its own and a diagram containing only unentangled excitations, then the associated change in entanglement entropy occurs at a different order in perturbation theory than the original diagram.

The diagram in figure 4.4 with the x, y contractions exchanged has no branch cuts in $u - y$, and so will be zero once we compute the corresponding commutators. As explained in 4.5.1, this is the real-time perturbation theory rule that every vertex must have at least one future-directed line that is not spacelike.

There are two allowed diagrams, and which one is non-zero depends on the location of x, y. The diagram in figure 4.4 corresponds exclusively to the causal entanglement of excitations. In contrast, when for example $u = x$ and $v = y$, the diagram in figure 4.5 corresponds exclusively to background state entanglement.

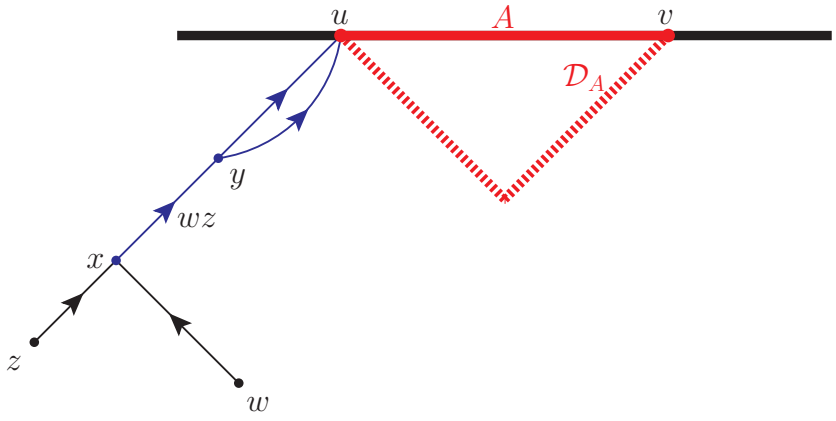

Figure 4.4: A non-zero diagram contributing to the $\mathcal{O}(J^2W^2)$ process. We have drawn one of the incoming lines as left-moving for clarity.

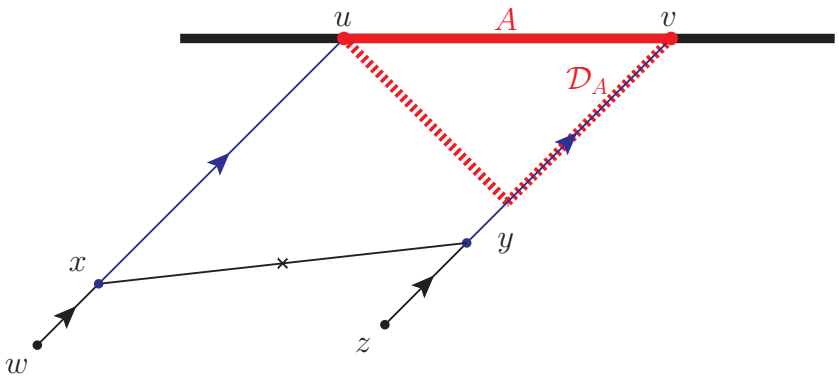

Figure 4.5: A diagram contributing to the $\mathcal{O}(J^2W^2)$ process. This diagram corresponds to a change in entanglement entropy due to background state correlations. A similar diagram contributes when $x, y = u$, in which case the entanglement is not due to background state correlations.

We compute the diagram in figure 4.4. The Euclidean signature integrand is

$$\mathcal{I}^E_{J^2W^2}(w,z,x,y) = \frac{1}{(w-x)^2(z-x)^2(x-y)^2(y-u)^2}. \tag{4.6.8}$$

Using the procedure in 4.5.1, it is straightforward to compute the commutator, although we will shortly use real-time Feynman rules to simplify the process further. Using the top sign in the top line of (4.2.13),

$$\begin{aligned}\mathcal{I}^{(1)}_{J^2W^2}(w,z,x,y) = &\left(\frac{1}{(w-x)^2} + i\pi\partial_{w-x}\delta(w-x)\right)\left(\frac{1}{(z-x)^2} + i\pi\partial_{z-x}\delta(z-x)\right)\\ &\times\left(\frac{1}{(x-y)^2} + i\pi\partial_{x-y}\,\delta(x-y)\right)\left(\frac{1}{(y-u)^2} + i\pi\partial_{y-u}\delta(y-u)\right).\end{aligned} \tag{4.6.9}$$

As in 4.5.1, we begin with the operator at u descend to compute the commutator.

$$\mathcal{I}_{J^2W^2}(w,z,x,y) = \partial_{w-x}\delta(w-x)\partial_{z-x}\delta(z-x)\partial_{x-y}\delta(x-y)\partial_{y-u}\delta(y-u). \tag{4.6.10}$$

We see that the W operators entangle the unentangled J excitations and entanglement travels according to the associated entanglement diagram. It is straightforward to integrate

this result against sources for the operators, as in (4.4.22).

$$\delta S_{J^2W^2} = \int d^2w d^2z d^2x d^2y \partial_w \mathcal{J}_J(w,\bar{w}) \partial_z \mathcal{J}_J(z,\bar{z}) \partial_x \mathcal{J}_W(x,\bar{x}) \partial_y \mathcal{J}_W(y,\bar{y}) \Big|_{w=z=x=y=u}, \tag{4.6.11}$$

where $\mathcal{J}_J, \mathcal{J}_W$ are the source functions for operators J, W.

Because we work in free field perturbation theory, real-time position space Feynman rules apply, and they simplify calculations further. We will need the Feynman rules for operators $\phi, \partial\phi$. When spacetime points a, b are causally connected, $\phi(a)\partial\phi(b)$ contributes a $\delta(a-b)$ and $\partial\phi(a)\partial\phi(b)$ contributes $\partial_{a-b}\delta(a-b)$. When a, b are spacelike-separated, $\phi(a)\partial\phi(b)$ contributes $1/(a-b)$ and $\partial\phi(a)\partial\phi(b)$ contributes $1/(a-b)^2$. We have omitted the overall numerical factors in these expressions.

Using the above Feynman rules, we can now easily compute the diagram in figure 4.5 in the kinematic regime $w = u, z = u$. We find the contribution

$$\mathcal{I}_{J^2W^2}(w,z,x,y) = \frac{1}{(y-x)^2} \partial_w \delta(w-x) \delta(x-u) \partial_z \delta(z-y) \delta(y-v). \tag{4.6.12}$$

We see that the background state entanglement decays in $y-x$. That this diagram decays in $y-x$ is expected from the spatial decay of vacuum correlations. In the regime $w = z = u$,

$$\mathcal{I}_{J^2W^2}(w,z,x,y) = \delta(y-u)\delta(x-u)\partial_y \delta(y-x) \partial_z \delta(z-y) \partial_w \delta(w-x). \tag{4.6.13}$$

At $\mathcal{O}(J^2W^2)$ performing the integration reveals similar features to the metric perturbation result (4.4.22), namely that the sources often must change across the lightcones of u, v in order to change entanglement entropy. This is a distinctly time-dependent feature of entanglement entropy and its interpretation is similar to that of (4.4.22). Diagrams in other kinematic regions are straightforward to obtain from the results we have given, and higher-order integrands are similarly easy to construct using the tools we have provided.

As all the operators we have used are fermion bilinears, the standard Wick contraction

between fermions would not have produced a diagram with a cubic vertex. However, the condition we gave in (4.5.9) identifies W as a cubic vertex. The bosonic field ϕ and entanglement diagrams naturally describe entanglement propagation in much the same straightforward way that the fermionic field ψ and spacetime Feynman diagrams naturally describe time-dependent corrections to local observables.

4.7 Discussion

In this work, we have investigated entanglement entropy in conformal field theory with a general time-dependent Hamiltonian. We have extended previous first-order studies by computing higher order corrections. Past first order, we found evidence of a universal entanglement structure in perturbation theory. We have conjectured that interactions entangle unentangled excitations. Using the free fermion as an illustrative example, we identified the spin-1 current J as an unentangled excitation, included the spin-3 current W as an entangled interaction and found that, when the interaction turns on where the two J excitations collide, the interaction entangles the excitations. We computed the corresponding J^2W^2 processes. Having identified unentangled excitations J and an entangled cubic vertex W, we show that the free fermion is a simple, tractable arena in which to investigate details of entanglement propagation.

We have conjectured that the flow of entanglement entropy is governed by "entanglement diagrams". Entanglement propagates only when there is a non-trivial entanglement diagram associated with the process. These diagrams are motivated by the accessory spacetime Feynman diagrams of real-time perturbation theory, but they are entirely independent of Feynman diagrams and obey certain rules specific to entanglement entropy. We provided a diagrammatic approach to streamline computations in real-time perturbation theory and found this approach makes causality properties of the correlators manifest. In the bosonized free fermion, entanglement diagrams are spacetime Feynman diagrams but for the boson ϕ rather than the fermion ψ. The procedure we propose for identifying vertices in entanglement

diagrams identifies W as a cubic vertex independently of the bosonization procedure that makes this fact manifest. More generally, we expect that further study of entanglement diagrams and the entanglement of excitations through interaction with entangled vertices may uncover natural variables for entanglement propagation in field theory.

4.7.1 Future directions

We detail several exciting directions of further study, some of which we hope to report on in the future.

Causality may place stringent constraints on the $1+1$ dimensional modular Hamiltonian via a bootstrap approach, order by order in perturbation theory. In 4.4 we found that entanglement causality places a non-trivial constraint on the integrand of the modular Hamiltonian if the integrand is function of local operators. Using the replica trick and Ward identities, one can compute the entanglement entropy due to metric perturbations to arbitrary order. Constraints on the modular Hamiltonian at a given order feed into its form at the next order. The ansatz can be checked for consistency against the exact expression, obtainable using standard perturbation theory [156]. At each order, the modular Hamiltonian must be consistent with entanglement causality due to perturbation by primary operators as well.

While local, explicit twist-operators are special to $1+1$ dimensional fermions, replica trick computations in the free scalar and fermions are in principle straightforward in general dimensions for a single interval [64]. One can clarify the relationship between entangled operators for excited states and Hamiltonian perturbations, as there is a correspondence between local operator excitations and Hamiltonian perturbations [2]. For example, vertex operators have a simple interpretation as building blocks of EPR states [64]. What is the entanglement propagation structure of vertex operators as Hamiltonian perturbations? The entangling interactions $\mathcal{O}_\lambda$ affect entanglement propagation. A concrete question to answer is: how does entanglement velocity depend on the choice of $\mathcal{O}_\lambda$? We have only addressed entanglement entropy, but one may investigate similar questions for other information theoretic measures.

Time-dependent Hamiltonian perturbations can serve as another probe of HRT. Specifically, approximate expressions for the conformal blocks dominating the $\langle \mathcal{O}\mathcal{O}\Phi_n\bar{\Phi}_n\rangle$ correlator are known in the large c limit for holographic CFTs [66, 157, 158]. This correlator gives the entanglement entropy to second order in the Hamiltonian perturbation $J(t)\mathcal{O}$, and one can compare the result to the bulk HRT calculation. Keeping $\Delta_{\mathcal{O}}/c$ fixed in the large-c limit corresponds to a non-perturbative bulk computation. In [159] one part of this CFT calculation was performed. $\Delta_{\mathcal{O}}(n) = n\Delta_O$ was used, while the full second order correction involves the operator $\sum_k^n J^k\mathcal{O}_k$, where $\Delta_{O_k} = k\Delta_{\mathcal{O}}$. On the other hand, holding $\Delta_{\mathcal{O}}$ fixed in the large-c limit corresponds to standard bulk semiclassical perturbation theory.

While we have so far discussed entanglement in flat spacetimes, it is well known that the structure of entanglement in AdS plays an important role in the AdS/CFT correspondence. In particular, one may investigate the entanglement spreading that we have described in flat space in AdS, and address its dual CFT interpretation. What is the CFT dual of bulk entanglement diagrams like figure 4.1? Specifically, tree-level Witten diagrams can be expressed as linear combinations of conformal blocks, see for example [160], and so we expect that bulk tree-level entanglement diagrams have a dual CFT description at the corresponding order in $1/N$. How do the UV data of the theory - the interactions - affect entanglement structure on a covariant measure of entanglement and entropy, namely light sheets [161,162]?

One can study loop-level effects in entanglement entropy. The loop-level integrals are challenging, but these may be addressed using modern machinery developed to calculate scattering amplitudes [34,163,164]. Integrating over the external sources is a task particular to real-time perturbation theory, but computing entanglement entropy order by order in interactions $\mathcal{O}_\lambda$ amounts to computing loop entanglement diagrams, and the integrals are analytic continuations of those that appear in loop-level scattering processes. Using the free scalar and fermion, and the perturbation theory tools we have presented here, one can investigate how UV behavior affects entanglement entropy.

Bibliography

[1] A. Sivaramakrishnan, "Color-Kinematic Duality in ABJM Theory Without Amplitude Relations," *Int. J. Mod. Phys.* **A32** (2017), no. 02n03 1750002, 1402.1821.

[2] A. Sivaramakrishnan, "Localized Excitations from Localized Unitary Operators," *Annals Phys.* **381** (2017) 41–67, 1604.00965.

[3] A. Sivaramakrishnan, "Entanglement Entropy with a Time-dependent Hamiltonian," 1709.09776.

[4] P. Kraus, A. Sivaramakrishnan, and R. Snively, "Black holes from CFT: Universality of correlators at large c," *JHEP* **08** (2017) 084, 1706.00771.

[5] Z. Bern, J. Carrasco, and H. Johansson, "New Relations for Gauge-Theory Amplitudes," *Phys.Rev.* **D78** (2008) 085011, 0805.3993.

[6] S. Henry Tye and Y. Zhang, "Dual Identities inside the Gluon and the Graviton Scattering Amplitudes," *JHEP* **1006** (2010) 071, 1003.1732.

[7] S. Stieberger, "Open and Closed vs. Pure Open String Disk Amplitudes," 0907.2211.

[8] N. Bjerrum-Bohr, P. H. Damgaard, T. Sondergaard, and P. Vanhove, "The Momentum Kernel of Gauge and Gravity Theories," *JHEP* **1101** (2011) 001, 1010.3933.

[9] Z. Bern, J. J. M. Carrasco, and H. Johansson, "Perturbative Quantum Gravity as a Double Copy of Gauge Theory," *Phys. Rev. Lett.* **105** (2010) 061602, 1004.0476.

[10] J. J. Carrasco and H. Johansson, "Five-Point Amplitudes in N=4 Super-Yang-Mills Theory and N=8 Supergravity," *Phys. Rev.* **D85** (2012) 025006, 1106.4711.

[11] E. Y. Yuan, "Virtual Color-Kinematics Duality: 6-pt 1-Loop MHV Amplitudes," *JHEP* **05** (2013) 070, 1210.1816.

[12] N. E. J. Bjerrum-Bohr, T. Dennen, R. Monteiro, and D. O'Connell, "Integrand Oxidation and One-Loop Colour-Dual Numerators in N=4 Gauge Theory," *JHEP* **07** (2013) 092, 1303.2913.

[13] Z. Bern, S. Davies, T. Dennen, Y.-t. Huang, and J. Nohle, "Color-Kinematics Duality for Pure Yang-Mills and Gravity at One and Two Loops," *Phys. Rev.* **D92** (2015), no. 4 045041, 1303.6605.

[14] Z. Bern, T. Dennen, Y.-t. Huang, and M. Kiermaier, "Gravity as the Square of Gauge Theory," *Phys.Rev.* **D82** (2010) 065003, 1004.0693.

[15] R. Monteiro and D. O'Connell, "The Kinematic Algebra From the Self-Dual Sector," *JHEP* **1107** (2011) 007, 1105.2565.

[16] M. Tolotti and S. Weinzierl, "Construction of an effective Yang-Mills Lagrangian with manifest BCJ duality," *JHEP* **1307** (2013) 111, 1306.2975.

[17] H. Kawai, D. Lewellen, and S. Tye, "A Relation Between Tree Amplitudes of Closed and Open Strings," *Nucl.Phys.* **B269** (1986) 1.

[18] Z. Bern, J. J. M. Carrasco, L. J. Dixon, H. Johansson, and R. Roiban, "Simplifying Multiloop Integrands and Ultraviolet Divergences of Gauge Theory and Gravity Amplitudes," *Phys. Rev.* **D85** (2012) 105014, 1201.5366.

[19] Z. Bern, S. Davies, T. Dennen, and Y.-t. Huang, "Absence of Three-Loop Four-Point Divergences in N=4 Supergravity," *Phys. Rev. Lett.* **108** (2012) 201301, 1202.3423.

[20] Z. Bern, S. Davies, T. Dennen, and Y.-t. Huang, "Ultraviolet Cancellations in Half-Maximal Supergravity as a Consequence of the Double-Copy Structure," *Phys. Rev.* **D86** (2012) 105014, 1209.2472.

[21] Z. Bern, S. Davies, T. Dennen, A. V. Smirnov, and V. A. Smirnov, "Ultraviolet Properties of N=4 Supergravity at Four Loops," *Phys. Rev. Lett.* **111** (2013), no. 23 231302, 1309.2498.

[22] D. Vaman and Y.-P. Yao, "Constraints and Generalized Gauge Transformations on Tree-Level Gluon and Graviton Amplitudes," *JHEP* **1011** (2010) 028, 1007.3475.

[23] R. H. Boels and R. S. Isermann, "On powercounting in perturbative quantum gravity theories through color-kinematic duality," *JHEP* **1306** (2013) 017, 1212.3473.

[24] S. Litsey and J. Stankowicz, "Kinematic Numerators and a Double-Copy Formula for N = 4 Super-Yang-Mills Residues," arXiv:1309.7681.

[25] N. Bjerrum-Bohr, P. H. Damgaard, and P. Vanhove, "Minimal Basis for Gauge Theory Amplitudes," *Phys.Rev.Lett.* **103** (2009) 161602, 0907.1425.

[26] T. Bargheer, S. He, and T. McLoughlin, "New Relations for Three-Dimensional Supersymmetric Scattering Amplitudes," *Phys.Rev.Lett.* **108** (2012) 231601, 1203.0562.

[27] Y.-t. Huang and H. Johansson, "Equivalent D=3 Supergravity Amplitudes from Double Copies of Three-Algebra and Two-Algebra Gauge Theories," *Phys.Rev.Lett.* **110** (2013) 171601, 1210.2255.

[28] Y.-t. Huang, H. Johansson, and S. Lee, "On Three-Algebra and Bi-Fundamental Matter Amplitudes and Integrability of Supergravity," 1307.2222.

[29] *See the ancillary file for the arXiv version of this manuscript.*

[30] F. Cachazo, S. He, and E. Y. Yuan, "Scattering of Massless Particles: Scalars, Gluons and Gravitons," *JHEP* **07** (2014) 033, 1309.0885.

[31] M. L. Mangano and S. J. Parke, "Multiparton amplitudes in gauge theories," *Phys. Rept.* **200** (1991) 301–367, hep-th/0509223.

[32] R. Kleiss and H. Kuijf, "Multigluon cross sections and 5-jet production at hadron colliders," *Nucl.Phys.* **B312** (1989) 616.

[33] O. Aharony, O. Bergman, D. L. Jafferis, and J. Maldacena, "N=6 superconformal Chern-Simons-matter theories, M2-branes and their gravity duals," *JHEP* **0810** (2008) 091, 0806.1218.

[34] H. Elvang and Y.-t. Huang, "Scattering Amplitudes," 1308.1697.

[35] D. Gang, Y.-t. Huang, E. Koh, S. Lee, and A. E. Lipstein, "Tree-level Recursion Relation and Dual Superconformal Symmetry of the ABJM Theory," *JHEP* **1103** (2011) 116, 1012.5032.

[36] O. T. Engelund and R. Roiban, "A twistor string for the ABJ(M) theory," *JHEP* **06** (2014) 088, 1401.6242.

[37] T. Hartman, C. A. Keller, and B. Stoica, "Universal Spectrum of 2d Conformal Field Theory in the Large c Limit," *JHEP* **09** (2014) 118, 1405.5137.

[38] D. Harlow, "Jerusalem Lectures on Black Holes and Quantum Information," *Rev. Mod. Phys.* **88** (2016) 15002, 1409.1231. [Rev. Mod. Phys.88,15002(2016)].

[39] S. D. Mathur, "The Information paradox: A Pedagogical introduction," *Class. Quant. Grav.* **26** (2009) 224001, 0909.1038.

[40] A. Almheiri, D. Marolf, J. Polchinski, and J. Sully, "Black Holes: Complementarity or Firewalls?," *JHEP* **02** (2013) 062, 1207.3123.

[41] S. Hellerman, "A Universal Inequality for CFT and Quantum Gravity," *JHEP* **08** (2011) 130, 0902.2790.

[42] A. Belin, C. A. Keller, and I. G. Zadeh, "Genus Two Partition Functions and Renyi Entropies of Large c CFTs," 1704.08250.

[43] J. Cardy, A. Maloney, and H. Maxfield, "A new handle on three-point coefficients: OPE asymptotics from genus two modular invariance," 1705.05855.

[44] A. Maloney, H. Maxfield, and G. S. Ng, "A conformal block Farey tail," 1609.02165.

[45] P. Kraus and A. Maloney, "A Cardy Formula for Three-Point Coefficients: How the Black Hole Got its Spots," 1608.03284.

[46] C.-M. Chang and Y.-H. Lin, "Bootstrapping 2D CFTs in the Semiclassical Limit," *JHEP* **08** (2016) 056, 1510.02464.

[47] C.-M. Chang and Y.-H. Lin, "Bootstrap, universality and horizons," *JHEP* **10** (2016) 068, 1604.01774.

[48] S. Collier, Y.-H. Lin, and X. Yin, "Modular Bootstrap Revisited," 1608.06241.

[49] S. Collier, P. Kravchuk, Y.-H. Lin, and X. Yin, "Bootstrapping the Spectral Function: On the Uniqueness of Liouville and the Universality of BTZ," 1702.00423.

[50] S. El-Showk and K. Papadodimas, "Emergent Spacetime and Holographic CFTs," *JHEP* **10** (2012) 106, 1101.4163.

[51] I. Heemskerk, J. Penedones, J. Polchinski, and J. Sully, "Holography from Conformal Field Theory," *JHEP* **10** (2009) 079, 0907.0151.

[52] A. Belin, B. Freivogel, R. A. Jefferson, and L. Kabir, "Sub-AdS scale locality in AdS_3/CFT_2," *JHEP* **04** (2017) 147, 1611.08601.

[53] D. Pappadopulo, S. Rychkov, J. Espin, and R. Rattazzi, "OPE Convergence in Conformal Field Theory," *Phys. Rev.* **D86** (2012) 105043, 1208.6449.

[54] J. M. Maldacena, "Eternal black holes in anti-de Sitter," *JHEP* **04** (2003) 021, hep-th/0106112.

[55] A. Belin, "Permutation Orbifolds and Chaos," 1705.08451.

[56] V. Balasubramanian, P. Kraus, and M. Shigemori, "Massless black holes and black rings as effective geometries of the D1-D5 system," *Class. Quant. Grav.* **22** (2005) 4803–4838, hep-th/0508110.

[57] E. Shaghoulian, "Modular forms and a generalized Cardy formula in higher dimensions," *Phys. Rev.* **D93** (2016), no. 12 126005, 1508.02728.

[58] E. Shaghoulian, "Black hole microstates in AdS," *Phys. Rev.* **D94** (2016), no. 10 104044, 1512.06855.

[59] A. Belin, J. de Boer, J. Kruthoff, B. Michel, E. Shaghoulian, and M. Shyani, "Universality of sparse $d > 2$ conformal field theory at large N," *JHEP* **03** (2017) 067, 1610.06186.

[60] E. Shaghoulian, "Modular invariance on $S^1 \times S^3$ and circle fibrations," 1612.05257.

[61] S. He, T. Numasawa, T. Takayanagi, and K. Watanabe, "Quantum Dimension as Entanglement Entropy in 2D CFTs," 1403.0702.

[62] M. Nozaki, "Notes on Quantum Entanglement of Local Operators," *JHEP* **10** (2014) 147, 1405.5875.

[63] P. Caputa, M. Nozaki, and T. Takayanagi, "Entanglement of local operators in large-N conformal field theories," *PTEP* **2014** (2014) 093B06, 1405.5946.

[64] M. Nozaki, T. Numasawa, and T. Takayanagi, "Quantum Entanglement of Local Operators in Conformal Field Theories," *Phys.Rev.Lett.* **112** (2014) 111602, 1401.0539.

[65] C. T. Asplund, A. Bernamonti, F. Galli, and T. Hartman, "Entanglement Scrambling in 2d Conformal Field Theory," *JHEP* **09** (2015) 110, 1506.03772.

[66] C. T. Asplund, A. Bernamonti, F. Galli, and T. Hartman, "Holographic Entanglement Entropy from 2d CFT: Heavy States and Local Quenches," *JHEP* **02** (2015) 171, 1410.1392.

[67] P. Caputa and A. Veliz-Osorio, "Entanglement constant for conformal families," *Phys. Rev.* **D92** (2015), no. 6 065010, 1507.00582.

[68] P. Caputa, J. Simón, A. Štikonas, and T. Takayanagi, "Quantum Entanglement of Localized Excited States at Finite Temperature," *JHEP* **01** (2015) 102, 1410.2287.

[69] J. Schwinger, "Brownian Motion of a Quantum Oscillator," *Journal of Mathematical Physics* **2** (1961), no. 3 407–432.

[70] L. V. Keldysh, "Diagram technique for nonequilibrium processes," *Zh. Eksp. Teor. Fiz.* **47** (1964) 1515–1527. [Sov. Phys. JETP20,1018(1965)].

[71] H. Reeh and S. Schlieder, "Bemerkungen zur unitäräquivalenz von lorentzinvarianten feldern," *Il Nuovo Cimento (1955-1965)* **22** (2008), no. 5 1051–1068.

[72] J. M. Knight, "Strict Localization in Quantum Field Theory," *Journal of Mathematical Physics* **2** (1961), no. 4 459–471.

[73] A. L. Licht, "Strict Localization," *Journal of Mathematical Physics* **4** (1963), no. 11 1443–1447.

[74] A. L. Licht, "Local States," *Journal of Mathematical Physics* **7** (1966), no. 9 1656–1669.

[75] M. Redhead, "More ado about nothing," *Foundations of Physics* **25** (1995), no. 1 123–137.

[76] K. E. Hellwig and K. Kraus, "Operations and measurements. II," *Communications in Mathematical Physics* **16** (1970), no. 2 142–147.

[77] T. D. Newton and E. P. Wigner, "Localized States for Elementary Systems," *Rev. Mod. Phys.* **21** (Jul, 1949) 400–406.

[78] H. Halvorson, "Reeh-Schlieder defeats Newton-Wigner: On alternative localization schemes in relativistic quantum field theory," *Phil. Sci.* **68** (2001) 111–133, `quant-ph/0007060`.

[79] D. Buchholz and E. Størmer, "Superposition, Transition Probabilities and Primitive Observables in Infinite Quantum Systems," *Communications in Mathematical Physics* **339** (2015), no. 1 309–325.

[80] D. F. Walls, "Squeezed states of light," *Nature* **306** (1983) 141.

[81] M. Kitagawa and M. Ueda, "Squeezed spin states," *Phys. Rev. A* **47** (Jun, 1993) 5138–5143.

[82] R. Gilmore, "On the properties of coherent states," *Rev. Mex. de Fisica* **23** (1972) 143.

[83] A. M. Perelomov, "Coherent States for Arbitrary Lie Group," *Commun. Math. Phys.* **26** (1972) 222.

[84] R. J. Glauber, "Coherent and Incoherent States of the Radiation Field," *Phys. Rev.* **131** (Sep, 1963) 2766–2788.

[85] T. Hartman, S. Jain, and S. Kundu, "Causality Constraints in Conformal Field Theory," 1509.00014.

[86] S. Leichenauer and M. Moosa, "Entanglement Tsunami in (1+1)-Dimensions," *Phys. Rev.* **D92** (2015) 126004, 1505.04225.

[87] M. Headrick, V. E. Hubeny, A. Lawrence, and M. Rangamani, "Causality & holographic entanglement entropy," *JHEP* **12** (2014) 162, 1408.6300.

[88] R. Haag, *Local quantum physics: fields, particles, algebras*. Texts and Monographs in Physics. Springer-Verlag, 1992.

[89] R. Streater and A. Wightman, *PCT, spin and statistics, and all that*. Mathematical physics monograph series. W.A. Benjamin, 1964.

[90] S. D. Mathur, "Is the Polyakov path integral prescription too restrictive?," hep-th/9306090.

[91] S. Weinberg, "Quantum contributions to cosmological correlations," *Phys.Rev.* **D72** (2005) 043514, hep-th/0506236.

[92] K. Skenderis and B. C. van Rees, "Real-time gauge/gravity duality: Prescription, Renormalization and Examples," *JHEP* **05** (2009) 085, 0812.2909.

[93] M. Musso, "A new diagrammatic representation for correlation functions in the in-in formalism," *JHEP* **1311** (2013) 184, hep-th/0611258.

[94] H. Casini, M. Huerta, and J. A. Rosabal, "Remarks on entanglement entropy for gauge fields," *Phys. Rev.* **D89** (2014), no. 8 085012, 1312.1183.

[95] R. M. Soni and S. P. Trivedi, "Aspects of Entanglement Entropy for Gauge Theories," *JHEP* **01** (2016) 136, 1510.07455.

[96] C.-T. Ma, "Entanglement with Centers," *JHEP* **01** (2016) 070, 1511.02671.

[97] G. C. Hegerfeldt, "Remark on causality and particle localization," *Phys. Rev. D* **10** (Nov, 1974) 3320–3321.

[98] J. Bhattacharya, V. E. Hubeny, M. Rangamani, and T. Takayanagi, "Entanglement density and gravitational thermodynamics," *Phys. Rev.* **D91** (2015), no. 10 106009, 1412.5472.

[99] H. Liu and S. J. Suh, "Entanglement Tsunami: Universal Scaling in Holographic Thermalization," *Phys. Rev. Lett.* **112** (2014) 011601, 1305.7244.

[100] V. E. Hubeny, M. Rangamani, and T. Takayanagi, "A Covariant holographic entanglement entropy proposal," *JHEP* **0707** (2007) 062, 0705.0016.

[101] S. Ryu and T. Takayanagi, "Holographic derivation of entanglement entropy from AdS/CFT," *Phys.Rev.Lett.* **96** (2006) 181602, hep-th/0603001.

[102] L. G. Yaffe, "Large N limits as classical mechanics," *Rev. Mod. Phys.* **54** (Apr, 1982) 407–435.

[103] A. M. Perelomov, "Obobshchennye kogerentnye sostoyaniya i nekotorye ikh primeneniya," *Uspekhi Fizicheskikh Nauk* **123** (1977), no. 9 23–55.

[104] V. Eisler and I. Peschel, "Evolution of entanglement after a local quench," *Journal of Statistical Mechanics: Theory and Experiment* **2007** (2007), no. 06 P06005.

[105] P. Calabrese and J. Cardy, "Entanglement and correlation functions following a local quench: a conformal field theory approach," *Journal of Statistical Mechanics: Theory and Experiment* **2007** (2007), no. 10 P10004.

[106] M. E. Peskin and D. V. Schroeder, *An introduction to quantum field theory*. Advanced book program. Westview Press Reading (Mass.), Boulder (Colo.), 1995. Autre tirage : 1997.

[107] R. Haag, "Quantum Field Theories with Composite Particles and Asymptotic Conditions," *Phys. Rev.* **112** (Oct, 1958) 669–673.

[108] P. Calabrese and J. Cardy, "Evolution of entanglement entropy in one-dimensional systems," *J. Stat. Mech.* **2005** (2005) 0503393.

[109] P. Calabrese and J. L. Cardy, "Entanglement entropy and quantum field theory," *J.Stat.Mech.* **0406** (2004) P06002, hep-th/0405152.

[110] C. Holzhey, F. Larsen, and F. Wilczek, "Geometric and renormalized entropy in conformal field theory," *Nucl.Phys.* **B424** (1994) 443–467, hep-th/9403108.

[111] P. Calabrese and J. Cardy, "Entanglement entropy and conformal field theory," *J.Phys.* **A42** (2009) 504005, 0905.4013.

[112] I. A. Morrison, "Boundary-to-bulk maps for AdS causal wedges and the Reeh-Schlieder property in holography," *JHEP* **05** (2014) 053, 1403.3426.

[113] S. Banerjee, J.-W. Bryan, K. Papadodimas, and S. Raju, "A toy model of black hole complementarity," 1603.02812.

[114] K. Papadodimas and S. Raju, "Black Hole Interior in the Holographic Correspondence and the Information Paradox," *Phys. Rev. Lett.* **112** (2014), no. 5 051301, 1310.6334.

[115] K. Papadodimas and S. Raju, "State-Dependent Bulk-Boundary Maps and Black Hole Complementarity," *Phys. Rev.* **D89** (2014), no. 8 086010, 1310.6335.

[116] K. Papadodimas and S. Raju, "Local Operators in the Eternal Black Hole," *Phys. Rev. Lett.* **115** (2015), no. 21 211601, 1502.06692.

[117] K. Papadodimas and S. Raju, "Remarks on the necessity and implications of state-dependence in the black hole interior," *Phys. Rev.* **D93** (2016), no. 8 084049, 1503.08825.

[118] J. M. Maldacena, "The Large N limit of superconformal field theories and supergravity," *Int.J.Theor.Phys.* **38** (1999) 1113–1133, hep-th/9711200.

[119] X. Dong, D. Harlow, and A. C. Wall, "Bulk Reconstruction in the Entanglement Wedge in AdS/CFT," 1601.05416.

[120] A. Almheiri, X. Dong, and D. Harlow, "Bulk Locality and Quantum Error Correction in AdS/CFT," *JHEP* **04** (2015) 163, 1411.7041.

[121] A. R. Brown, D. A. Roberts, L. Susskind, B. Swingle, and Y. Zhao, "Holographic Complexity Equals Bulk Action?," *Phys. Rev. Lett.* **116** (2016), no. 19 191301, 1509.07876.

[122] T. Hartman and J. Maldacena, "Time Evolution of Entanglement Entropy from Black Hole Interiors," *JHEP* **05** (2013) 014, 1303.1080.

[123] D. L. Jafferis, A. Lewkowycz, J. Maldacena, and S. J. Suh, "Relative entropy equals bulk relative entropy," 1512.06431.

[124] A. Almheiri, D. Marolf, J. Polchinski, and J. Sully, "Black Holes: Complementarity or Firewalls?," *JHEP* **02** (2013) 062, 1207.3123.

[125] D. Harlow, "Jerusalem Lectures on Black Holes and Quantum Information," *Rev. Mod. Phys.* **88** (2016) 15002, 1409.1231. [Rev. Mod. Phys.88,15002(2016)].

[126] A. Lewkowycz and J. Maldacena, "Generalized gravitational entropy," *JHEP* **1308** (2013) 090, 1304.4926.

[127] X. Dong, A. Lewkowycz, and M. Rangamani, "Deriving covariant holographic entanglement," *JHEP* **11** (2016) 028, 1607.07506.

[128] T. Faulkner, M. Guica, T. Hartman, R. C. Myers, and M. Van Raamsdonk, "Gravitation from Entanglement in Holographic CFTs," *JHEP* **1403** (2014) 051, 1312.7856.

[129] H. Casini, M. Huerta, and R. C. Myers, "Towards a derivation of holographic entanglement entropy," *JHEP* **1105** (2011) 036, 1102.0440.

[130] N. Afkhami-Jeddi, T. Hartman, S. Kundu, and A. Tajdini, "Shockwaves from the Operator Product Expansion," 1709.03597.

[131] T. Ugajin, "Two dimensional quantum quenches and holography," 1311.2562.

[132] P. Calabrese and J. Cardy, "Quantum Quenches in Extended Systems," *J. Stat. Mech.* **0706** (2007) P06008, 0704.1880.

[133] S. R. Das, D. A. Galante, and R. C. Myers, "Universal scaling in fast quantum quenches in conformal field theories," *Phys.Rev.Lett.* **112** (2014) 171601, 1401.0560.

[134] S. R. Das, D. A. Galante, and R. C. Myers, "Universality in fast quantum quenches," *JHEP* **1502** (2015) 167, 1411.7710.

[135] V. Rosenhaus and M. Smolkin, "Entanglement Entropy: A Perturbative Calculation," 1403.3733.

[136] V. Rosenhaus and M. Smolkin, "Entanglement Entropy for Relevant and Geometric Perturbations," *JHEP* **02** (2015) 015, 1410.6530.

[137] S. Leichenauer, M. Moosa, and M. Smolkin, "Dynamics of the Area Law of Entanglement Entropy," *JHEP* **09** (2016) 035, 1604.00388.

[138] S. Datta, J. R. David, M. Ferlaino, and S. P. Kumar, "Higher spin entanglement entropy from CFT," *JHEP* **1406** (2014) 096, 1402.0007.

[139] D. Berenstein and A. Miller, "Conformal perturbation theory, dimensional regularization, and AdS/CFT correspondence," *Phys. Rev.* **D90** (2014), no. 8 086011, 1406.4142.

[140] M. Lüscher and G. Mack, "Global conformal invariance in quantum field theory," *Comm. Math. Phys.* **41** (1975), no. 3 203–234.

[141] K. Osterwalder and R. Schrader, "Axioms for Euclidean Green's functions," *Communications in Mathematical Physics* **31** (Jun, 1973) 83–112.

[142] K. Osterwalder and R. Schrader, "Axioms for Euclidean Green's functions II," *Communications in Mathematical Physics* **42** (Oct, 1975) 281–305.

[143] W. Greiner and J. Reinhardt, *Quantum Electrodynamics*. Physics and Astronomy. Springer Berlin Heidelberg, 2008.

[144] N. Birrell and P. Davies, *Quantum Fields in Curved Space*. Cambridge Monographs on Mathematical Physics. Cambridge University Press, 1984.

[145] H. Ooguri, "Spectrum of Hawking radiation and the Huygens principle," *Phys. Rev. D* **33** (Jun, 1986) 3573–3580.

[146] H. Casini, C. Fosco, and M. Huerta, "Entanglement and alpha entropies for a massive Dirac field in two dimensions," *J.Stat.Mech.* **0507** (2005) P07007, `cond-mat/0505563`.

[147] H. Casini and M. Huerta, "Entanglement entropy in free quantum field theory," *J.Phys.* **A42** (2009) 504007, `0905.2562`.

[148] H. Casini and M. Huerta, "Remarks on the entanglement entropy for disconnected regions," *JHEP* **0903** (2009) 048, `0812.1773`.

[149] V. Balasubramanian and P. Kraus, "A Stress tensor for Anti-de Sitter gravity," *Commun. Math. Phys.* **208** (1999) 413–428, `hep-th/9902121`.

[150] J. D. Brown and M. Henneaux, "Central Charges in the Canonical Realization of Asymptotic Symmetries: An Example from Three-Dimensional Gravity," *Commun. Math. Phys.* **104** (1986) 207–226.

[151] K. Krasnov, "On holomorphic factorization in asymptotically AdS 3-D gravity," *Class.Quant.Grav.* **20** (2003) 4015–4042, hep-th/0109198.

[152] M. Banados, "Three-dimensional quantum geometry and black holes," hep-th/9901148. [AIP Conf. Proc.484,147(1999)].

[153] E. D'Hoker, P. Kraus, and A. Shah, "RG Flow of Magnetic Brane Correlators," *JHEP* **04** (2011) 039, 1012.5072.

[154] M. M. Roberts, "Time evolution of entanglement entropy from a pulse," *JHEP* **1212** (2012) 027, 1204.1982.

[155] C. N. Pope, "Lectures on W algebras and W gravity," in *Proceedings, Summer School in High-energy Physics and Cosmology: Trieste, Italy, June 17-August 9, 1991. Vol. 1, 2*, pp. 827–867, 1991. hep-th/9112076.

[156] T. Faulkner, F. M. Haehl, E. Hijano, O. Parrikar, C. Rabideau, and M. Van Raamsdonk, "Nonlinear Gravity from Entanglement in Conformal Field Theories," *JHEP* **08** (2017) 057, 1705.03026.

[157] A. L. Fitzpatrick, J. Kaplan, and M. T. Walters, "Universality of Long-Distance AdS Physics from the CFT Bootstrap," *JHEP* **08** (2014) 145, 1403.6829.

[158] A. L. Fitzpatrick, J. Kaplan, and M. T. Walters, "Virasoro Conformal Blocks and Thermality from Classical Background Fields," *JHEP* **11** (2015) 200, 1501.05315.

[159] T. Anous, T. Hartman, A. Rovai, and J. Sonner, "Black Hole Collapse in the 1/c Expansion," *JHEP* **07** (2016) 123, 1603.04856.

[160] E. Hijano, P. Kraus, E. Perlmutter, and R. Snively, "Witten Diagrams Revisited: The AdS Geometry of Conformal Blocks," *JHEP* **01** (2016) 146, 1508.00501.

[161] R. Bousso, "A Covariant entropy conjecture," *JHEP* **07** (1999) 004, hep-th/9905177.

[162] R. Bousso, H. Casini, Z. Fisher, and J. Maldacena, "Proof of a Quantum Bousso Bound," *Phys. Rev.* **D90** (2014), no. 4 044002, 1404.5635.

[163] J. M. Henn, "Lectures on differential equations for Feynman integrals," *J. Phys.* **A48** (2015) 153001, 1412.2296.

[164] V. Smirnov, *Evaluating Feynman Integrals*. Springer Tracts in Modern Physics. Springer Berlin Heidelberg, 2005.